

T-Pos224 ONCOMODULIN: ^1H NMR and OPTICAL STOPPED-FLOW SPECTROSCOPIC STUDIES of its METAL-BINDING PROPERTIES. T.C. Williams, D.C. Corson, J.P. MacManus†, and B.D. Sykes (*MRC Group in Protein Structure and Function, and the Department of Biochemistry, University of Alberta; †Division of Biological Sciences, NRC, Ottawa*)

We have shown by ^1H NMR and optical stopped-flow spectroscopic methods that oncomodulin has significantly different $\text{Ca(II)} \rightarrow \text{Ln(III)}$ exchange characteristics compared to parvalbumins, despite its extensive amino acid sequence homology with these calcium binding proteins. ^1H NMR-monitored Lu(III) titration of Ca -oncomodulin indicated that the EF-site calcium ion was readily displaced by this small lanthanide ion, the relative stability of these chelates, $\text{rel}\beta$, being approximately 10^3 ; displacement of Ca(II) from the CD site was approximately 30x more difficult. The relative ease of Lu(III) exchange at the EF site as compared to exchange at the CD site is also common in parvalbumins. However, the kinetics of the release of Yb(III) from the EF site of oncomodulin indicated that the $\text{abs}\beta$ for small Ln(III) s is nearly 100x weaker than for parvalbumins; the stability of the Ca(II) EF-site chelate was estimated at $3 \times 10^7 \text{ M}^{-1}$, nearly 5x weaker than for most parvalbumins. In addition, lineshape analysis of several ^1H NMR resonances indicated that $\text{Ca(II)} \rightarrow \text{Lu(III)}$ exchange at the CD site was approximately 20 sec^{-1} , many times faster than for the CD site of parvalbumins. This we attribute in large part to substitution of an Asp for a Glu at the -X position in the CD site of oncomodulin (residue 59). Furthermore, analysis of the kinetics of Yb(III) -release from Yb -oncomodulin indicated that chelation of Yb(III) at the CD site enhances the stability of Yb(III) bound at the EF site by approximately 20-fold.

T-Pos225 EQUILIBRIUM BINDING CONSTANTS FOR THE GROUP I METAL CATIONS WITH GRAMICIDIN A DETERMINED BY COMPETITION STUDIES AND Tl^+ -205 NMR SPECTROSCOPY. R. E. Koeppe II, J. F. Hinton, W. L. Whaley, D. Shungu, and F. S. Millett, Department of Chemistry, University of Arkansas, Fayetteville, Arkansas 72701.

The cation selectivity of gramicidin A has been investigated through measurements of the equilibrium binding constants for Tl^+ , Li^+ , Na^+ , K^+ , Rb^+ and Cs^+ , all of which can be transported through the channel. Thallium-205, because of its relatively tight binding to gramicidin and its highly sensitive NMR properties, has served as a useful probe for studying all of these ions by a competitive displacement technique. Tl^+ -205 binds to gramicidin A in aqueous dispersions of lysophosphatidylcholine (lyso-PC) with an association constant of 582 M^{-1} and a bound chemical shift of 127 ppm relative to Tl^+ in dilute aqueous solution. We have measured the Tl^+ -205 NMR chemical shift at 34°C for 15 mM Tl^+ as a function of varying Group I cation concentration in the presence of 5 mM gramicidin dimer and 100 mM lyso-PC. The data fit a theoretical model in which all ions compete for a common binding site on the gramicidin. The values of the binding constants are 32.2 M^{-1} (Li), 36.9 (Na), 52.6 (K), 55.9 (Rb) and 54.0 M^{-1} (Cs). The range of these binding constants is smaller than the corresponding range of single-channel conductances for this series of ions, and the sequence ($\text{Li} < \text{Na} < \text{K} = \text{Rb} = \text{Cs}$) is the same as the reported sequence of voltage-independent association rate constants with gramicidin A channels in planar lipid bilayers. Supported in part by NSF grant PCM-8300065 and NIH grants GM-34968 and NS-00648.

T-Pos226 METAL NMR STUDIES OF LITHIUM TRANSPORT IN HUMAN ERYTHROCYTES, Mary C. Espanol and Duarte Mota de Freitas (Intr. by Joan S. Valentine), Department of Chemistry, Loyola University of Chicago, 6525 N. Sheridan Road, Chicago, IL 60626.

Lithium transport in red blood cells (RBC) has been previously investigated by atomic absorption (AA) photometry. On the basis of these studies, it has been postulated that the major influx pathways for Li^+ in human erythrocytes are the leak and anion-exchange systems whereas Li^+ efflux takes place predominantly via the Na^+ - Li^+ countertransport system and to a small extent through $(\text{Na}^+, \text{K}^+)\text{-ATPase}$. The reported transport rate constants obtained for red cells of healthy individuals, hypertensive, and manic-depressive patients have varied extensively and have even in some cases overlapped. This discrepancy is most likely due to the invasive nature of the experimental procedure previously used, namely physical separation of intracellular and extracellular pools of Li^+ is required prior to determination of $[\text{Li}^+]$ concentration in the two compartments by AA. We found that Gupta's shift reagent, dysprosium(III) tripolyphosphate, resolves intracellular and extracellular lithium resonances and is therefore suitable to study Li^+ transport non-invasively in red cells by Li-7 NMR. The chemical shift difference measured by Li-7 NMR between intracellular and extracellular components of RBC in the presence of 5 mM Dy(PPP)_3 is approximately 4.0 ppm which is about half of that typically observed for Na-23 NMR after addition of 1 mM LiCl to a suspension of RBC. A two-fold decrease in intracellular $[\text{Na}^+]$ concentration was observed within the first 10 minutes following addition of 1 mM LiCl . This observation suggests for the first time that Li^+ influx takes place, at least in part, via a Na^+ -dependent pathway. The identification of transport mechanisms for Na^+ and Li^+ fluxes in RBCs by specific transport inhibitors will be addressed.

T-Pos227 EPR AND ELECTRON SPIN ECHO STUDIES OF IRON-SULFUR CLUSTERS S-1 and S-2 IN BEEF HEART SUCCINATE DEHYDROGENASE. R. LoBrutto, P. E. Haley, C.-A. Yu, T. Ohnishi and J. S. Leigh, Dept. of Biochem. & Biophysics, University of Pennsylvania, Philadelphia, PA 19104.

The ligands of the two iron-sulfur clusters S-1 and S-2 in beef-heart succinate dehydrogenase (SDH) have not been determined to date. We have made a detailed comparison of the electron spin-echo envelope modulation (ESEEM) spectra from cluster S-1 as a function of g-value, with spectra obtained from two better-characterized iron-sulfur proteins. X-ray crystallographic data (1) confirm that the 2Fe-2S cluster in *Spirulina platensis* ferredoxin has four sulfur ligands, but that there are several nitrogens from the polypeptide backbone that are close enough to form NH...S hydrogen bonds to the cluster. The ESEEM spectrum of the dithionite-reduced protein shows intense modulations characteristic of ^{14}N at all g-values. At $g = 2.01$, four distinct modulation frequencies are evident: 0.8, 1.7, 3.0 and 4.3 MHz. The highest frequency is most likely due to a nuclear transition of the type $\Delta m_I = 2$. The ESEEM spectrum of spinach ferredoxin is virtually identical to that of *S. platensis* ferredoxin at $g = 2.01$, and at most other g-values. The ESEEM spectrum of S-1 in BH-SDH contains very similar frequencies, although the ratios of the line intensities in the Fourier transformed spectrum is different. We conclude that S-1 probably also has all sulfur ligands, but that its immediate protein environment is somewhat different from that of the two ferredoxins. We will also present ESEEM and spin relaxation rate data from dithionite-reduced SDH, which reflect the ligation and environment of the S-2 cluster.

(1) T. Tsukihara, et al., J. Biochem. 90, 1763-1773 (1981).

T-Pos228 C-13 NMR CHEMICAL SHIFT STUDIES ON THE MICELLE AGGREGATION NUMBER OF THE NON-IONIC MEMBRANE-SOLUBILIZING DETERGENT OCTYLGLUCOSIDE. Raja G. Khalifah*, Elizabeth S. Rowe* and Robert Roxby**. *Biochemistry Department, University of Kansas School of Medicine and Veterans Administration Medical Center, Kansas City MO 64128 and **Biochemistry Department, University of Maine, Orono ME 04469.

Octyl- β -D-glucoside is a highly useful non-ionic detergent with a high critical micelle concentration that facilitates its solubilization of lipids and membrane-bound proteins. Previous ultracentrifugation studies have revealed that the micelle aggregation number increases from about 50 to 90 with increasing concentration above the critical micelle concentration. We have carried out C-13 NMR studies on the structure and formation of micelles of this detergent and have developed a full non-linear least squares method of analysis to objectively determine the micelle aggregation number n . We find that n is 20 (s.d. 7) and is concentration independent. Our analysis reveals that, in contrast to previous claims, the C-13 NMR shift change that accompanies micelle formation reflects only the first-formed micellar aggregate and cannot monitor changes in aggregation numbers. (Supported by grants from the Medical Research Service of the Veterans Administration (R.G.K. and E.S.R.), from the Public Health Service (AA 05371-02 to E.S.R. and AM 18852 to R.R.) and from the Maine Agriculture Experimental Station (ME 08403 to R.R.)).

T-Pos229 DEUTERIUM, OXYGEN-17 AND SODIUM-23 NMR OF MYOFIBRILLAR PROTEIN INTERACTIONS WITH ELECTROLYTES IN SOLUTIONS AND POWDERS. I. C. Baianu*, P. J. Bechtel, T. S. Lioutas and M. P. Steinberg, Department of Food Science, University of Illinois at Urbana*, Phys. Chemistry & NMR Laboratories, 1304 W. Pennsylvania Ave., Urbana, IL 61801.

Sorption isotherms of myofibrillar proteins with sodium chloride and water are compared with high field nuclear magnetic resonance (NMR) data in order to determine the molecular mechanisms of the sorption process and its relationship to the interactions of myofibrillar proteins with electrolytes and water. Upon addition of salt, the amount of water in the first hydration layer of myofibrillar proteins increased significantly, as did the total amount of water hydrating these proteins. The fraction of Na^+ 'bound' to the myofibrillar (MF) proteins increased with the myofibrillar protein concentration to a maximum of about 500 moles Na^+ per 10^6 g MF proteins. From the ^{23}Na and ^{17}O NMR data at 5.4 Tesla, correlation times were calculated for 'bound' Na^+ and water, respectively. Surprisingly, the correlation time of bound Na^+ to MF proteins (about 28ps) is three times shorter than the corresponding value for lysozyme (about 76ps). The addition of Na^+ to MF proteins increased substantially the ^{23}Na NMR linewidth in comparison with that of the corresponding sodium chloride solution. Furthermore, instead of gradual changes in the NMR linewidths with concentration, we observed well-defined regions of distinct, linear dependences on concentration. Such data are related to previous work on lysozyme interactions with electrolytes and water (1-3).

REFERENCES: 1. Halle, B. et al. (1981). J. Amer. Chem. Soc. 103:500-508; 2. Baianu, I. C. et al. (1985). Biophys. J. 47:330a; 3. Lioutas, T., Baianu, I. C. and Steinberg, M. P. (1985). Biophys. J. 47:210a.

T-Pos230 APPLICATIONS OF ^{15}N NMR TO LARGE BIOMOLECULES DEMONSTRATED WITH DNA.

Kathleen M. Morden* and Stanley J. Opella[†], *Dept. of Biochemistry, Louisiana State University, Baton Rouge, LA 70803 and [†]Dept. of Chemistry, University of Pennsylvania, Philadelphia PA 19104.

In recent years NMR has become a very powerful technique for the study of structure in biological molecules. Most of this progress has been due to the development of two-dimensional NMR techniques. One of the most useful of these techniques is the NOESY experiment, a two-dimensional NMR method used to determine through space interactions that can lead to the elucidation of the three dimensional structure of the molecule. One of the major drawbacks of the solution techniques is the limitation to relatively small molecules (< 30,000 MW). In an attempt to look at larger biomolecules we have utilized the techniques of solid state NMR. We have investigated the use of ^{15}N NMR as a tool in the structure determination of large pieces of DNA. The system that was studied was the replicative form of the fd virus in E. Coli. The DNA was isotopically labeled by growing the E. Coli in a medium containing $(^{15}\text{NH}_4)_2\text{SO}_4$ as the sole source of nitrogen. ^{15}N - ^{15}N spin exchange experiments, the solid state equivalent of the NOESY experiments, were carried out on a hydrated sample of DNA. Both inter and intra-base spin exchange interactions were observed. One and two-dimensional ^{15}N spectra of this system will be shown. Results of using several selective spin exchange experiments on the model compound 1,3 ^{15}N -Cytosine will also be shown. The prospects for ^{15}N NMR on large biomolecules will be discussed.

T-Pos231 ^{15}N AMIDE CHEMICAL SHIFT TENSORS OF SEVERAL DIPEPTIDES. Terrence G. Oas¹, Cynthia J. Hartzell², Frederick W. Dahlquist¹ and Gary Drobny.² ¹Institute of Molecular Biology, University of Oregon, Eugene, OR 97403, ²Department of Chemistry, University of Washington, Seattle, WA 98195.

We have obtained ^{15}N powder and magic-angle spinning spectra of several dipeptides of the form N-acetylglycyl-X-amide enriched in ^{13}C at the glycyl carbonyl carbon and in ^{15}N at the amide nitrogen of the X residue. These spectra have allowed us to determine the principal values and orientations of the ^{15}N chemical shift tensors of these molecules. Our results indicate significant differences in both the orientation and principal values of the shift tensors of these dipeptides. These differences are due in part to different lattice environments of the molecules. These results suggest that it is invalid to assume a canonical shift tensor for ^{15}N amides in proteins when using ^{15}N chemical shift to determine the orientation of peptide groups in studies on oriented protein molecules.

T-Pos232 USING THE NOESY EXPERIMENT TO PROBE LIPID DYNAMICS

R.E. Stark* and M.S. Broido#

*Department of Chemistry, College of Staten Island, C.U.N.Y., Staten Island, NY 10301

#Department of Chemistry, Hunter College, C.U.N.Y., New York, NY 10021

Lipolytic enzymes exhibit enhanced activity toward substrates solubilized in detergent micelles, and assessments of lipid dynamics and packing in these aggregates may thus be quite informative with regard to enzyme mechanism. Though a qualitative picture of acyl chain motion and micellar structure has been developed from ^1H NMR linewidths and ^1H spin-lattice relaxation rates (R_1 's) in bile salt-phospholipid (BS-PC) mixtures, a more quantitative investigative strategy may be based on a combination of ^1H R_1 and two-dimensional NOE (NOESY) experiments. We have observed NOESY cross peaks in BS-PC spectra for protons which are spatially very distant but which are linked by a rigid molecular network. In order to probe the motional characteristics of the spin communication that are suggested by these results (as well as the inherent spatial information of the dipolar interactions), we have performed a series of selective and nonselective R_1 measurements at different field strengths and temperatures. These results support the potential of NOESY as a dynamic as well as spatial probe of molecular organization in model bile mixtures.

T-Pos233 IN VIVO ^{19}F NMR MEASUREMENTS OF HALOTHANE METABOLISM IN RAT LIVER. Barry S. Selinsky, Morrow Thompson, Lisa M. Jeffreys, and Robert E. London. National Institute of Environmental Health Sciences, PO Box 12233, Research Triangle Park, NC 27709.

The hepatic metabolism of the inhalation anesthetic halothane (2-chloro-2-bromo-1,1,1-trifluoroethane) has been examined in rats using in vivo surface coil ^{19}F NMR spectroscopy. ^{19}F NMR resonances for halothane and three halothane metabolites are clearly seen using the technique of London et al. (*J. Biochem. Biophys. Meth.*, 1985, **11**, 21-19) for noninvasive observation of the liver. Halothane and its metabolites are cleared slowly from rat liver, remaining at observable concentrations 36 hours after exposure to halothane. Rat liver extract studies demonstrate that all of the in vivo resonances correspond to different chemical species, and not the same species in different physical environments within the liver. Also, an additional ^{19}F resonance is observed which could not be detected in vivo. Three of the halothane metabolites have been tentatively identified as trifluoroacetic acid, 2-chloro-1,1-difluoroethene, and 2-chloro-1,1,1-trifluoroethane. This study demonstrates the usefulness of ^{19}F surface coil NMR spectroscopy for the examination of metabolism and clearance of halothane, and for in vivo measurements of fluorinated agents in general.

T-Pos234 IN VITRO AND IN VIVO HIGH RESOLUTION PROTON NMR DETECTION OF METABOLITES IN RAT AND MOUSE BRAIN, WITH EFFICIENT WATER PEAK SUPPRESSION
Thomas M. Eads*, Jerzy Szumowski & Robert G. Bryant, Dept. Radiology, Univ. Rochester Med. Ctr., Rochester, NY 14642 (*present address: Kraft, Inc. R&D, Basic Food Science Laboratory, 801 Waukegan Rd., Glenview, IL 60025).

Low molecular weight solutes (glucose, lactate, etc.) are detected with excellent resolution and sensitivity at their natural concentrations (mM) in brain tissue using high resolution proton nuclear magnetic resonance spectroscopy (270 MHz) by application of a method which suppresses the water proton peak. Water in tissue has complex magnetic behavior: A large fraction of water having a very short T2 is allowed to decay in the transverse plane during a spin echo pulse train. The resulting spin echo spectrum has a narrow residual water peak of sufficiently low intensity that metabolites are easily detected. Spectra of intact mouse and rat brains are shown. In minced brain tissue, addition of Mn^{2+} (few tenths mM) further reduces the contribution from water with long T2, with the dramatic result that resonances with 0.12 ppm of the H2O peak are detectable. Control of water T2 by a paramagnetic reagent, and detection after a Carr-Purcell-Meiboom-Gill spin echo pulse train (Bryant & Eads, *J. Magn. Res.* in press (1985)) is a general method. Both reagent and detection scheme may be varied for particular applications to fluids, cells, and tissues. We also show high resolution spectra from live animals, using surface coils with an imaging spectrometer operating at 2 Tesla (85 MHz). Thus it is possible to obtain high resolution proton nmr spectra, with water peak suppression, in vivo, by taking advantage of naturally short water T2.

T-Pos235 NUCLEAR MAGNETIC RESONANCE STUDIES OF INTRACELLULAR POTASSIUM IN *E. COLI*. B. Richey, S. Cayley, C. F. Anderson and M. T. Record, Jr., Depts. of Chemistry and Biochemistry, University of Wisconsin, Madison, WI. 53706.

The in vitro interactions of proteins with nucleic acids are invariably observed to depend strongly on the concentration of electrolyte ions. Thus, the intracellular concentrations of these ions should influence the strength of protein-nucleic acid interactions in vivo. The major intracellular cation in *E. coli* is potassium. The total concentration of this ion varies over the range as 0.1-0.6 M in response to changes in the osmolarity of the external growth media (Epstein, W. and Schultz, S. G. (1965) *J. Gen. Physiol.* **49**, 221-239). Since these levels of potassium ion are sufficient to strongly inhibit protein-DNA interactions in vitro, we have undertaken ^{39}K NMR measurements on concentrated cell suspensions of *E. coli* to determine the physical state of intracellular K^+ ions. We have compared the concentration of NMR-visible potassium in the cell with total potassium concentration as determined by atomic absorption spectroscopy and cell volume measurements. It appears that the majority of intracellular K^+ is NMR-visible with a linewidth which is qualitatively similar to that observed for potassium ion in DNA solutions of comparable concentration. This is consistent with its thermodynamic role as an osmoprotectant for *E. coli* in environments of high osmotic strength. Supported by NSF grant CHE-8509625 (MTR) and NIH fellowship F32 GM10895 (BR).

- T-Pos236** EFFECTS OF DILTIAZEM ON CARDIAC LEVELS OF PCr AND ATP DURING HYPOXIA AS MONITORED BY ^{31}P -NMR. Steven D. Buchthal, Truman R. Brown, Fox Chase Cancer Center, Philadelphia, PA and Ingrid L. Grupp, Arnold Schwartz, University of Cincinnati, Cincinnati, OH.

Isolated perfused rat hearts were made hypoxic by changing the gas composition of the perfusate from 95% O_2 :5% CO_2 to 20% O_2 :5% CO_2 , bal N_2 and the amounts of PCr, ATP and Pi were monitored by ^{31}P -NMR. After 30 min. of hypoxia, PCr dropped to $70 \pm 4.6\%$ of control levels. In contrast, in hearts that were pretreated with $2 \times 10^{-7}\text{M}$ diltiazem PCr levels dropped to only $82.5 \pm 4.3\%$ ($p < .05$, $n=4$). Following reoxygenation of the heart during which PCr levels rose to 120% of control levels \pm diltiazem, a second period of hypoxia in which the drug was given to untreated hearts and washed out of treated hearts caused PCr levels to fall to $82.5 \pm 9.2\%$ with, and $62.3 \pm 1.4\%$ without diltiazem ($p < .05$). ATP levels as measured by the γ -phosphate peak fell slightly ($90 \pm 6.8\%$) during hypoxia without diltiazem but dropped to $78.8 \pm 3.8\%$ in its presence. The second round of hypoxia saw ATP levels drop to $58.8 \pm 3.8\%$ in the absence of diltiazem and $78.8 \pm 4.7\%$ ($p < .05$) in the presence of diltiazem. These results suggest that diltiazem affects the control of cardiac metabolism during hypoxia. (Supported by NIH HL22619.)

- T-Pos237** PHOSPHONATE ANALOGS OF AMINO ACIDS AS ^{31}P NMR INDICATORS OF INTRACELLULAR pH. Benjamin S. Szwergold, Truman R. Brown and Jerome J. Freed. Fox Chase Cancer Center, Phila., PA

In order to understand the correlation of intracellular pH mitogenic stimulation, we have undertaken studies of the regulation of intracellular pH in a well characterized model, the mouse 3T3 fibroblast. Because these cells have very low levels of intracellular inorganic phosphate under well energized conditions, another pH indicator is required in this system. The ^{31}P NMR indicators, deoxyglucose 6P, and methyl phosphonate, have for different reasons, also proven unsatisfactory in our work. Because of this, we have explored the possible use of a series of phosphono-amino acids as such indicators. Of the compounds studied, the best thus far have proven to be 2-amino-5-phosphonovaleric acid and 2-amino-6-phosphonohexanoic acid. Their properties include:

- Physiological pKa, 7.1 and 7.5, respectively
- Sensitivity greater than 1 ppm/1 pH unit
- Resonant frequency far from the phosphate region
- Low toxicity.

This combination of attributes should make these compounds useful in other NMR studies of intracellular pH.

- T-Pos238 FAR ULTRAVIOLET RESONANCE RAMAN STUDIES OF PROTEIN COMPONENTS: PROLINE BONDS AND HISTIDINE.** Leland Mayne, Greg Harhay and Bruce Hudson, Department of Chemistry & Institute of Molecular Biology, University of Oregon, Eugene, OR 97403

As part of a continuing study we have been investigating the far ultraviolet resonant Raman spectra of proteins and protein components. The Raman bands of X-proline bonds can be strongly enhanced relative to normal peptide bonds with excitation around 235 nm. This may permit UV Raman studies to monitor the state of cis-trans isomerism of these bonds. The Raman bands of imidazole show considerable variations depending upon the state of ionization or deuteration. In protein studies these changes might be useful in clarifying the state of ionization and the solvent accessibility of this enzymatically important residue.

* "UV Resonance Raman Studies of Peptide Components", L. C. Mayne, T. Ramahi, T. Oas, and B. Hudson, *Biophys. J.*, **45**, 322a (1984); "UV Resonance Raman Spectroscopy of Proteins and Protein Components", L. C. Mayne, G. Harhay, and B. Hudson, *Biophys. J.*, **47**, 88a (1985); "Ultraviolet Resonance Raman Spectroscopy of Biopolymers", B. Hudson and L. C. Mayne, *Methods in Enzymology*, in press; "Ultraviolet Resonance Raman Studies of N-methylacetamide", L. C. Mayne, L. D. Ziegler, and B. Hudson, *J. Phys. Chem.*, **89**, 6399 (1985); "Peptides & Protein Side Chains", B. Hudson and L. C. Mayne, in "Biological Applications of Resonance Raman", in "Resonance Raman Spectra of Polyenes and Aromatics", T. Spiro, ed., in press.

T-Pos239 UV RESONANCE RAMAN STUDIES OF AROMATIC AMINO ACIDS AND PROTEINS. S. A. Asher, C. R. Johnson, M. Ludwig, Department of Chemistry, University of Pittsburgh, Pittsburgh, PA 15260

UV resonance Raman studies of phenylalanine, tyrosine and tryptophan show strong enhancement of ring vibrations for excitation in the 217-260 nm spectral region. Raman excitation profiles detail the vibronic structure which underlie the absorption bands. We will explain the observed selectivity of resonance enhancement for particular vibrational modes in the 217-300 nm absorption bands. The excitation profile data indicate that little charge transfer character underlies the L_a absorption band of tyrosinate. The excitation profiles of aromatic amino acids in proteins qualitatively resemble those of the aromatic amino acid monomers. Thus, these excitation profiles can be used to specify excitation wavelengths to selectively enhance particular types of aromatic amino acids in proteins. The $830/850\text{ cm}^{-1}$ tyrosine doublet typically used in normal Raman to monitor tyrosine environment is strongly enhanced in the UV. Photochemistry and optical saturation phenomena complicate UV Raman measurements. The dependence of these processes on incident laser power density will be described in detail.

T-Pos240 UV RESONANCE RAMAN STUDIES OF PYRENE IN SOLUTION AND IN BIOLOGICAL MATRICES. C. M. Jones, S. A. Asher, Department of Chemistry, University of Pittsburgh, Pittsburgh, PA 15260

UV resonance Raman studies of polycyclic aromatic hydrocarbon (PAH's) such as pyrene and naphthalene demonstrate extraordinarily large Raman cross sections. The modes enhanced are mainly due to symmetric in-plane ring breathing vibrations. The Raman excitation profiles in the S_2 , S_3 , and S_4 states of pyrene detail these vibrations which are Franck-Condon active in each absorption band. The excitation profiles measured between 217-300 nm show the positions of the 0-0 transitions and clarify the underlying vibronic components within the absorption bands. The Raman spectral frequencies and intensities strongly depend upon ring peripheral substitution. Because of the ring substitution spectral dependence and because of the dramatic resonance Raman enhancements it is easy to detect, speciate and quantitate PAH's present in complicated biological matrices. We demonstrate detection of naphthalene derivatives in rat liver microsome samples at 10^{-3} M naphthalene concentrations.

T-Pos241 RAMAN SPECTROSCOPY OF OXIDIZED AND REDUCED NICOTINAMIDE ADENINE DINUCLEOTIDES. Kwok To Yue, Charlotte Martin, Dehuai Chen, Paula Nelson, Donald Sloan, and Robert Callender. Departments of Physics (D.C. and R.C.) and Chemistry (C.M., P.N., and D.S.), City College of New York, New York 10031 and Department of Physics (K.T.Y.), Emory University, Atlanta, GA 30322.

We have measured the Raman spectra of oxidized nicotinamide adenine dinucleotide NAD^+ , and its reduced form, NADH, as well as a series of fragments and analogs of NAD^+ and NADH. In addition, we have studied the effects of pH as well as deuteration of the exchangeable protons on the Raman spectra of these molecules. In comparing the positions and intensities of the peaks in the fragment and analog spectra with those of NADH and NAD^+ , we find that it is useful to consider these large molecules as consisting of component parts, namely adenosine, two ribose groups, two phosphate groups and nicotinamide, for the purposes of assigning their spectral features. The Raman bands of NADH and NAD^+ are found to generally arise from molecular motions arising from one or another of these molecular moieties, although some peaks are not quite so easily identified in this way. This type of assignment is the first step in a detailed understanding of the Raman spectra of NAD^+ and NADH. This is needed to understand the binding properties of NADH and NAD^+ acting as coenzymes with the NAD-linked dehydrogenases as deduced recently using Raman spectroscopy (see e.g. Yue et al., this conference).

T-Pos242 RAMAN STUDIES OF THE BINDING OF NADH AND NAD⁺ TO ALCOHOL DEHYDROGENASES. Kwok To Yue, Dehuai Chen, Donald Sloan, and Robert Callender. Physics (D. C. and R. C.) and Chemistry (D. S.) Departments, City College of N.Y., N.Y. 10031 and Physics Department (K. T. Y.), Emory University, Atlanta, GA 30322.

We have extended our Raman studies (*Biochemistry* 23, 6480, 1984) on the binding of reduced nicotinamide adenine dinucleotide (NADH) to liver alcohol dehydrogenase (LADH) to include the binding of the oxidized coenzyme (NAD⁺) to LADH and the binding of both reduced and oxidized coenzymes to yeast alcohol dehydrogenase (YADH). The Raman spectrum of NAD⁺ bound to LADH is identical to that of NADH bound to LADH, suggesting that the coenzymes have changed into a common conformation which will facilitate the next step in the enzymatic reaction. Furthermore, we found no pH dependence of the Raman spectra of either NADH or NAD⁺ between 6.5 and 9.6 when bound to LADH. We have also examined the effect of inhibitors to the Raman spectra of the bound coenzymes. Very small changes were observed on the bound NADH spectrum by the presence of excess isobutyramide and dimethyl sulfoxide. However, significant changes occur when pyrazole binds to the binary complex LADH/NAD⁺, indicating the involvement of the coenzyme in the binding of pyrazole. In contrast to the results found for LADH, the spectra of NADH and NAD⁺ when bound to YADH are almost identical to their respective spectra in solution, suggesting that both coenzymes are only loosely bound to YADH.

T-Pos243 THE GROUND AND EXCITED STATE PK_a'S OF AROMATIC COMPOUNDS COMPLEXED WITH β-CYCLODEXTRIN. A. Ürstan¹, W.R. Laws², J.F. Wojcik³, and J.B.A. Ross¹.
¹Department of Biochemistry and ²the Center for Polypeptide and Membrane Research, The Mount Sinai School of Medicine, One Gustave L. Levy Place, New York, N.Y. 10029; ³Department of Chemistry, Villanova University, Villanova, PA 19085.

β-Cyclodextrins have catalytic properties¹ and have also been used as models for the steroid-binding sites of high-affinity steroid-binding proteins². To further understand the physical-chemical properties of β-cyclodextrin complexes, we have examined the perturbation of ground and excited state pK_a's (pK_a and pK_a^{*}, respectively) of 2-naphthol, 2-naphthoic acid, acridine, salicylic acid and related compounds when complexed with β-cyclodextrin. pK_a's of free and complexed dyes were measured using absorption and fluorescence methods. pK_a^{*}'s of the complexed dyes were estimated from Förster cycle calculations. The pK_a shifts upon complex formation are in the same direction as the shifts in pK_a to pK_a^{*} in the unbound dyes, indicating that complexation with β-cyclodextrin may perturb the electronic structure of the bound dyes. The β-cyclodextrin-dye complexes have also been characterized by fluorescence quenching and lifetime experiments.

¹D.W. Griffiths and M.L. Bender, *Adv. Catal.*, **23**, 209 (1973).

²A. Ürstan, M.F. Lulka, B. Eide, P.H. Petra and J.B.A. Ross, submitted to *Biochemistry*.

T-Pos244 EXCITED-STATE PROTONATION OF SEROTONIN AND RELATED INDOLES: TIME-RESOLVED STUDIES

Jay R. Knutson, Raymond F. Chen, Pia Chaudhuri, Carrie S. Scott, and Robert L. Bowman
 Laboratory of Technical Development, NHLBI, NIH, Bethesda, MD 20892

Serotonin (5-hydroxytryptamine) and related hydroxy- and alkoxyindoles such as melatonin are important neurotransmitters. Like tryptophan, they are maximally excited at 280 nm and emit at about 340 nm, but they have the unique property of exhibiting a green emission at about 540 nm when excited at 280 nm in acid (Bowman et al, *Science* 122, 32, 1955). The origin of this unusual emission was suggested to be the protonation of the excited fluorophore (Chen, *Proc. Nat. Acad. Sci.* 60, 598, 1968). Using a modelocked, cavity-dumped tunable dye laser source in a time-resolved spectrofluorometer with multiple scanning (T-format) detection, we have followed the growth of the green emission on the picosecond time scale, confirming that the emission is due to excited-state protonation. The reaction is essentially irreversible with $k(S^* \rightarrow S) = 2.6 \times 10^8 \text{ sec}^{-1}$, $k(S^* \rightarrow SH^*) = 2.5 \times 10^9 \text{ sec}^{-1} \text{ M}^{-1}$, and $k(SH^* \rightarrow SH) = 1.9 \times 10^8 \text{ sec}^{-1}$. In detail, one can also add correction terms for static and dynamic quenching, by including steady state data. This system serves as a model for excited state protonation and has significance for indole photophysics.

T-Pos245 CHARACTERIZATION OF BINDING OF CHARGE SHIFT PROBES TO RED CELL MEMBRANES AND RENAL BRUSH BORDER MEMBRANE VESICLES. Eric N. Fluhler, A. S. Verkman, Leslie M. Loew and James A. Dix, Department of Chemistry, State University of New York, Binghamton, NY 13901; University of Connecticut Health Center, Farmington, CT 06032; University of California, San Francisco, CA 94143.

Fluorescent probes based on the aminostyrylpyridinium (ASP) chromophore respond rapidly (<1 usec) to changes in membrane potential. We have characterized the interaction of the ASP derivative, di-4-ANEPPS, with human red cell membranes and renal brush border membrane vesicles (BBMV) isolated from the proximal tubule of rabbit kidney. Fluorescence stopped-flow kinetic studies in red cells revealed a biexponential increase of probe fluorescence (time constants, τ_1 = 0.15 and 1.36 sec at 25 °C). For BBMV, a biexponential increase was also observed (τ_1 = 20 msec and 150-500 msec at 25 °C); τ_1 for the fast time course was concentration independent while τ_2 for the slower time course increased with concentration over the range 0.1 to 10 μ M. A single fluorescence lifetime was observed in homogeneous solvents and in membrane systems (lifetimes, in ns: ethanol, 0.40; ethylene glycol, 0.63; glycerol, 1.16; PC liposomes, 2.00; lauryl alcohol, 2.90; BBMV, 3.96; ghosts, 4.62). Measurements of anisotropy and differential tangents suggest that the probe's rotation is anisotropic and significantly hindered (anisotropy, differential tangents: ghosts, 0.280, 0.041; BBMV, 0.247, 0.032; PC liposomes, 0.256, 0.040; ethanol, 0.200, 0.035). Variation of membrane potential with valinomycin-induced potassium diffusion potentials in red cells showed that the probe responds primarily by an increase of fluorescence at the excitation and emission maxima; the calibration of probe response was 0.068%/mV. Supported by NIH HL29488 and GM35063.

T-Pos246 THE ROTAMER MODEL AND THE FLUORESCENCE DECAY KINETICS OF SINGLE TRYPTOPHAN-CONTAINING POLYPEPTIDES. M.F. Lulka(1), W.R. Laws(2), A. Buku(2), J.D. Glass(3), H.R. Wyssbrod(2, 3), and J.B.A. Ross(1), Departments of Biochemistry(1) and Physiology and Biophysics(3) and the Center for Polypeptide and Membrane Research(2), The Mount Sinai School of Medicine, One Gustave L. Levy Place, New York, NY 10029.

The origin of multiexponential fluorescence decay kinetics observed for single tryptophan-containing compounds is still unresolved. Many explanations have been suggested. We have tested the proposal that the complex kinetics could be due to ground-state heterogeneity resulting from rotamers about the C α -C β (χ^1) and C β -C γ (χ^2) bonds. Data analysis assumed a model where the rotamers do not interconvert during the lifetime of the excited state. This model allows the pre-exponential terms (amplitudes) to be linked to the rotamer populations. Using this linked-function data analysis approach (Ross et al., *Photochem. Photobiol.*, in press), the multiexponential fluorescence decay of single tyrosine residues in polypeptides can be explained by a rotamer model (Laws et al. and Ross et al., *Biochemistry*, in press). We have examined the fluorescence decay kinetics of similar single tryptophan systems, including [2-Trp]oxytocin and cyclo(-D-Trp-Pro-Gly-D-Ala-Pro-). Ground-state distributions of the various tryptophan side-chain rotamers have been calculated from 1 H-NMR coupling constants. The results of the rotamer model analysis will be compared with other kinetic models for the decay of tryptophan fluorescence.

T-Pos247 FLUORESCENCE DECAY STUDIES OF MUTANT AND WILD TYPE FORMS OF STAPHYLOCOCCAL NUCLEASE. J. Rudzki, J. Beechem, A. Kimball, D. Implicito, A. Chun and L. Brand. Department of Biology, The Johns Hopkins University, Baltimore, MD 21218.

Staphylococcal nuclease consists of a single polypeptide chain with 149 amino acid residues and no disulfide bridges. Its lone tryptophan (Trp 140) is surrounded, in part, by two lysine residues (Lys 110 and 133) and a glutamic acid residue (Glu 129). Shortle (Shortle, *Gene* (1983), 22, 181; Shortle and Lin, *Genetics* (1985), 110, 539) has cloned the gene encoding nuclease from *Staphylococcus aureus* and developed a plasmid-based genetic system utilizing *Escherichia coli* as the host cell. Wild type nuclease derived from *E. coli*, as well as single-site mutants of nuclease, were studied in 25 mM phosphate, 0.1 M NaCl pH 7.0 at 24 °C. Tryptophan fluorescence resulting from photoexcitation at 295 nm was monitored by time-correlated single photon counting, and analyzed as a sum of exponentials. Wild type nuclease exhibits biexponential fluorescence with lifetimes τ_1 = 4.5 ns (α_1 = 0.60) and τ_2 = 6.5 ns (α_2 = 0.40). Mutant K133T, in which threonine replaces Lys 133, shows biexponential behavior as well, with τ_1 = 3.3 ns (α_1 = 0.55) and τ_2 = 6.1 ns (α_2 = 0.45). In contrast, mutant E129K (Glu 129 replaced by lysine) exhibits an altered UV-absorbance spectrum and triexponential fluorescence kinetics: τ_1 = 3.1 ns (α_1 = 0.41), τ_2 = 5.9 ns (α_2 = 0.36) and τ_3 = 0.5 ns (α_3 = 0.23). A mutant (R87C) in which a cysteine replaces Arg 87 at the active site of the enzyme, away from the Trp 140 residue, shows fluorescence behavior very similar to that of the wild type protein (τ_1 = 4.6 ns (α_1 = 0.62), τ_2 = 6.6 ns (α_2 = 0.38)). Interpretation of these data in terms of single tryptophan proteins will be presented. Supported by NIH grant No. GM11632.

T-Pos248 FLUORESCENCE DEPOLARIZATION OF PROTEIN-DYE CONJUGATES. EXCITATION WAVELENGTH DEPENDENCE OF PERRIN PLOTS. D.L. VanderMeulen, Baylor Research Foundation, Dallas, TX 75246; B.W. VanderMeer, V. Thomas and D.M. Jameson, Dept. of Pharmacology, UTHSCD, Dallas, TX 75235

The intrinsic polarization, P_0 , for a fluorophore is usually wavelength dependent; excitation into the lowest energy absorption band typically yields high (positive) values of P_0 . Most studies on protein hydrodynamics utilizing polarization techniques have involved excitation wavelengths which give rise to high positive P_0 values. To detect anisotropic rotations we have studied the polarization of various protein-dye complexes, while varying temperature and solvent viscosity using wavelengths corresponding to both positive and negative P_0 values. Our studies include multifrequency phase lifetime data and steady-state polarizations on conjugates of eosin and fluorescein with a number of protein systems including skeletal muscle myosin, pig heart mitochondrial malate dehydrogenase, bovine serum albumin and lysozyme. A striking observation in protein-dye conjugates is that increasing solvent viscosity leads to increasing polarization (less negative) values, regardless of whether the starting P values are positive or negative. Fluorophores free in solution do not show this anomalous behavior in the negative polarization regime, suggesting that asymmetries of rotation about protein-dye bonds are important. These results are interpreted in terms of rotator models which take into account limited local rotation of the dye about one or two directions in addition to the global rotation of the protein. Our experimental and modeling studies extend previous work in this area (e.g., Witholt and Brand, *Biochem. J.* 2, 1948 (1970)). Supported by NIH grant 5R01 HL 26881 (DVM) and NSF grant PCM-8402663 (DMJ)

T-Pos249 TIME RESOLVED TRYPTOPHAN FLUORESCENCE OF M13 COAT PROTEIN. Iain Johnson, Lynn Thomason and Bruce Hudson. Department of Chemistry & Institute of Molecular Biology, University of Oregon, Eugene, OR 97403.

Several recent investigations have demonstrated the utility of time resolved fluorescence measurements for examining the influence of membrane proteins on lipid bilayer dynamics. The converse application is described here. The total fluorescence decays of M13 coat protein Trp-26 in deoxycholate (DOC) micelles and phospholipid bilayers (DMPC) are rather similar ($\langle \tau \rangle = 4.1$ ns and 3.9 ns respectively) and the steady state fluorescence spectra are identical. Fluorescence anisotropy decays in the two hydrophobic environments monitor different aspects of rotational diffusion behavior. In DOC micelles, Trp-26 has little internal flexibility (concurring with NMR measurements) and the principal rotational correlation time is compatible with whole body rotation of the micelle. The corresponding motion for DMPC proteoliposomes is too slow to cause fluorescence depolarization. Two resolved decay components are observed, presumably reflecting slow internal reorientation of Trp-26, with correlation times of around 2 ns and 100 ns. Both show discontinuities of rate (but not of amplitude) in the vicinity of the lipid phase transition. Possible interpretations of these motions will be discussed.

T-Pos250 HEAVY ATOM EFFECTS ON ENERGY TRANSFER IN POLYNUCLEOTIDES. V.W. Burns, Dept. Physiological Sciences, University of California Davis, CA.

Using the fluorophore Tb^{3+} as a reporter, the effect of thallium on transfer of energy in polynucleotides at room temperature in solution has been studied. In certain polynucleotides- $p(G)$, $p(G,I)$, $pd(G)_6$ - thallium greatly increases the transfer of UV energy absorbed by the bases to Tb^{3+} . In the cases of DNA, $p(G,U)$, $p(G,A)$, $p(A,U)$, $P(X)$, $p(A)$, $p(U)$, $P(I)$, $pd(G,A)_6$, and $pd(G,T)_5$ there is little or no effect of thallium. It is known that overlap of excited triplets of bases with the excited singlet state of Tb^{3+} permits energy transfer. The effects of thallium can be explained using the Medinger-Wilkinson theory of heavy atom quenching of excited singlet states to excited triplet states (1). On this basis thallium increases intersystem crossing, but this occurs only in the three G containing polynucleotides. In those G and X containing polynucleotides showing little thallium effect the evidence suggests that intersystem crossing is comparatively high to begin with. These polynucleotides, including DNA, appear to transfer absorbed energy to triplet states efficiently at room temperature.

1. V.W. Burns (1985), *Biopolymers* 24, 1293-1300.

T-Pos251 NITROTYROSINE RESIDUES IN A SOLUBLE TYPE I COLLAGEN. Robert L. Karvonen, Diane M. Sasaki, Felix R. Fernandez-Madrid, and Mauricio A. Lande. (Intr. by Lana Lee) A soluble nitrotyrosyl derivative of rabbit type I scleral collagen was produced with tetranitromethane in the presence of guanidine-HCl with a 57% yield of alpha-chains. Some intermolecular crosslinking had occurred during nitration indicated by an increased amount of soluble, high molecular weight aggregates. An average of five tyrosyl residues per molecule of non-crosslinked monomeric collagen were nitrated based on amino acid composition. A comparison of the spectral titrations of nitrated and unmodified alpha-chains in the presence of guanidine-HCl, produced an absorbance maximum at 428 nm under alkaline conditions, at 360 nm under acidic conditions, and an isosbestic point at 381 nm. This spectrum is consistent with the presence of free phenolic hydroxyl groups on the nitrotyrosyl moiety. The maximum molar extinction coefficients for the nitrotyrosine residues in the monomeric alpha chains of collagen at 360 nm, 381 nm, and 428 nm, were 4430, 3740, and 6360 $M^{-1}cm^{-1}$, respectively. A pK value of 6.7 for the collagen nitrotyrosine was calculated from the titration at 428 nm. Since the telopeptide regions, believed to be important in fibrillogenesis, are the only tyrosine containing regions in the collagen, the nitrotyrosine chromophore may serve as a reporter group for microenvironmental changes in that region.

T-Pos252 SECONDARY STRUCTURE OF HALORHODOPSIN

Bing K. Jap and S.-H. Kong, (Intr. by Kenneth H. Downing) Donner Laboratory, Lawrence Berkeley Laboratory, University of California, Berkeley, CA 94720

Ultraviolet circular dichroism (CD) spectra of halorhodopsin (hR), a light-driven chloride pump from *Halobacterium halobium*, has been obtained in the interval from 190 to 240 nm. The resulting CD spectrum of hR in octylglucoside was fitted with standard basis functions yielding an α helical content of about 50% and a β structure content of about 30%. The CD spectrum is unaffected by the presence or absence of chloride ions and by the ionic strength of the medium. The CD spectrum of hR is very similar to that of octylglucoside-solubilized bacteriorhodopsin, a light-driven "proton" pump from the same bacteria. This indicates that these two light-driven ion pumps have nearly identical fractions of α and β secondary structure. Similarity in the structures surrounding the retinal of these pumps has also been suggested by resonance Raman spectroscopy study¹. The result reported here is consistent with, but does not prove, the hypothesis that the folding of these two pumps is similar. If a similarity in the detailed molecular structures does indeed exist, these pumps may share a common mechanism of ion transport.

¹Smith, S.O., Marvin, M.J., Bogomolni, R.A. and Mathies, R.A. (1984). J. Biol. Chem. 259, 12326-12329.

T-Pos253 OPTICAL ACTIVITY OF ALPHA-HELICAL PROTEINS: A CRITICAL COMPARISON OF EXPERIMENT AND THEORY. N.J. Gibson and J.Y. Cassim, Department of Microbiology and Program in Biophysics, The Ohio State University, Columbus, Ohio 43210

Quantum theories have been proposed to explain the prominent amide electronic optical activity of α -helical proteins*. Although attempts have been made in the past to confirm experimentally the predictions of these theories, the results were never entirely convincing. Since the optical activity of the helix depends on the orientation of the helix relative to the direction of the incident light propagation, critical comparison of experiment and theory are only possible if the optical activity of the helix can be measured with the incident light oriented parallel and perpendicular to the helical axis. Solution of this formidable technical problem, which has eluded researchers for many years, has now been achieved in this laboratory. The oriented and randomized spectra are related by $\Theta_{\perp} = \frac{1}{2}[3\langle\Theta\rangle - \Theta_{\parallel}]$, where Θ_{\perp} , $\langle\Theta\rangle$ and Θ_{\parallel} are the amide ellipticities when the incident light is oriented perpendicular, random and parallel to the helical axes, respectively. We have measured $\langle\Theta\rangle$ and Θ_{\parallel} under the same conditions from 183 to 250 nm by utilizing films of the purple membrane of *Halobacterium halobium*. This membrane contains a single protein, bacteriorhodopsin, which is highly α -helical and whose helical segments are oriented nearly perpendicular to the membrane plane. By orienting the membrane plane perpendicular to the incident light in a film, Θ_{\parallel} is obtained. By treating the same film with ethanol, without changing the protein secondary structure or the film thickness, $\langle\Theta\rangle$ is obtained. Analysis of these spectra provide excellent confirmation of the predictions of theory in regards to the positions and polarizations of the rotatory bands.

* For an excellent review see Sears, D.W. and S. Beychok (1973). In Physical Principles and Techniques of Protein Chemistry. S.S. Leach, editor. Academic Press, New York. Part C. pp. 446-593.

T-Pos254 CD AND EPR STUDIES OF CU(II)-THIOETHER LIGATIONS OF CU(II)-CYCLO(L-METHIONYL-L-HISTIDYL) COMPLEXES. Shigeo Kubota, Jen Tsi Yang and Mark S. Crowder*. Cardiovascular Res. Inst. Univ. of Calif., San Francisco, CA 94143 and *IBM, San Jose, CA 95110.

Cu(II)-thioether ligations in the Cu(II)-c(Met-His) complexes are relevant to the Cu(II)(type 1) active center of plastocyanins and azurins with a Cu(II)N₂(His)S(Cys)S*(Met) set. The CD spectra of a 1:4 [Cu(II)]-c[c(Met-His)] solution in 0.1 M NaCl at pH 7.8-8.1 showed a positive band at 415 nm and a shoulder near 470 nm with $[\theta]_{\text{Cu}} = 70$ and 29 deg cm²/dmol, respectively. The solution of the complexes became turbid between pH 8.2 and 11.9 but clear again at higher pHs. For a solution at pH 12.1 the positive CD band turned into a negative shoulder and the positive shoulder red-shifted by about 10 nm; the corresponding $[\theta]_{\text{Cu}}$ at 430 and 480 was -190 and 35 deg cm²/dmol, respectively. In aqueous 80% methanol at pH(apparent) 7.9 the CD spectrum had an enhanced positive band and a weak shoulder with $[\theta]_{\text{Cu}} = 250$ and 20 deg cm²/dmol at 400 and 470 respectively. These spectral features were unaffected by the use of excess peptide, e.g. [c(Met-His)]/[Cu(II)] varied from 2 to 10. The two bands might be assigned to $\sigma(\text{S}^*)\rightarrow\text{Cu(II)}$ LMCT bands because they were not observed for parent Cu(II)-c(His-His) complexes at various pHs [Kubota and Yang (1984) Proc. Natl. Acad. Sci. USA 81: 3283-3286]. EPR spectra of these complexes indicated that at most two N atoms, probably from histidyl imidazoles, could be associated with a Cu(II) ion regardless of the molar peptide/metal ratios used. We propose that the complex has a Cu(II)N₂(His)S*X_n set at pH 8, where X is exogenous ligands and n either 1 or 2. Further, one Cu(II)-S* bonding would be equatorial with a CD band at 415 nm and the other apical with a lower energy band at 470 nm. Supported by USPHS Grant GM-10880.

T-Pos255 A DOUBLE-STRANDED SECONDARY STRUCTURE FOR HYALURONIC ACID IN AQUEOUS-ORGANIC SOLVENT AS REVEALED BY VACUUM UV CIRCULAR DICHROISM

Paul W. Staskus and W. Curtis Johnson, Jr. Dept. Biochem. & Biophys., OSU, Corvallis, OR 97331

The self-association of oligo hyaluronic acid has been investigated by means of circular dichroism (CD) spectroscopy in the vacuum ultraviolet region. Oligomers of hyaluronate were produced by limited digestion of polymer with bovine testicular hyaluronidase and separated by gel exclusion chromatography. CD spectra were recorded for the polymer and some oligomers in a solvent system similar to that which accentuates the elastic character of hyaluronic acid. Integrity of sample materials during this investigation was assessed by electrophoresis on polyacrylamide gels.

At about 2mM concentration of repeating disaccharide, oligomers longer than eight disaccharides exhibit a chain-length sensitivity to the difference in CD between aqueous and aqueous-organic solvent. This is most pronounced in the energy region assigned to $\pi\text{-}\pi^*$ transitions of the hyaluronic acid chromophores. The CD of oligomers from twelve to sixteen disaccharides in length is quite sensitive to sample concentration, representing clear spectroscopic evidence of molecular association for hyaluronic acid in aqueous-organic solvent. Sets of CD spectra recorded as a function of sample concentration or solvent composition at a given temperature can be fit within the noise level of the data by two basis spectra. Assuming two environments for sample chromophores, data recorded as a function of sample concentration, temperature and oligomeric chain length are most simply modeled by a cooperative association of two strands of hyaluronic acid.

T-Pos256 EVALUATION OF APPROXIMATIONS IN MOLECULAR EXCITON THEORY WITH APPLICATIONS TO PHOTOSYNTHETIC SYSTEMS, D. E. LaLonde, J. D. Petke & G. M. Maggiora*, Depts. of Chemistry and Biochemistry, University of Kansas, Lawrence, KS 66045.

The singlet electronic states and spectra of one-dimensional arrays of "stacked" bacteriochlorin (BC) and methyl bacteriochlorophyllide a (MeBPh) molecules have been computed within the framework of molecular exciton theory. The exciton treatment features the inclusion of up to ten excited singlet states in each monomer, covering both the visible and Soret bands. Exciton matrix elements were evaluated using dipole-moment conserving point-charge representations of quantum mechanically derived state and transition densities, as opposed to the usual dipole approximation. The calculated red shifts of the Q_y band range from 300-350 cm⁻¹ in dimeric to 800-850 cm⁻¹ in octameric systems depending on the number and type of approximations employed. Moreover, the shifts were shown to arise principally from excitonic interactions among monomer Q states, with insignificant interactions from Soret states. Additional studies of two- and three-dimensional arrays of BC molecules produced only small changes from the shifts obtained in the one-dimensional case. The Q_y band of MeBPh crystals is red shifted ca. 1600 cm⁻¹ relative to the Q_y band of monomeric MeBPh. Thus, while the present calculations can account for a number of specific intermolecular effects, the computed red shift is little more than half that observed experimentally. More sophisticated quantum mechanical treatments are currently being employed to help elucidate the nature of the deficiencies inherent in the exciton approach.

*Present address: The Upjohn Company, Kalamazoo, MI 49001.

T-Pos257 LUMINESCENCE STUDIES OF LANTHANIDE - ONCOMODULIN COMPLEXES. Michael T. Henzl, Raymond C. Hapak and Edward R. Birnbaum, Department of Chemistry, New Mexico State University, Las Cruces, NM 88003.

Oncomodulin, a parvalbumin-like calcium-binding protein, was studied using the luminescent lanthanide ions Eu^{3+} and Tb^{3+} . As with parvalbumin, these ions bind with great avidity, displacing bound Ca^{2+} ions. Titrations indicated the presence of two high-affinity binding sites for lanthanide ions. The laser-induced $F_0 \rightarrow {}^5D_0$ excitation spectrum of oncomodulin-bound Eu^{3+} ion was also obtained. At pH 5.5, the spectrum of the fully-bound protein consists of a single peak centered at 5796Å, having a linewidth of ~6Å. At higher pH, this spectrum is replaced by a broad, symmetrical peak centered at 5782Å. This behavior is quite similar to that observed with pike parvalbumin III, further evidence for the close relationship between the two proteins.

T-Pos258 QUANTITATION OF RADIATION INDUCED OXYGEN-RADICAL PRODUCTION IN POLYMORPHONUCLEAR LEUKOCYTES; AN IN VITRO STUDY. Andrea E. Lunsford, K.F. McCarthy and C.E. Swenberg; Armed Forces Radiobiology Research Institute, Bethesda, Maryland 20814-5145.

Quantitation of radiation induced reactive oxygen derivatives such as the hydroxyl radical is difficult to achieve within cellular matrices for a number of reasons (e.g. a large variety of solutes are present in the cytosol to react with the radicals). In the last several years a fluorogenic compound, 2',7'-dichlorofluorescein diacetate (DCFH-DA) has been successfully employed, in combination with flow cytometric methods, to evaluate the amount of H_2O_2 produced by phagocytizing and agent-stimulated polymorphonuclear leukocytes (PMNL). We have adapted this technique to evaluate the amount of reactive oxygen derivatives produced in PMNL in response to Co-60 gamma irradiation. PMNL isolated from canine blood were incubated with DCFH-DA, a nonpolar compound which readily diffuses through the cellular membrane. The absorbed DCFH-DA is consequently deacetylated by cellular enzymes, but remains nonfluorescent unless exposed to oxidizing compounds. Oxidation generates dichlorofluorescein (*DCF), a highly fluorescent compound ($\text{Ex } \lambda = 485\text{nm}$, $\text{Em } \lambda = 525\text{nm}$). In this study relative fluorescence intensity was monitored on a FACS II (Becton-Dickinson) cell sorter equipped with a 4-watt argon laser excitation source (488nm emission, 530nm bandpass filter, PMT at 450V). Fluorescence was monitored over a 30 min. interval for resting (control) PMNL and for PMNL stimulated with: 1) H_2O_2 (25, 50, 100 μM), 2) phorbol myristate acetate (100 nm/ml) and 3) varying doses of Co-60 gamma radiation (100, 200, 500 rads). The increase in fluorescence with time ($\text{amole } *DCF/\text{cell}/\text{min.}$) is directly proportional to the number of oxidizing agents produced within the cytosol per unit time.

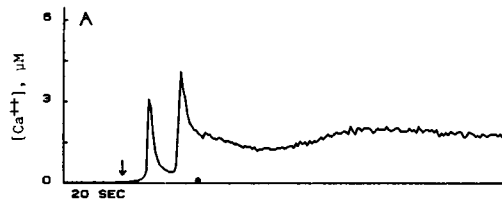
T-Pos259 MICROENVIRONMENT OF MEMBRANE-BOUND PENTACHLOROPHENOL. P. Smejtek, W. Barstad and K. Hsu, Environmental Sciences and Resources/Physics Program, Portland State University, Portland, Oregon 97207.

Pentachlorophenol (PCP) changes biophysical properties of membranes such as surface and interfacial potentials, and induces electrical conductivity associated with transmembrane translocation of protons. We present results of UV absorption studies of the neutral (HA) and ionized (A^-) forms of PCP in solvents of differing dielectric constant and hydrogen bonding ability and of the adsorbed PCP on phosphatidylcholine and phosphatidylglycerol liposomes to find how the membrane microenvironment changes physical properties of PCP. The solvent effects on the 305 nm band of HA are negligible compared to those on the 320-330 nm band of A^- . The increase of dielectric constant induces red shift, whereas hydrogen bonding causes blue shift of the UV absorption band of A^- . The spectrum of A^- adsorbed on PC liposomes resembles that of A^- in octanol--a membrane model solvent, and that for PG liposomes is comparable to A^- in methanol. The presence of negative charge on PG causes the blue shift, indicating hydrogen bonding of A^- . Using UV spectral titration we have found the pK_a 's of membrane bound PCP to be 5.9 and 6.9 on PC and PG, respectively, whereas the aqueous pK_a is only 4.8. Thus PCP bound to membrane acts as a much weaker acid. This finding is consistent with the pH shifts of conductivity maxima observed earlier on PC and PG membranes.* The ionization pH shift explains in part why PCP is such an effective xenobiotic, since both the HA and A^- forms must be present in membranes in order to effect maximum proton translocation. Supported by NIH grant 5R01 ES00937-11.

*P. Smejtek, K. Hsu and W. H. Perman, Biophys. J. 16:319, 1976.

T-Pos260 $[Ca^{++}]_i$ CHANGES IN SINGLE RAT PERITONEAL MAST CELLS MEASURED WITH THE FLUORESCENT Ca INDICATOR FURA-2. W. Almers & E. Neher, Max Planck Inst. f. biophysikal. Chemie, 3400 Göttingen, FRG.

When mast cells encounter antigen, they release histamine and other mediators in an explosive episode of exocytosis, called degranulation. Degranulation is thought to be accompanied, and perhaps triggered by, an increase in cytoplasmic $[Ca^{++}]$, $[Ca^{++}]_i$. We determined $[Ca^{++}]_i$ from the ratio of fluorescence intensities observed (Grynkiewicz et al., JBC 260, 3440) when single, fura-2 loaded mast cells were illuminated alternately with 350-360 and 390 nm light. First, cells were loaded by incubation with membrane-impermeant fura-2 ester. The dye reported an apparent $[Ca^{++}]_i$ of 250 ± 34 nM (SEM, $n=25$). During antigen-simulated degranulation, $[Ca^{++}]$ seemed to change little, but half the fluorescence at both wavelengths was lost, as if half the dye had accumulated in the secretory granules and was lost during exocytosis. Next, the membrane-impermeant fura-2 salt was loaded into the cytoplasm through the orifice of a patch pipette. After the pipette was removed, the dye reported $[Ca^{++}]_i = 155 \pm 16$ nM ($n=33$). On adding antigen (arrow in fig.) or 48/80, we saw only transient fluorescence changes that indicated one or more large, transient increases in $[Ca^{++}]_i$ preceding degranulation. (Degranulation started at the dot in fig.) Ca transients and degranulation could be elicited also in Ca-free external solutions. Evidently mast cells have internal stores that can release Ca when antigen binds to the cell membrane.



T-Pos261 EFFECTS OF A CALMODULIN INHIBITOR (W-7) AND CYCLIC NUCLEOTIDES ON ELECTRICAL UNCOUPLING OF CRAYFISH SEPTATE AXONS. Camillo Peracchia, Department of Physiology, University of Rochester, Rochester, NY 14642

Calmodulin(CaM)-like proteins may be involved in the regulation of cell-to-cell channel permeability. This hypothesis is based on evidence for CaM binding to the lens, liver and crayfish gap junction proteins, in gel overlay experiments, and on data showing the inhibitory effect of CaM blockers such as TFP and calmidazolium on CO₂-induced uncoupling in Amphibian embryos (Peracchia and Girsch, Am. J. Physiol. 248, H765, 1985). To test the effects of CaM inhibitors on coupling regulation in a two cell system where both the junctional (R_j) and surface membrane (R_{m1} , R_{m2}) resistances can be measured independently, four microelectrodes were inserted into a crayfish septate axon, two on each side of the septum. Hyperpolarizing current pulses (150 nA) were injected alternatively in the caudal (C_1) and rostral (C_2) segment of the lateral giant axon and the resulting electrotonic potentials (V_1 , V_2 , V_{1*} and V_{2*}) were recorded and measured to calculate R_{j1} , R_{j2} , R_{m1} and R_{m2} (Bennett, Ann N.Y. Acad. Sci., 137, 509, 1966). The axons were uncoupled at regular intervals by superfusing them with acetate containing saline solution (pH 6.3) in the presence or absence of W-7 (50-100 μM), a CaM-inhibitor, or as a control its non-chlorinated form (W-5). W-7 strongly inhibits the acetate-induced increase in junctional resistance while W-5 is ineffective. The uncoupling inhibition is reversible only after short exposures to W-7. Uncoupling inhibition does not seem to be caused by an increase in cAMP or cGMP concentration, because exposures to db-cAMP or db-cGMP (up to 1 mM) influence neither basic values of R_j nor their changes with acetate. Supported by NIH GM20113.

T-Pos262 Novel Effects of Ca²⁺ Ionophores and Cyclosporin A in Human Lymphocytes. L. TRON, S. DAMJANOVICH and A. SZALOS*. Department of Biophysics, Medical School of Debrecen, Debrecen, Hungary and *Department of Drug Biology, Food and Drug Administration, Washington, D.C. 20204. We have recently found that ionomycin, in the range of 2 to 8 μg/ml depolarizes the plasma membrane of human lymphocytes. This membrane depolarization occurs in a dose dependent manner and parallels the dose dependent influx of Ca²⁺ as measured with Indo-1 (cell permeable) the Ca²⁺ specific fluorescence indicator. The plasma depolarization is due to the K⁺ efflux, which also occurred in a dose dependent manner and was monitored by ⁴²K⁺ efflux measurements according to the technique of Segal and Lichtman (Exp. Cell Res. 112, 95, 1978). The same general phenomena were shown to occur when human lymphocytes were treated with the other Ca²⁺ ionophore A23187, in the dose range of 0.5 to 5 μg/ml cell suspension and with the immunosuppressive agent cyclosporin A in the dose range of 0.5 to 40 μg/ml cell suspension. Valinomycin was used as the control for membrane depolarization and ⁴²K⁺ efflux measurements. We have concluded that ionomycin, A23187 and cyclosporin A simultaneously affect K⁺ efflux and Ca²⁺ influx in human lymphocytes.

T-Pos263 HEALING-OVER PROCESS IN HEART. INTERACTION BETWEEN Ca AND PROTONS. Walmor C. De Mello, Department of Pharmacology, Medical Sciences Campus, UPR, GPO Box 5067, San Juan, P. R. 00936.

The injury potential caused by damage of cardiac muscle soon vanishes (healing-over) because a high resistance barrier is established near lesion. Ca, which is essential for the sealing process (De Mello et al., 1969), diffuses through the cut-end and decreases the junctional conductance. Protons also interact with gap junctional molecules and promotes sealing, but only if pH₀ is 5.5 or lower (De Mello, 1983). Studies of the interaction between Ca and protons on the sealing process indicate that when acidity (pH₀ - 6) is produced: a) protons compete with Ca for the binding sites; b) the Hill coefficient for protons is 0.66 while for Ca is 1; c) the results are compatible with a model in which each binding site has two sub-sites. Ca interacts with both sub-sites and promotes healing-over. Protons also interact with both sub-sites but one of them has a greater affinity for H ions than the other. In order to promote sealing protons must occupy both sub-sites (pH₀ - 5.5 or lower).

(Supported by Grant HL-34353 from NIH.)

T-Pos264 AGGREGATION KINETICS OF ANTIBODY COATED SPLEEN CELLS WITH P388D1 MACROPHAGES

D.G. Covell, D. Segal (Intr. by Sanzo Miyazawa). NIH, Bethesda, MD 20892

Communication between cells is thought to involve interactions between complementary pairs of adhesive molecules at the cell:cell interface. Biological processes where such interactions are essential include fertilization, differentiation, phagocytosis and cytolysis. Kinetic models have been developed to examine the formation of cellular aggregates, called conjugates, composed of a central macrophage with known surface density of Fc receptors surrounded by IgG-coated spleen cells. The models were tested against experimental data obtained using flow cytometry (Segal, et al. J Immunology 132(4):1924, 1984) where the surface densities of Fc receptors on macrophages and IgG antibodies on spleen cells were varied. The forward rate constant, K, for the model of bimolecular collisions between heterophilic particles is decomposed into elemental processes that include as parameters; 1) the collision rate, R, of particles falling under 1 G in a closed rotating chamber and 2) the probability, P, that each collision results in a successful attachment of a spleen cell and a macrophage. The net rate constant, K, is found to be independent of cell density. The collision rate, R, is found to be a nonlinear function of particle size and speed of rotation of the mixing chamber. The probability of sticking, P, is found to be a nonlinear function of the surface density of complementary bridging molecules. Comparisons between the proposed model and the experimental data indicate that a) a maximum of three spleen cells can bind to a macrophage and b) Populations of macrophages and spleen cells are heterogenous with respect to their ability to attach to one another. Our results suggest that ten percent of the total cell population cannot form stable aggregates.

T-Pos265 ADSORPTION OF AMINOPYRIDINES TO PHOSPHATIDYL SERINE MEMBRANES. P. Smejtek*, W.K. Riker**, A. Oxyzoglou**, C. Wright* and M. Bennett#, *Dept. of Physics, Portland State University, **Dept. of Pharmacology, #Dept. of Anesthesiology, Oregon Health Sciences University, Portland, Oregon.

Aminopyridines are membrane active compounds known to enhance synaptic transmission. Matsumoto and Riker (1) studied calcium dependence of compound action potential in isolated frog sympathetic ganglia and found that aminopyridines could restore transmission at low calcium concentrations. We have studied adsorption of aminopyridines, calcium, and several cations to phosphatidylserine vesicles at pH 7.2 by means of electrophoretic determination of zeta potentials. Our results for calcium and monovalent cations agreed with published data (2). We found the association constant of 3,4-diaminopyridine (3,4-DAP) and 4-aminopyridine (4-AP) to be 5 and 3 l/M, respectively. Thus the strength of their binding is less, but comparable to calcium, which is about 10 l/M. The effect of 3-aminopyridine (3-AP) on zeta potential of PS vesicles was small even though the negatively charged PS surface could significantly enhance 3-AP ionization. The ability of aminopyridines to restore synaptic transmission decreases as follows: 3,4-DAP > 4-AP > 3-AP, which is in the same order as the sequence of PS-membrane association constants. The data suggest that 3,4-DAP and 4-AP can effectively depolarize the negatively charged membrane and facilitate entry of calcium into the prejunctional nerve terminal. Supported by NIH grant 5R01 ES00937-11.

(1) M. Matsumoto and W.K. Riker, J. Pharmacol. Exp. Theor. 228:573, 1984, (2) M. Eisenberg, T. Gresalfi, T. Riccio and S. McLaughlin, Biochemistry 18:5213, 1979, and S. McLaughlin, N. Mulrine, T. Gresalfi, G. Vaio and A. McLaughlin, J. Gen. Physiol. 77:445, 1981.

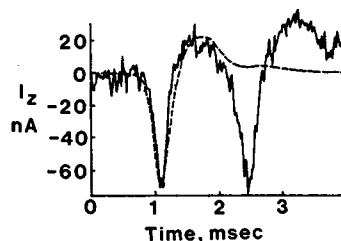
T-Pos266 MODULATION OF CELL-TO-CELL COUPLING BY cAMP IN MOUSE ISLETS OF LANGERHANS

R. M. Santos, P. Meda and E. Rojas LCB&G, N.I.H., Bethesda

Cellular levels of cAMP are mainly controlled by the activity of the membrane bound enzyme adenylate cyclase and the cytosolic enzyme phosphodiesterase. Glucose-induced B-cell electrical activity and insulin release from mouse islets of Langerhans are potentiated by application of stimulators of adenylate cyclase such as forskolin. Using the fluorescent dye lucifer yellow to mark impaled cells responding to 11 mM glucose with a burst pattern of electrical activity, and a rhodamine conjugated fluorescent antibody against either insulin, glucagon, somatostatin or pancreatic polypeptide to identify the cell type, we have confirmed B-cell-to-B-cell dye coupling in microdissected mouse islets of Langerhans. Using two microelectrodes, one to inject current (i) (response V_1) and the other to probe electrical coupling (response V_2) we studied the effects of forskolin on V_1 and on the coupling ratio V_2/V_1 . In presence of a substimulatory concentration of glucose (7 mM), 5 μ M forskolin induced a transient depolarization of the membrane and the appearance of a bursting electrical activity. In presence of 11 mM glucose, 5 μ M forskolin stimulated electrical activity. B-cell input resistance (V_1/i) was found to decrease by an average 12% in both instances, a 10% increase in coupling ratio V_2/V_1 being detected when forskolin was applied in the presence of 11 mM glucose. These results suggest that B-cell-to-B-cell coupling is enhanced in presence of an elevated cytosolic cAMP level.

T-Pos267 ACTION CURRENT PROPAGATION ACROSS AN ELECTRICAL SYNAPSE: MAGNETIC MEASUREMENTS ON A SEPTATED EARTHWORM AXON. F. Gielen¹, B. Roth¹, J. Wikswo¹ and P. Brink². ¹Dept. of Physics & Astr., Vanderbilt U., Nashville, TN. ²Dept. Anatomical Sciences, SUNY at Stony Brook.

A segment of the medial axon between two septa was visualized by microelectrode injection of a fluorescein dye. The axial, intracellular action current was determined by measuring the associated magnetic field using a toroid, and the transmembrane action potential was recorded with the microelectrode. The figure shows the action current from first the medial and later the two lateral axons. By treating the axon as if it was uniform along its length, we can use a volume conductor model to calculate an average axial current from the transmembrane potential. The amplitudes of the calculated (dashed) and measured (solid) curves match when the effective internal resistivity is $111 \pm 30 \Omega \text{cm}$. We searched for perturbations in the axial current associated with the septa by scanning the toroid along the axis of the nerve. Using a 0.7 mm wide toroid, we can say that changes in the amplitude of the axial current were less than $\pm 15\%$, and septal propagation delay, averaged over the toroid width, was less than 20 μ s. However, since the septal spacing was only 40% greater than the width of the toroid, narrower and quieter toroids will be required before definitive statements can be made regarding the effect of septa on propagation of the action potential. The accurate fit of the model and the absence of detected axial variation suggest that the action current passes directly through the septa without significant perturbation.

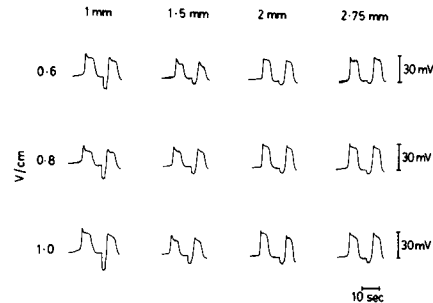
**T-Pos268** KINETIC PROPERTIES OF THE CRAYFISH RECTIFYING ELECTROTONIC SYNAPSE UNDER VOLTAGE-CLAMP CONTROL. Stewart W. Jaslove and Peter R. Brink, Department of Anatomical Sciences, HSC, SUNY at Stony Brook, Long Island, New York 11794.

The motor giant synapse of the crayfish abdominal nerve cord is composed of morphologically typical gap-junctional channels with the unusual ability to rectify current flow peripherally. Using the double-voltage-clamp and intracellular perfusion techniques we have previously found that the rectification depends only on transjunctional potential; steady-state synaptic conductance varying from about 0.1 μ S when the postsynaptic side is depolarized to about 10 μ S when hyperpolarized (Jaslove and Brink, *J. Gen. Physiol.* 86:17a, 1985). We can now show that when measured "instantaneously" the I/V relation approaches linearity and that new steady-state conductance levels are approached with at least two exponential time constants. The fast time constant is strongly temperature dependent ($Q_{10} \sim 15$), being 5-10 msec at 10°C and <5 msec at 20°C. This time constant does not appear to be strongly voltage dependent. The long time constant is 100-1000 msec at 10°C. Possible faster kinetic components on the order of .2 msec duration (such as a sigmoidal onset of activation) have not yet been resolved. Kinetics gradually disappear during the course of an experiment (up to 3 hr.), leaving the synapse symmetrically conducting; a wash-out of axoplasmic gating intermediates by perfusion may be involved. [Supported by NIH grants 24905 and 31299.]

T-Pos269 ELECTROTTONIC CURRENT SPREAD IN THE CIRCULAR MUSCLE LAYER OF THE DOG COLON.

J.D. Huizinga and E. Chow. McMaster University, Dept. of Neurosciences, Intestinal Disease Research Unit, Hamilton, Ontario, Canada.

Asynchrony of motor events at adjacent sites of the human colon is a characteristic of its basal motor activity. This could be due to poor electrical coupling between muscle cells. We studied therefore the passive electrical properties of the colon. Electrottonic current pulses were applied using an Abe-Tomita type stimulation bath. Spread of current was measured with microelectrodes at different distances from the site of current injection. Current spread was measured along the long axis of the circular muscle cells and in the direction perpendicular to it. The space constant was measured with different stimulus intensities. 24 series of measurements were performed in 8 muscle preparations. The space constant and time constant along the long axis of the muscle cells were 2.15 ± 0.39 mm and 164 ± 23 sec respectively. Current spread across the circular muscle cells was poor, even with underlying longitudinal muscle, with estimated space and time constants of 0.43 ± 0.15 mm and 304 ± 49 sec respectively. These data suggest that synchrony of electrical activity in circumferential direction is facilitated by low resistance pathways. However, coupling of activity in the axial direction of the colon may rely on mechanisms other than low resistance pathways.



T-Pos270 A MODEL FOR THE LATERAL ORGANIZATION OF GAP JUNCTIONS. James R. Abney, Jochen Braun, and John C. Owicki, Department of Biophysics & Medical Physics, University of California, and Division of Biology and Medicine, Lawrence Berkeley Laboratory, University of California, Berkeley, CA 94720.

As we reported previously, forces between integral membrane proteins can be deduced from freeze-fracture electron micrographs [J.B., J.R.A., & J.C.O. (1984) *Nature* 310: 316]. For gap junctions in mouse liver, in which plaques of aggregated protein dyads bridge two apposed cell membranes, this analysis demonstrated purely repulsive lateral forces between dyads. These forces create a lateral pressure tending to minimize repulsive encounters between dyads by enlarging the junction. Since the dyads remain aggregated, we propose a model of gap junction structure based on a balance of lateral pressure between the junction and the surrounding extracellular space. The pressure from *inside* the junction arises entirely from interactions between dyads; this allows for its accurate determination

from experimental data: $\Pi/kT = \rho + (\rho^2/4kT) \int_0^\infty r f(r) g(r) 2\pi r dr$. Here Π is the lateral pressure, k Boltzmann's constant,

T the absolute temperature, ρ the number density of dyads, and $f(r)$ and $g(r)$ the interdyad pair force and radial distribution function, respectively. The balancing pressure from *outside* the junction arises primarily from the compression of the glycocalyx, and is modeled with mixing, elastic, and osmotic terms adapted from Flory-Krigbaum and McMillan-Mayer theories. This pressure fundamentally reflects repulsions between the closely apposed membranes. The inner and outer pressures agree well, which supports the pressure-balance model of the lateral structure of gap junctions. Supported by grants from N.I.H. (B.R.S.G.) and the U.C. Cancer Research Coordinating Committee.

T-Pos271 PERMEABILITY CHARACTERISTICS OF THE INTERCELLULAR CHANNEL OF THE GAP JUNCTION. P.R. Brink, S.W. Jaslove and D. Joseph. Department of Anatomical Sciences, HSC, SUNY at Stony Brook, New York 11794.

The permeability of the gap junction was measured for three fluorescent probes in the septate giant axon system of earthworm via the method of Brink and Ramanan (Biophys.J. 48:299-309, 1985). Dichlorofluorescein (2CLFL, $1.26 \times 1.23 \times 0.7$ nm), Fluorescein-5-maleimide (FL-M, $1.16 \times 1.35 \times 0.7$ nm) and Carboxyfluorescein (CFL, $1.16 \times 1.27 \times 0.7$ nm) were studied. 2CLFL and FL-M have only one charged carboxyl group at pH 7.0. CFL has two charged carboxyl groups one of which lies on the outer edge of the 1.27 nm dimension of the molecule. The critical dimension for transit through the intercellular channel is 1.23 nm for 2CLFL, 1.35 nm for FL-M and 1.27 nm for CFL. FL-M has a lower apparent junctional membrane permeability than 2CLFL (1.7×10^{-5} cm/s $n=5$ vs. 2×10^{-6} cm/s $n=5$). Based on size determinants CFL would be predicted to have a permeability in between 2CLFL and FL-M. But its permeability is even less than FL-M (8×10^{-6} cm/s $n=5$). This discrepancy is best explained by charge discrimination and hydration size due to solute charge. All three probes had cytoplasmic diffusion coefficients in the range of 5×10^{-7} cm²/s. The diffusion constants for the probes were unchanged with time. Because the cytoplasmic diffusion coefficients are the same and unchanged with time for all three probes the effects cannot be explained by ascribing different free pool concentrations to the three probes. Supported by NIH grant 24905.

T-Pos272 COMPARISON OF TWO FLUORESCENT DYE TRANSFER RATES THROUGH GAP JUNCTIONS IN NOVIKOFF HEPATOMA CELLS. R.P. BIEGON, M.M. ATKINSON AND J.D. SHERIDAN. Dept. of Anatomy, Univ. of Minnesota Med. Sch., Minneapolis, Mn. 55455. (Intr. by Hon-Cheung Lee).

We have developed a method to measure junctional permeance of fluorescent dyes in isolated pairs of cultured mammalian cells. A small volume of dye is microinjected into cell 1 of a pair and the subsequent transfer of dye to cell 2 is videotaped through a SIT camera. An Apple II+ computer equipped with a digisector board generates a best-fit line relating the log difference of dye concentration in cell 1 and cell 2 to the time elapsed since the end of the microinjection. Permeance—the product of the permeability coefficient P and the junctional area A —is derived from the slope of the line and the estimated cell volumes. Permeance for the dye Lucifer Yellow CH (LY, MW=457.2) ranges widely, from 0.08 to $26.7 \times 10^{-11} \text{ cm}^3/\text{sec}$. This range likely reflects variations in A (size of junctions) rather than in P ; however, our method cannot distinguish between differences in numbers of channels only and differences in cross-sectional area of individual open channels. To address more directly the question of channel heterogeneity, we coinjected a somewhat larger dye, lis-samine rhodamine B (LRB, MW=571) along with LY, i.e., in the same microelectrode. Transfer of the two dyes was monitored separately, by alternating the appropriate filter assemblies at predetermined times after microinjection. Permeance of LRB in Novikoff cells is, on average, one-eighth that of LY; variations in the ratios of the two permeances have been found and may signify channel heterogeneity from cell pair to cell pair. Furthermore, since LRB would not be expected to diffuse eight times slower than LY through cytoplasm-containing channels, there must be some retardation of LRB within the channels or total exclusion of LRB from some channels. Supported by CA 16335.

T-Pos273 MODULATION OF GAP JUNCTIONAL CONDUCTANCE IN THE GIANT LATERAL AXON OF CRAYFISH (*Procambarus clarkii*). A. Moreno, D. Spray* & F. Ramón. Centro de Investigación del IPN, México. *A. Einstein Coll. Med., New York.

Electrotonic coupling between lateral axons of the crayfish abdominal nerve cord is sensitive to intracellular pH. Junctional conductance (g_j) decreases when the extracellular NaCl is replaced by Na acetate, a maneuver that increases intracellular acidity. Due to the importance of crayfish diurnal cycles we studied the gap junctional sensitivity to pH_i in two groups of animals: a) at daytime (9 to 12 hrs.) and b) at night (18 to 24 hrs.). The junctional conductance was calculated from measurements of voltage changes and current injections via microelectrodes. Intracellular pH was measured by pH sensitive microelectrodes. The minimum g_j value of night axons reached after acetate was 50% less than that of day axons and the pK value shifted from 6.52 ± 0.06 ($n=6$) during the day to 6.29 ± 0.07 ($n=4$) at night. In crayfish, the diurnal cycles are induced by hormonal substances from the glands in the eyestalk. Because of this, experiments were performed in animals with eyestalks removed at the same time as the experiments described above. Gap junctions from destalked crayfish lost their sensitivity to uncoupling by acetate, but while in day crayfish it lasted 1 hour to 2 days, in night axons it lasted up to 5 days. The pK of axons from night animals destalked 1 hour before was lower than 6.3. These results suggest the existence of a cellular control of g_j through a modulation of gap protein sensitivity to uncoupling by cations.

T-Pos274 VARIATIONS IN GAP JUNCTION STRUCTURES MEASURED BY INCOHERENT SCATTERING -- Sunil Maulik*, D.L.D. Caspar, W.C. Phillips, & D.A. Goodenough⁺, *Graduate Biophysics Program and Rosenstiel Center, Brandeis University, Waltham, MA., 02254. ⁺Dept. of Anatomy, Harvard Medical School, Boston, MA., 02115.

Because the averaged gap junction membrane-pair profile is centrosymmetric about the gap center, the coherent diffracted intensity must be zero at the nodes of the average membrane-pair transform. At these nodes we have observed finite intensity which has the same angular distribution as the coherent diffraction maxima. This intensity is incoherent scatter arising from variations in the profiles of the membrane units within the specimen. The total meridional diffraction, which is the sum of the coherent and incoherent intensities, has been measured by angular deconvolution (Makowski, L., (1978) J. Appl. Cryst. 11:273-283). The coherent intensity is the product of the square of the average membrane-pair transform and the interference function, defined respectively by the average membrane-pair profile and the pair-correlation function. The coherent intensity has been calculated by refining models for these functions against the diffraction data (Maulik, S. et al (1985) Biophys. J. 47, 106a). The incoherent intensity was then determined by subtracting the calculated coherent intensity from the measured meridional intensity. This incoherent intensity can then be accounted for by small variations in the bilayer-pair separation and in the amount and distribution of protein on the cytoplasmic surfaces of the membranes. A model for these structural fluctuations, together with those used to calculate the coherent intensity, was then refined to fit the total measured meridional diffraction to within the noise level of the measurements.

T-Pos275 CONNEXON LATTICE IN GAP JUNCTIONS IS COMPACTED BY DEHYDRATION AND BY LIPID EXTRACTION

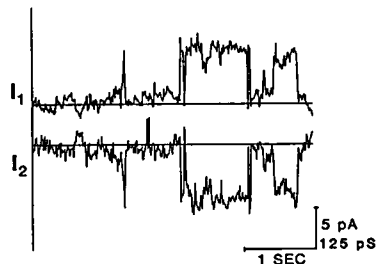
Thomas T. Tibbitts, Dan A. Goodenough, Walter C. Phillips and Donald L. D. Caspar.

Rosenstiel Research Center, Brandeis University and Department of Anatomy, Harvard Medical School.

Controlled variation of the water content in pellets of stacked gap junction plaques affects both the stacking period and the average center-to-center spacing of connexons within the plaques. Analysis of low-angle x-ray diffraction reveals that slow, stepwise dehydration induces a graded compaction of both the lamellar stacks and the connexon hexagonal lattice. This reversible compaction has been observed in unfixed specimens derived from three different rat liver preparations. The spacing of the hexagonally packed connexons is about 90 Å when fully hydrated and decreases to about 75 Å when the relative humidity (RH) is less than 82%. As the connexons move closer together, intensities of equatorial and off-equatorial reflections change relative to one another, indicating that a redistribution of mass within the connexon protein units accompanies lattice compaction. Reflections characteristic of stacked lipid bilayers appear on the meridian of diffraction patterns from specimens at less than 75% RH, presumably due to lipid extruded from the membrane lattice. Disappearance of these reflections generally accompanies re-expansion of the lattice, unless the specimen was previously subjected to less than 50% RH. Reversible compaction is not an intrinsic property of the connexon lattice, since unfixed specimens derived from another rat liver preparation show a lattice spacing, invariant to dehydration, of 86 Å. Treatment with 1% w/v sodium deoxycholate, followed by several washes to remove the detergent, reduces this spacing to 76.5 Å. These results show that connexons can be driven to closer packing either by dehydration or by detergent-mediated lipid extraction.

T-Pos276 SINGLE GAP JUNCTIONAL CHANNEL ACTIVITY IN EMBRYONIC CHICK HEART CELLS. R. D. Veenstra and R.L. DeHaan, Dept. of Anatomy and Cell Biology, Emory University, Atlanta, Ga. 30322

Adhering pairs of ventricular cells, isolated from the heart of 7 day chick embryos and cultured for 1 day *in vitro*, were voltage-clamped using the whole-cell patch clamp technique. Two patch pipettes, filled with a high-K, low-Na, low-Ca solution and having tip resistances of 4 - 8 Mohms, were used to control the voltage of each cell independently. When a constant transjunctional potential gradient (V_j) of 10mV was applied and the membrane potential (V_m) of both cells varied over 160mV (-90 to +70mV in cell 1 and -80 to +80mV in cell 2), the junctional conductance (G_j) in 7 cell pairs was 2-6 nS, and was independent of V_m . When V_j was varied between -60 and +60mV, G_j was unaffected, and showed no rectification. Current through channels in the non-junctional membrane of one cell was seen with the same polarity in the other cell, but was reduced in magnitude by the voltage drop across G_j . Junctional channel currents, in contrast, were recorded with opposite polarity and equal size, and were proportional to V_j . With constant V_j , junctional current was inward for the more negative cell and outward for the other. Using these criteria, we have identified large step-like G_j events (Figure) averaging 156 ± 19 pS ($n=34$). Smaller conductance fluctuations of about 50 and 90 pS have also been observed. (Supported by NIH Grants HL27385 to RLD and HL06909 to RDV)



T-Pos277 CALCIUM CHANNELS FROM INTRACELLULAR MEMBRANES RECONSTITUTED IN PATCH-CLAMPED BILAYERS. P. Vassilev, M. Kanazirska, and H. Ti Tien, Department of Physiology, Michigan State University, East Lansing, MI 48824

In nerve cells the Ca^{2+} -storing vesicles of smooth endoplasmic reticulum are involved in the regulation of the excitation-secretion coupling in the presynaptic nerve terminals. The Ca^{2+} uptake is controlled mainly by membrane Ca^{2+} , Mg^{2+} -ATPases. However, the mechanism of Ca^{2+} efflux from the intracellular organelles is not well understood. A channel mechanism was tested using the bilayer lipid membrane (BLM) system. The BLMs were formed on the tips of patch-clamp pipettes after passing them through monolayers containing lipids and proteolipid isolated from cattle cardiac sarcoplasmic reticulum, or from brain microsomes. Single channel events with similar characteristics were observed in both types of membranes. Current displacements with large amplitude (4.5 pA) were found even at 0 mV. From the current-voltage relationship a large unit single channel conductance of 175 pS (in 5×10^{-2} M CaCl_2) was defined. A tendency for periodical changes in channel activity was observed. ATP (10^{-3} M) stimulated the channel activity mainly by increasing the mean open time. Ruthenium red (10^{-6} M) as well as Ca^{3+} inhibited the channel opening. Channels with large unit conductance functioning in the millisecond range are very probable candidates for explaining the fast kinetics of the Ca^{2+} release from the sarcoplasmic reticulum in muscle cells. However, their presence in brain microsomal fractions is surprising, which may be responsible for the Ca^{2+} efflux from the smooth endoplasmic reticulum in the presynaptic terminals, thereby stimulating the exocytosis of neurotransmitter-containing vesicles. [Supported by NIH GM 14971]

T-Pos278 CALCIUM CHANNEL BLOCKADE AND RELATED PROBLEMS FROM THE PERSPECTIVE OF EXTRACELLULAR CALCIUM IN RABBIT ATRIUM.

D.W. Hilgemann, Department of Physiology, UCLA School of Medicine, Los Angeles, Calif. 90024

Fast extracellular calcium (Ca) transients in mammalian heart are broadly consistent with current concepts of E-C coupling as demonstrated by recent simulations (Noble and Hilgemann, *J Physiol*, abstr in press). The present work addresses the role of Ca channel in extracellular Ca depletion. The early Ca depletion rate (ECDR; measured between 3 and 6 ms after excitation) is 0.1 $\mu\text{M}/\text{Kg}$ wet wt/5 ms with 130 μM free Ca (2 mM tetramethylammonium; 200 μM total Ca). Interventions which minimize SR Ca release without blocking SR Ca uptake (e.g., early excitations or ryanodine pretreatment) result in almost linear depletions for up to 200 ms; at contractions potentiated by a few premature excitations depletion stops within 20 ms. ECDR is decreased by 50 to 75% with 1 μM nifedipine. By projection, ECDR corresponds to the lower range of Ca currents measured in isolated myocytes. Verapamil is without effect on ECDR at low extracellular Ca and frequencies up to 2 Hz. Accordingly, depolarization alone does not invoke block by verapamil; however, ECDR is suppressed by verapamil with interventions which are presumed to indirectly enhance Ca channel inactivation via internal Ca release (e.g., potentiation of contraction by premature excitations). The following two-step formulation of Ca channel inactivation allows simulation: Intracellular Ca binds to a regulatory site to produce an inactivated state (Eckert and Chad, *Prog Biophys Mol Biol* 44:215); subsequently, a voltage-dependent process "preserves" the inactivation, largely preventing reactivation of the Ca channel by relaxation of intracellular free Ca; verapamil "stabilizes" the voltage-induced inactivation state (Kanaya et al., *J Mol Cell Cardiol* 15:145). Supported by the AHA-GLAA.

T-Pos279 DEPENDENCE OF CARDIAC TWITCH TENSION ON MEMBRANE HOLDING POTENTIAL AND INTRACELLULAR SODIUM: ROLE FOR NA-CA EXCHANGE. Craig T. January (Intr. by Gordon A. Jamieson), The University of Chicago, Chicago, IL 60637

In cardiac Purkinje fibers, the intracellular sodium ion activity (a_{Na}) and twitch tension amplitude are a function of the membrane holding potential. In these experiments, the membrane potential of sheep and canine Purkinje fibers was controlled using a voltage clamp, twitch tension was monitored, and a_{Na} was measured using liquid ion exchange microelectrodes. Depolarizing voltage steps to 0 mV for 100-200 msec were applied at 0.1 Hz in order to evoke twitches. Decreasing or increasing the holding potential (range -40 to -110 mV) caused a_{Na} to decrease or increase monotonically over several minutes to a new steady state level. Twitch tension amplitude also decreased or increased, respectively, but with a more complex timecourse. Following an increase in holding potential (causing a_{Na} to gradually rise) twitch tension amplitude first decreased slightly before increasing over several minutes to a new steady state level. After returning to the original holding potential (causing a_{Na} to fall to its initial level) twitch tension amplitude first briefly increased before gradually declining to the original level. Using a model of Na-Ca exchange, the changes in twitch tension amplitude resulting from changes in holding potential are similar to changes predicted for the intracellular calcium ion activity, and suggests important roles for both voltage and sodium dependence of Na-Ca exchange.

T-Pos280 VICINAL DITHIOL GROUPS AND ACTIVATION OF THE CARDIAC SODIUM-CALCIUM EXCHANGE SYSTEM. Carole A. Bailey and John P. Reeves. Roche Institute of Molecular Biology, Roche Research Center, Nutley, NJ 07110 USA.

Na-Ca exchange activity in cardiac sarcolemmal vesicles was inhibited by a wide variety of sulfhydryl reagents, with the following order of effectiveness: $\text{Hg}^{2+} > \text{p-chloromercuribenzenesulfonate (pCMBS)} > 5,5\text{'-dithiobis(2-nitrobenzoic acid)} > \text{diamide} \sim \text{N-ethylmaleimide} > \text{glutathione-S-maleimide}$. Transport activity was also inhibited by the trivalent arsenic compounds phenylarsine oxide and equimolar amounts of Na m-arsenite and 2,3-dimercaptopropanol (As-BAL), which are thought to react specifically with vicinal dithiols. The concentration profile for inhibition by pCMBS and As-BAL was biphasic, with 40-60% inhibition occurring at concentrations below 40 μM and 1 mM respectively, and more gradual inhibition of activity occurring at higher concentrations. For vesicles in which transport activity was stimulated 3-fold or more by treatment with chymotrypsin or redox reagents (Biophys. J. 47: 81a, 1985), more than 85% of the activity was sensitive to concentrations of pCMBS and As-BAL below 40 μM and 1 mM, respectively. To assess the involvement of vicinal dithiols in activation of Na-Ca exchange activity, native vesicles were pretreated with 5 mM As-BAL and then washed free of this reagent. Exchange activity in the treated vesicles was approximately 50% of that in untreated controls; however, this treatment markedly reduced the stimulation of exchange activity by either chymotrypsin or redox reagents. These results suggest a role for vicinal sulfhydryl groups in both the normal function of the Na-Ca exchange protein as well as its activation by proteolysis or redox reagents in cardiac sarcolemmal vesicles.

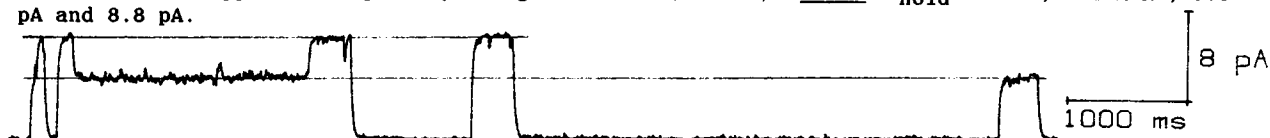
T-Pos281 "CREEP CURRENT" REVERSAL POTENTIAL MEASUREMENTS ARE CONSISTENT WITH A NA/CA-EXCHANGE MECHANISM. J.R. Hume and A. Uehara. Department of Pharmacology and Toxicology, Michigan State University, East Lansing, MI 48824. Na^+ -loading single frog atrial cells produces changes in membrane current which resemble: (i) the "creep currents" previously observed in cardiac Purkinje fibers during exposure to low K solutions and (ii) currents generated by a theoretical model of electrogenic Na/Ca-exchange (Uehara and Hume, Biophys. J. 47:460a, 1985). In contrast to Purkinje fibers, Na-loading atrial cells results in the appearance of creep currents without accompanying transient inward currents (ITs). Creep currents are unlikely to be generated by voltage-gated membrane channels since they are insensitive to antagonists of Na, Ca or K channels but are blocked by low doses of several compounds which block Na/Ca-exchange flux activity in isolated sarcolemmal vesicles (Hadley et al., J. Physiol. in press, 1985). We have further investigated the ionic basis of creep currents by making reversal potential measurements. Our results indicate that creep currents display a genuine reversal of current direction only under equilibrium conditions, and that voltage displacements away from the holding potential rapidly alter equilibrium conditions. Current-voltage relations for inward creep currents are labile and shift along the voltage axis in response to changes in either duration or amplitude of preceeding voltage clamp pulses, suggesting that creep currents are importantly influenced by changes in ion concentration gradients. These properties of creep currents are consistent with an electrogenic Na/Ca-exchange mechanism and inconsistent with a non-selective membrane channel activated by $(\text{Ca})_i$. Moreover, this behavior of inward creep currents can be simulated using a mathematical model of electrogenic Na/Ca-exchange and its dependence upon changes in $(\text{Ca})_i$. Supported by NIH grant HL30143 and a grant-in-aid from the American Heart Association and its Michigan Affiliate.

T-Pos282 CELL SURFACE INTERFERENCE WITH CALCIUM MICROELECTRODE RESPONSE. Milton L. Pressler¹, Jurg Streit², and Daniel D. Gretler², Dept. of Medicine¹, Ind. Univ. School Med., Indpls., IN. and Dept. of Physiology², Univ. of Berne, Berne, Switzerland.

Many limitations exist to Ca^{2+} -selective microelectrode determinations of free intracellular calcium concentration ($[\text{Ca}^{2+}]_i$) in cardiac tissue. In this paper, we report our experience with Ca^{2+} -microelectrodes (0.6-1.2 μm diameter) incorporating the liquid Ca-sensor of Oehme et al. (ETH 1001) in a polyvinylchloride matrix. Resting sheep Purkinje fibers (35.0 $^{\circ}\text{C}$) were impaled with conventional KCl and Ca^{2+} -selective microelectrodes. Ca-electrodes were calibrated before and after impalement in EGTA-buffered solutions containing (μM): 155 K^+ , 10 Na^+ , and 3 Mg^{2+} (fixed interference method). Tyrode solution ($[\text{K}^+]$ 5.4 mM; $[\text{Ca}^{2+}]$ 2.0 mM) defined the zero reference point. Drastic alterations of the Ca-electrode response were evident after penetration of the cardiac cells. The slope of the Ca-electrode response to free $[\text{Ca}^{2+}]$ markedly flattened after impalement: pCa 5.75-6.5, 18.2 ± 5.9 mV/decade (PRE) to 5.0 ± 2.8 mV/decade (POST); pCa 6.5-7.2, 6.7 ± 4.7 mV/decade (PRE) to 1.6 ± 1.4 mV/decade (POST) [n=18; $P < 0.001$]. Even in stable and drift-free records, the flat response made it difficult to quantitate $[\text{Ca}^{2+}]_i$; better than ± 0.5 -1 log unit. Similar attenuation of the Ca-response could be produced by 1) simple contact of the electrode tip to the fiber surface or 2) insertion and withdrawal from a block of 1.5% agar. Furthermore, exposure to dextran or starch solutions mimicked the interference whereas silicon oil or 0.5-10% albumin had little effect. We suggest that some of the difficulties associated with cellular measurements using Ca-electrodes may be secondary to cell surface interference by complex polysaccharides. (Supported by grants from the NHLBI and IN Heart Assn)

T-Pos283 RECONSTITUTION OF A HIGHLY CONDUCTIVE K CHANNEL FROM CANINE VENTRICULAR SARCOLEMMA. Joseph A. Hill, Jr., Roberto Coronado, Harold C. Strauss. (Intr. by T.J. McManus). Departments of Medicine and Pharmacology, Duke University Medical Center, Durham, NC 27710 and Department of Pharmacology, University of North Carolina, Chapel Hill, NC

We have used bilayers of the Mueller-Rudin type (PE:PS) formed in large apertures to record single K-conducting channels from ventricular sarcolemma (Jones et al., J Biol Chem 255: 9971-9980, 1980). One channel exhibited two conducting states O_1 (190 pS, ± 5 (SE), $n=7$, inset) and O_2 (108 pS, ± 2) in the presence of 0.1M K^+ . The ratio of $O_2:O_1$ conductances was relatively constant at 57% (± 1). The current-voltage relation was ohmic over the range ± 70 mV and the single channel opening probability increased with increasingly positive holding potentials. O_1 and O_2 communicate with each other and also with the closed state. Calcium, apamin and ATP were without apparent effects. The $P_{Na}:P_K$ ratio as measured under bilionic conditions was 0.5 and the $P_{Rb}:P_K$ ratio was approximately unity. These data provide evidence for the existence in cardiac sarcolemma of a highly conductive, Ca^{2+} -insensitive cationic channel that is previously undescribed. (Supported in part by NIH grants 19216, 17670). Inset: $V_{hold}=+50$ mV, 0.1 M K^+ ; 5.3 pA and 8.8 pA.



T-Pos284 INDIRECT AND DIRECT DETERMINATION OF INTRACELLULAR K^+ CONCENTRATION IN ISOLATED CANINE PURKINJE MYOCYTES. Karl Dresdner and Penelope Boyden, Dept. of Pharmacology, Columbia University, College of Physicians and Surgeons, New York New York.

Free intracellular K^+ concentration ($[K]_i$) has been determined in multicellular preparations by directly measuring intracellular K^+ activity with an ion sensitive microelectrode or by first determining the reversal potential of the resting potential and then indirectly estimating $[K]_i$. We have compared these two methods by determining $[K]_i$ using in isolated myocytes from free running Purkinje strands (SPCs) at 36.5°C. Method 1 (Indirect). Changes in resting potential (RP) of SPC ($n=7$) were recorded in response to step changes in $[K]_o$ (3.8 to 100mM). $[K]_o$ near the myocyte surface was monitored with a K^+ sensitive microelectrode (K-ISE). RP was linearly dependent upon $[K]_o$ for $[K]_o > 20$ mM (mean slope = 52.9 mV). Using linear regressions extrapolated to 0mV, mean $[K]_i$ was estimated to be 140mM, indicating that $E_K = -97$ mV in 3.8mM $[K]_o$ (where mean RP = -87mV). Method 2 (Direct) Two intracellular microelectrodes in a single SPC (a conventional 3M KCl electrode and a K-ISE) were used to measure $[K]_i$ directly. The RP of the SPC was subtracted from the K-ISE recording and the intracellular K^+ activity (a_{Ki}) was calculated. Assuming that the intracellular K^+ activity coefficient = 0.75, then $[K]_i = a_{Ki}/0.75$. For $n=7$ myocytes, the calculated mean $[K]_i = 139$ mM. We conclude: 1) both methods will yield similar $[K]_i$ values in SPCs, and 2) because each method has its limitations and disadvantages, it is best to check the results of one method against the other when feasible. Supported by NIH HL 34470.

T-Pos285 ROLE OF ELECTRICAL UNCOUPLING ON IMPULSE PROPAGATION IN SHEEP CARDIAC PURKINJE FIBERS.

Serge Sicouri, Mario Delmar and Jose Jalife. SUNY/Upstate Med. Ctr., Syracuse, NY 13210

Changes in cell-to-cell coupling may play a role in heart rhythm and conduction disturbances. To analyze the relative importance of electrical coupling in action potential propagation, we used microelectrodes and linear Purkinje fibers, and studied the changes in conduction velocity (CV) and upstroke velocity (\dot{V}_{max}) induced by the uncoupler heptanol (1.2 - 3.0 mM). In addition, heptanol effects on intercellular resistance (R_i) were measured by cable analysis and compared with those estimated from the equations of active propagation in excitable cells. Heptanol superfusion reversibly led to a major decline in CV (80.2%), while reducing \dot{V}_{max} only slightly (32%), before complete block occurred. The drug led to a small decrease in maximum diastolic potential and induced "foot" potentials associated with conduction delays. This brought the take-off potential to less negative levels and partially explained the decrease in \dot{V}_{max} induced by heptanol. More importantly, complete blockade was correlated with a five-fold increase in R_i , while excitability was unchanged, as demonstrated by the presence of "non-propagated" action potentials at the site of intracellular current injection. Very similar results were obtained by superfusing the preparation with 0.1 μ M ouabain instead of heptanol. When, in the absence of drug, the \dot{V}_{max} vs CV relationship was studied during superfusion with 20 mM KCl, a major decrease in \dot{V}_{max} (84.9%) produced only a 31.6% decrease in CV. No significant changes in R_i were observed during 20 mM KCl superfusion. We conclude that electrical uncoupling is the most important factor leading to conduction blockade by heptanol or ouabain under our experimental conditions. The results underscore the importance of electrical uncoupling in cardiac arrhythmias and conduction disturbances.

T-Pos286 MATHEMATICAL MODEL OF THE PURKINJE FIBER Na PUMP REVEALS DISTORTION OF ITS K SENSITIVITY ATTRIBUTABLE TO EFFECTS OF RESTRICTED DIFFUSION IN CLEFT SPACES.

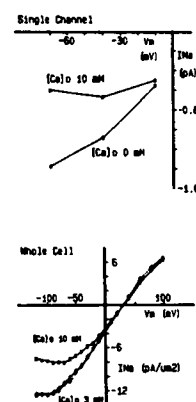
Robert TenEick, David Mogul, Helge Rasmussen (Introd. by A.L. Bassett)

Depts. of Pharmacology and Medicine, Northwestern University, Chicago, IL 60611

Many studies of the Na-pump in sheep Purkinje strands have involved intracellular Na-loading by exposure to 0 mM K followed by re-exposure to K (K-activated Na-pumping). The K concentration for half maximal pump stimulation ($K_{0.5}$) in such experiments is said to be higher than $K_{0.5}$ determined under steady state conditions. We developed a model to determine if gradients in the K concentration in unstirred extracellular fluid layers can account for the discrepancy. Pump activity was assumed to be linearly dependent on intracellular Na and dependent on extracellular K according to Michaelis-Menten kinetics. The model simulated slow diffusion of K across unstirred layers and pump-induced K depletion in extracellular clefts. Even with substantial delay in achieving a steady state K concentration following reexposure to K after Na loading, a linear relationship between the simulated pump current and intracellular Na, a monoexponential decay of current and independence of the rate constants for the decay of the Na-load at physiologically relevant extracellular K^+ concentrations was maintained. However, large systematic errors in estimates of $K_{0.5}$ were produced. Such errors may account for the discrepancy between the kinetic and steady state estimates of $K_{0.5}$. The simulations suggest that a reduction in pump rate induced by reducing the size of the Na load or lowering the temperature may reduce the amount of error in experimental estimates of $K_{0.5}$ for K activated Na pumping. They also imply a linear dependence of pump rate on intracellular (Na), monoexponential decay of pump current, and apparent Michaelis-Menten kinetics should not be regarded as sufficient evidence that pump induced depletion has not introduced artefact into determinations of $K_{0.5}$.

T-Pos287 CALCIUM DEPENDENCE OF SINGLE Na CHANNEL RECTIFICATION AND INSTANTANEOUS IV RELATION IN CARDIAC PURKINJE CELLS. D.A. Hanck, M.F. Sheets, B.E. Scanley, J.C. Makielski, & H.A. Fozzard. Cardiac Electrophysiology Lab, The University of Chicago, Chicago, Illinois.

Calcium-dependent rectification of the Na channel current has been seen in the negative potential range in squid (eg Taylor, et al, Biophys.J. 16:27a, 1976) and in neuroblastoma cells (Yamamoto et al, Biophys.J. 45:337, 1984). Rectification in cardiac cells (Cachelin et al, J.Physiol. 340:389, 1983) could also be influenced by saturation of Na channels or by bandwidth limitation in recording a flickering channel. We compared the Ca dependence of the instantaneous IV relation of I_{Na} in cardiac Purkinje cells with a large bore glass suction pipette voltage clamp (sampled at 300kHz, 17°C) to single Na channels recorded by cell-attached patches (filtered at 2kHz, 11°C). Single channel IV relations were strongly dependent on Ca_o between 0 and 10 mM. Rectification of the whole cell instantaneous IV relation was similarly dependent on Ca_o between 3.0 and 10 mM with 15 mM Na_i and 120 mM Na_o , and the relation was not altered by reducing Na_o to 45 mM. We conclude that Na channel rectification is independent of Na_o in the physiological range and is not the result of bandwidth limitations. It appears to be the result of a direct interaction of Ca with the channel, and it would partly explain the effect of Ca on cardiac excitability. Supported by HL20592, K11HL01447, K11HL01572, & T32GM07281.

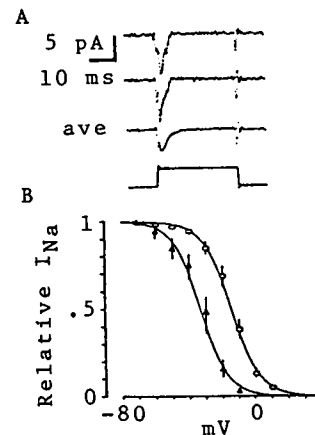


T-Pos288 *THE GATING PROPERTIES OF BATRACHOTOXIN MODIFIED Na CHANNELS IN CARDIAC CELLS. Li-Yen Mae Huang⁺, Atsuko Yatani⁺, and Arthur M. Brown⁺. * Department of Physiology and Biophysics, Marine Biomedical Institute, University of Texas Medical Branch, Galveston, TX 77550. + Department of Physiology and Molecular Biophysics, Baylor College of Medicine, Houston, TX 77030.

The gating properties of batrachotoxin (BTX)-modified Na channels were studied in single dissociated ventricular myocytes from neonatal rat heart. Whole-cell Na currents were measured under voltage clamp conditions using the patch clamp method. K and Ca currents were completely suppressed by TEA, Cs and Co. The onset of BTX effects was slow, and the complete reversibility of the effects was not obtained. Cardiac cells were relatively insensitive to BTX. In the presence of 10 μ M BTX, about 80% of the Na channels were affected, whereas almost all of the Na channels in neuroblastoma cells were modified with 2-5 μ M BTX. The BTX-modified Na channels were studied under the condition where a portion of the Na channels was modified.

BTX-modified cardiac Na currents activated at hyperpolarizing potential (-100 to -90 mV) with first order kinetics. The rate of activation was much slower than the normal Na currents. The peak conductance-voltage curve was shifted about 50 mV in the hyperpolarizing direction compared to the curve for normal Na currents. Fast inactivation of Na channels examined with 500 ms pre-pulse duration was completely eliminated by BTX. BTX also reduced the slow inactivation obtained with 2 min repulse. Although the affinity of cardiac Na channel for BTX is lower, the properties of BTX-modified cardiac Na channels are similar to those found in nerve cells.

T-Pos289 VOLTAGE-DEPENDENT ACTION OF TETRODOTOXIN ON SINGLE Na^+ CHANNEL CURRENTS IN GUINEA-PIG VENTRICULAR MYOCYTES. P.M. Vassilev, R.W. Hadley, K.S. Lee* and J.R. Hume. Department of Pharmacology and Toxicology, Michigan State University, East Lansing, MI 48824 and *Cardiovascular Disease Research, The Upjohn Company, Kalamazoo, MI 49001. In guinea-pig papillary muscles, TTX block of V_{max} exhibits steady-state voltage dependence (Baer et al., Nature 263:344-345, 1976), yet direct measurements of Na^+ currents in rabbit Purkinje fibers did not reveal a voltage-dependent action of TTX (Cohen et al., J. Gen. Physiol. 78:383-411, 1981). We have reexamined this issue in isolated guinea-pig ventricular myocytes by directly assessing the action of TTX on Na^+ channel availability determined from single Na^+ channel current measurements in cell attached patches. The voltage dependence of channel availability was obtained from ensemble averages of Na^+ channel openings during depolarizing test potential steps (+40 mV relative to average V_r of -80 mV) from 8-10 different patch holding potentials in each patch (Fig. 1A). In 6 control patches, the mean value of V_h was -15 mV (relative to V_r); in 8 patches, the pipette contained 1.0 μM TTX and mean value of V_h was -32 mV (Fig. 1B). Similar results were obtained with pulses applied at frequencies of either 1.0 or 0.067 Hz. These observations confirm that TTX block of ventricular myocardial Na^+ channels is voltage-dependent. Supported by NIH grant HL30143 and a grant from M.S.U.



T-Pos290 ROLE OF RATIO ($a_{\text{Na}}^o/a_{\text{Na}}^i$) OF EXTRA- AND INTRA-CELLULAR SODIUM ACTIVITIES IN THE CONTROL OF CONTRACTILE FORCE IN CARDIAC PURKINJE FIBERS. J.K. Sonn and C.O. Lee. Department of Physiology, Cornell University Medical College, New York, N.Y. 10021

Role of $a_{\text{Na}}^o/a_{\text{Na}}^i$ in the control of contractile force (T) in canine cardiac Purkinje fibers driven at 1.0 Hz was studied by simultaneously measuring a_{Na}^i and T when extracellular Na^+ concentration ($[\text{Na}^+]_o$) of 149.4 mM was reduced by 20%, 40%, 60%, and 100%. In a steady-state, a_{Na}^o in each solution was determined from $[\text{Na}^+]_o$ and activity coefficient of corresponding solution. Reductions of $[\text{Na}^+]_o$ by 20%, 40% and 60% decreased a_{Na}^i from 8.6 ± 0.4 mM (n=4) to 7.4 ± 0.5 (n=3), 5.9 ± 0.1 (n=4) and 4.4 ± 0.1 mM (n=3), and increased T by $84 \pm 17\%$, $251 \pm 75\%$ and $481 \pm 143\%$ respectively. Determination of $a_{\text{Na}}^o/a_{\text{Na}}^i$ at normal and low $[\text{Na}^+]_o$ revealed that reductions of $[\text{Na}^+]_o$ by 20%, 40% and 60% decreased the $a_{\text{Na}}^o/a_{\text{Na}}^i$ from 12.8 ± 0.6 (n=4) to 12.2 ± 0.8 (n=3), 11.6 ± 0.2 (n=4) and 10.6 ± 0.3 (n=3). The results indicate that the decrease in $a_{\text{Na}}^o/a_{\text{Na}}^i$ is related to the increase in T and the $a_{\text{Na}}^o/a_{\text{Na}}^i$ plays an important role in the control of T presumably through a Na-Ca exchange. Reduction of $[\text{Na}^+]_o$ by 100% decreased a_{Na}^i from 9.4 ± 0.7 mM (n=5) to -0.3 ± 0.5 mM. The decline in a_{Na}^i could be divided into fast and slow phases. Strophanthidin (5×10^{-7} M) increased a_{Na}^i and T in normal, high and low $[\text{Na}^+]_o$. T and a_{Na}^i during exposure to strophanthidin were plotted against each other on logarithmic coordinates. The data fit well on a single line. The slope obtained at normal $[\text{Na}^+]_o$ was 5.9 ± 1.1 (n=7). The slopes obtained at high (20% increase) and low (20% reduction) $[\text{Na}^+]_o$ were 5.5 ± 1.5 (n=4) and 5.0 ± 0.9 (n=5) respectively. The results indicate that the slopes obtained at high and low $[\text{Na}^+]_o$ are not significantly different from that obtained at normal $[\text{Na}^+]_o$. However, the intercept of the relationship between contractile force and a_{Na}^i was changed by increasing and decreasing $[\text{Na}^+]_o$. Supported by USPHS HL 21136.

T-Pos291 INTRACELLULAR pH IN SUBENDOCARDIAL CANINE PURKINJE FIBERS FROM ONE DAY OLD INFARCTS USING DOUBLE-BARREL ION SELECTIVE MICROELECTRODES: COMPARISON WITH MAXIMUM DIASTOLIC POTENTIAL. K.P. Dresdner, R.P. Kline, A.L. Wit. Pharmacology Department, Columbia University, College of Physicians and Surgeons, New York, NY 10032

Double-barrel microelectrodes selective for H^+ (Fluka #82500 neutral carrier proton cocktail) were used to measure maximum diastolic potential (MDP) simultaneously with intracellular pH (pHi) in normal Purkinje fibers (NPF), and in ischemic Purkinje fibers (IPF) surviving in strips of subendocardium removed from one-day old infarcted left ventricle. Infarcts were caused by complete occlusion of the anterior descending coronary artery. Tyrodes superfusate (4 mM K^+ , 2.8 mM Ca^{++} ; gassed with 95% O_2 , 5% CO_2) contained either 12 or 24 mM HCO_3^- . In 12 mM HCO_3^- , bath pH was 7.05 ± 0.05 and NPF pHi was 6.83 ± 0.08 (n=37; mean \pm S.D.). In 24 mM HCO_3^- , bath pH was 7.30 ± 0.09 and NPF pHi was 6.92 ± 0.12 (n=39). IPF had depressed MDP which improved during 3-4 hours of Tyrodes superfusion: a) from -47.5 ± 12.1 mV (n=18; first hour) to -77.2 ± 6.8 mV (n=58) in 12 mM HCO_3^- ; and b) from -47.1 ± 12.1 mV (n=14; first hour) to -74.3 ± 11.7 mV (n=20) in 24 mM HCO_3^- . NPF MDP was similar in 12 and 24 mM HCO_3^- (-83.5 ± 3.7 and -82.1 ± 3.7 mV).

IPF pHi values were initially more alkaline than NPF pHi for both bicarbonate values. They became more acidic during a) from 6.93 ± 0.11 to 6.88 ± 0.12 , but remained the same during b) from 7.15 ± 0.09 to 7.14 ± 0.06 . However, superfusion of NPF with hypoxic Tyrodes (gassed with 95% N_2 , 5% CO_2 ; 18 mM HCO_3^-) readily induced acidic shifts in pHi of 0.1 to 0.3 units as would be expected during acute ischemia. We conclude that reversible and irreversible MDP depression in IPF from one day old infarcts is not associated with cellular acidosis.

T-Pos292 GTP BINDING PROTEIN COUPLES MUSCARINIC ACH RECEPTOR TO A K CHANNEL. Paul J. Pfaffinger, Jennifer M. Martin, Dale D. Hunter, Neil M. Nathanson & Bertil Hille, Physiol. & Biophys. and Pharmacol. Depts., Univ. of Washington, Seattle, WA 98195.

We have investigated coupling of muscarinic acetylcholine receptors (mAChR) in embryonic chick atrial cells to an inward rectifying K channel using the whole-cell voltage clamp technique. Intracellular solution exchange was optimized by recording from cells smaller than 15 by 40 μm and using 2-4 megohm pipettes. Cells were allowed to equilibrate with the pipette/intracellular solution for 5 min. ACh (5-10 μM) was then added to the bath and the ACh-activated K currents were calculated as the increase in current 1-2 min after the addition of ACh. As in other heart cells, ACh activated K channels whose I-V curve showed inward rectification. The response could be completely prevented by atropine (10 μM); thus the receptor is a mAChR. The induced current had the properties of an inward rectifying K channel: its reversal potential and gating shifted with the external [K]; the current could be blocked by 1 mM Ba^{+2} or Cs^{+} . We examined the coupling between the mAChR and the K channel by changing the composition of our pipette solution. The response to ACh required GTP (100 μM) in the pipette solution. In addition, overnight treatment of the cells with IAP (Islet Activating Protein from *Bordetella pertussis*) prevented activation of the current by ACh. In our cells IAP specifically ADP ribosylates two GTP binding proteins N_1 and N_0 which are known to interact with mAChR's. We therefore conclude that a GTP binding protein is a necessary link between the mAChR and the inward rectifying K channel. A GTP binding protein may also be required for the shutting of M current channels by muscarine, LHRH, and substance P in frog sympathetic ganglia. Supported by NIH grants NS08174, HL30639, GM07270, RR00374; the AHA and the USARO.

T-Pos293 Muscarinic Receptor and Guanine Nucleotide Mediated Inhibition of I_{Ca} in Single Cells from Bullfrog Atrium. E.F. Shibata, J.K. Northup, Y. Momose and W. Giles, Univ. of Calgary, Calgary, Canada T2N 4N1.

Single microelectrode whole-cell voltage clamp techniques have been used to study the effects of muscarinic agonists (MA) and guanine nucleotides on β -agonist enhanced I_{Ca} in bullfrog atrial cells. As expected, isoproterenol (ISO, 10^{-6} M) produces a large increase in I_{Ca} (5-fold at 0 mV); and intracellularly applied 8-Bromo cyclic AMP (8-BcAMP, 0.1 mM) mimics this ISO effect. Bath applied acetylcholine (ACh, 10^{-5} M), oxotremorine (Oxo, 10^{-5} M) and carbamylcholine (Carb, 10^{-5} M) each completely inhibit both the ISO and 8-BcAMP increases in I_{Ca} ; and these MA effects are antagonized completely by atropine (10 μM). Doses of ACh $> 10^{-6}$ M and Oxo $> 10^{-5}$ M consistently produce two additional effects: (i) inhibition (50-100%) of control I_{Ca} , (ii) activation of a steady inwardly-rectifying K⁺ current (cf. Momose, Giles and Szabo, 1984).

Intracellular application of nonhydrolyzable guanine nucleotides (GN), GTP γS (10^{-5} M) and Gpp(NH)p (10^{-3} M) mimic the MA-induced inhibition of the ISO-enhanced I_{Ca} ; in addition, these agents substantially reduce the 8-BcAMP induced increase in I_{Ca} . In contrast intracellular ATP γS was ineffective. Pretreatment of populations of cells with pertussis toxin (PTX, 3 $\mu\text{g}/\text{ml}$ for 24-36 hr) failed to remove the MA response or its GN dependence. Thus a GN binding protein(s) which is not a PTX substrate, may be involved in MA control of I_{Ca} ; however, the control site appears independent of cAMP metabolism.

Supported by NIH Awards HL-27454 and HL-33662 to W. Giles; and Canadian MRC, CHF, and AHFMR Awards to W. Giles and J.K. Northup.

T-Pos294 BLOCK OF Na^{+} CURRENT IN CARDIAC MYOCYTES BY TTX. C.H. Follmer and J.Z. Yeh. Department of Pharmacology Northwestern Univ. Med. Sch., Chicago, IL 60611 (Intr. by M. Yoshii)

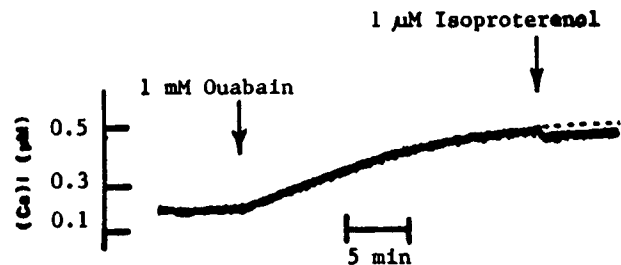
Using the single suction pipette voltage-clamp, the kinetics of TTX block of I_{Na} in human and cat atrial, cat ventricular, and canine Purkinje cells was examined. In each cell type, TTX (1 μM) produced about 70% resting block of I_{Na} , and did not affect steady-state inactivation defined using a two-pulse protocol (holding potential (V_h) = -140 mV, 50 and 200 msec prepulse, $T = 21^\circ\text{C}$). TTX produced use-dependent block (UDB) of I_{Na} (0.05-5 Hz @ 21°C). UDB was enhanced by increasing pulse rate and only slightly increased by increases in pulse duration (2-200 msec) or holding potential. Results using a twin-pulse method showed two distinct phases of block onset: fast ($\tau < 1$ msec) and slow ($\tau > 1$ sec). A train of 1-2 msec conditioning pulses to various potentials revealed voltage dependence of block closely associated with increases in G_{Na} ($V_{1/2} = -50$ mV, slope = 6.4 mV/e-fold). In the presence of TTX, recovery from inactivation at $V_h = -100$ mV was biphasic, a fast and a very slow phase ($\tau > 3$ sec). At $V_h = -120$ to -160 mV, recovery was multiphasic, a fast recovery phase (V_h dependent), followed by a net blocking phase and a very slow recovery phase (V_h independent). In conclusion, the multiphasic recovery time course at different V_h could be explained if it reflects recovery of inactivated unbound channels, toxin binding to recovered rested state channels, and recovery of inactivated toxin bound channels. While the fast phase of block is consistent with the blocking rate constant for open channels by TTX, the net blocking phase during the recovery time course supports the notion that development of UDB block may reflect slow binding of TTX to rested state channels and occur during the interpulse interval. Since little block was associated with fast inactivation (2-100 msec), the slow component most likely involves slow inactivation.

T-Pos295 ⁸⁶Rb FLUXES IN CARDIAC SARCOLEMMA VESICLES. A.S. Otero and G. Szabo, Department of Physiology & Biophysics, University of Texas Medical Branch, Galveston, Texas 77550.

A high yield procedure for the purification of cardiac sarcolemma was developed with the objective of characterizing transmembrane ion fluxes. A crude microsomal fraction obtained from bullfrog heart by differential centrifugation was fractionated in a step density gradient of HypaqueTM. The sarcolemmal fraction was collected at the 0/18% (w/v) Hypaque interface. Purification factors (relative to homogenate) were 20-fold for Na⁺, K⁺-ATPase and 25-fold for muscarinic cholinergic binding sites, while recoveries were respectively 25% and 36%. The Na⁺, K⁺-ATPase activity of the isolated preparation was increased 8 to 10-fold by detergent treatment, indicating that ~90% of the sarcolemmal membranes formed vesicles impermeable to small solutes. K⁺-gradient dependent ⁸⁶Rb uptake was measured by the method of Garty et al. (J. Biol. Chem. 258: 10394, 1983). The vesicles were prepared to contain 50 mM KCl. Assays were performed at external KCl concentration (KCl_o) ranging from nominally 0 to 50 mM. At KCl_o=0 the uptake of ⁸⁶Rb was rapid and large, reaching a maximal level at 20-30 min and decaying slowly in a process that extended for several hours. Addition of low concentrations of KCl (1 to 5 mM) to the medium decreased both the rate and extent of uptake. BaCl₂ (1mM) inhibited the uptake observed in the presence of 2.5mM KCl_o. When KCl_o was 50mM the uptake of ⁸⁶Rb was abolished. Addition of various alkali metal chloride salts to the assay medium lowered the uptake of ⁸⁶Rb to different extents, the efficacy order being Rb⁺ > K⁺ > Cs⁺ > Li⁺ > Na⁺. In the presence of gramicidin D, Na⁺ was as effective as K⁺ in decreasing ⁸⁶Rb uptake. (Supported by American Heart Association, Texas Affiliate, and DHHS HL-24820).

T-Pos296 ISOPROTERENOL DECREASES CYTOSOLIC CALCIUM CONCENTRATION OF RAT VENTRICULAR MYOCYTES DURING NA-K PUMP INHIBITION. By S-S. Sheu, V.K. Sharma, and M. Korth. Department of Pharmacology, University of Rochester, Rochester, NY 14642.

β-adrenoceptor agonists are known to have profound effects on cardiac contraction. Two important examples are the positive inotropic effect and the relaxant effect. Three possible mechanisms, which all involve cAMP-dependent protein phosphorylation, have been proposed for the relaxant effect: 1) accelerated uptake of Ca²⁺ into sarcoplasmic reticulum; 2) decreased sensitivity of myofilaments to Ca²⁺; and 3) stimulation of the Na-K pump and hence, enhancement of Ca²⁺ efflux via Na-Ca exchange. In the present study, we have examined the role of Na-K pump in isoproterenol-induced relaxant effect by measuring cytosolic Ca²⁺ concentration with quin-2 or fura-2 in cardiac myocytes of rat ventricle. As indicated in the figure, inhibition of Na-K pump by exposing the cells to 1 mM ouabain, resulted in an increase in cytosolic Ca²⁺ concentration. Subsequent addition to 1 μM isoproterenol caused a reduction in cytosolic Ca²⁺ concentration. The results suggest that some other mechanism(s), such as uptake of Ca²⁺ into sarcoplasmic reticulum, must be involved in the reduction of cytosolic Ca²⁺ concentration by isoproterenol.

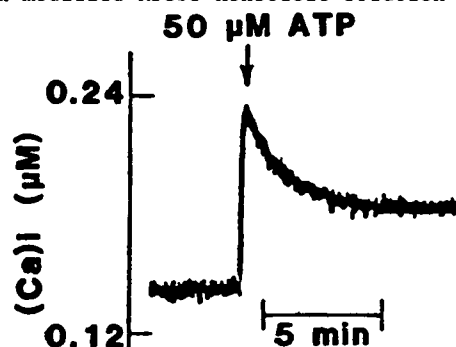


T-Pos297 EFFECTS OF KCl AND VERAPAMIL ON CYTOSOLIC CA²⁺ OF ISOLATED FELINE VENTRICULAR MYOCYTES. W.H. duBell and S.R. Houser. Department of Physiology, Temple University School of Medicine, Philadelphia, PA 19140

It is generally accepted that cytosolic Ca²⁺ is greater in rat myocardial cells than in those of other mammalian species. A previous study using the Ca²⁺ indicator Quin-2 to measure the cytosolic free Ca²⁺ in rat myocytes has yielded a value of 137.1 ± 2.6 nM ($\bar{X} \pm \text{se}$) [Powell et al. (1984) Biochem. Biophys. Res. Comm. 122:1012-1022]. The purpose of this study was to use Quin-2 to determine the cytosolic free Ca²⁺ (Ca_i²⁺) in isolated feline ventricular myocytes. Cells were loaded with Quin2 (25μM) for 30 minutes in Krebs Henseleit medium containing 5.4 mM KCl and 1.0 mM Ca²⁺. The cells were washed twice in KH medium, with 30 minutes for settling between washes. Final suspension was in KH medium with 2.0 mM or 0.2 mM Ca²⁺. Fluorescence was recorded on a Perkin-Elmer LS-5 Fluorescence Spectrophotometer. Resting Ca_i²⁺ was found to be 62 ± 5 nM, lower than in the rat. Addition of KCl to 20.4 mM caused an increase in Ca_i²⁺ to 81 ± 13 nM. Further addition to 50.4 mM raised Ca_i²⁺ to 230 ± 35 nM. Verapamil (at 10^{-5} M), while having no effect on resting Ca_i²⁺, blocked most of the KCl depolarization induced increase in Ca_i²⁺. In additional experiments done with an extracellular Ca²⁺ of 0.2mM, Ca_i²⁺ was found to be 43 ± 8 nM. This work demonstrates that Ca_i²⁺ is lower in the cat than in the rat. It also demonstrates some dependence of Ca_i²⁺ on Ca_o²⁺. In addition, the experiments with and without verapamil in the presence of KCl induced depolarization support the idea that the increase in Ca_i²⁺ under these conditions is due to entry of extracellular Ca²⁺ rather than release from an intracellular store. (Supported by NIH Grants HL33921 and HL33648)

T-Pos298 MICROMOLAR EXTRACELLULAR ATP INCREASES INTRACELLULAR CALCIUM CONCENTRATION IN ISOLATED RAT VENTRICULAR MYOCYTES. By V.K. Sharma and S-S. Sheu. Department of Pharmacology, University of Rochester, Rochester, NY 14642.

Many studies have shown that exogenous ATP causes perturbation of membrane permeability in several types of intact cells. However, the physiological significance of this ATP effect has not been established. Using the fluorescent indicators, quin-2 and fura-2, we investigated the effect of ATP on cytosolic Ca^{2+} concentration in isolated rat ventricular myocytes. Addition of extracellular ATP (1-500 μM) to cell suspensions (incubated in modified Krebs-Henseleit solution containing 2 mM Ca^{2+} and 2 mM Mg^{2+}) results in a dose-dependent increase in cytosolic Ca^{2+} concentration. As shown in the representative figure, treatment with 50 μM ATP resulted in a rapid increase on cytosolic Ca^{2+} concentration. After reaching the peak value, the cytosolic Ca^{2+} then declined gradually to a new steady level. Other adenosine derivatives, including AMP, Adenosine, and AMPPNP (a non-hydrolyzable ATP analog) did not produce a similar effect. Current experiments are directed at discerning the mechanism of this ATP effect--e.g. affect Ca^{2+} permeability of the plasma membrane or release of Ca^{2+} from sarcoplasmic reticulum.



T-Pos299 PACEMAKER CURRENT (i_f) AND THE INWARD RECTIFIER (i_{k1}) IN SINGLE RIGHT ATRIAL MYOCYTES FROM CAT HEART. S. Lipsius, J. Vereecke, E. Carmeliet; Loyola University Medical Center, Dept. of Physiology, Maywood, IL USA; Universiteit Leuven, Laboratorium voor Fysiologie, Campus Gasthuisberg, Leuven, Belgium.

Whole cell voltage clamp technique was used to study ionic currents that may participate in atrial subsidiary pacemaker activity. Right atrial myocytes, excluding the SA node, were obtained by collagenase dispersion. Tyrode's contained 5.4 mM K^+ and pipette solution contained in mM: 120 K-acetyl-glycinate, 20 KCl, 5 Na_2ATP , 5 EGTA, 0.685 CaCl_2 , 5 HEPES, pH 7.2. Hyperpolarizing clamps produced one of three different current patterns. In some cells small hyperpolarizing steps elicited only a time-independent inward current. With larger steps the current partially decayed as a function of time. External Ba (2 mM) blocked this current. The Ba-sensitive current inwardly rectified and reversed near -95 mV. In other cells however, hyperpolarizing clamps elicited a net inward current which increased as a function of time. Current amplitude became larger at more negative potentials and did not reverse even at potentials of -160 mV. Ba had no effect but 2 mM Cs blocked this current. In other cells, current was biphasic at strongly negative potentials. After an initial decay the current became more inward again. Ba blocked the initial current but had little effect on the late current, thus revealing a net inward current blocked by Cs. We conclude that right atrial myocytes can exhibit a pacemaker current (i_f) or the inward rectifier current (i_{k1}) or both. When both are present the inward rectifier can mask the onset of pacemaker current activation. The ratio of these currents may contribute to determining whether an atrial cell will display automaticity or remain quiescent.

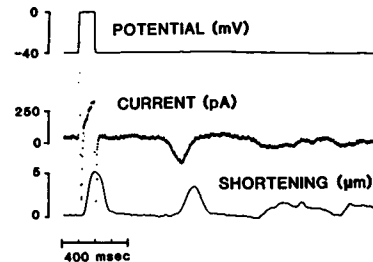
T-Pos300 The Effects of Heart Rate on the Extracellular Volume of Hamster Ventricle. Donald D. Macchia and Cathy Carruthers. Indiana University School of Medicine, Northwest Center for Medical Education, Gary, IN 46411.

It has recently been shown that hibernating hamsters have smaller ventricular extracellular volumes (ECV) than non-hibernators (Exper. 39:364, 83). From this study, the decrease in ECV could be a result of either the decreased temperature (5 $^{\circ}\text{C}$ in the hibernators) or the decreased heart rate (20 bpm in hibernators as compared to 450 bpm in non-hibernators). With the above in mind, the ECV was measured in hamster ventricles perfused in vitro at 38 $^{\circ}\text{C}$ and 22 $^{\circ}\text{C}$ and allowed to beat spontaneously at < 150 bpm. When the perfusate temperature was 38 $^{\circ}\text{C}$, the same as the in situ hamster body temperature, the mean morphometrically determined ECV of 0.077 ± 0.006 (n=4) was found to be less than the morphometric ECV of 0.24 ± 0.007 (n=12) for in situ hearts. When the perfusate temperature was decreased to 22 $^{\circ}\text{C}$ (maintaining the heart rate the same as at 38 $^{\circ}\text{C}$) the morphometric space of 0.084 ± 0.006 (n=4) was similar to that observed at 38 $^{\circ}\text{C}$. These data suggest that the ECV of hamster ventricle is dependent upon heart rate and not temperature. When sulfate distribution was used to measure the ECV in hamster ventricle, the sulfate space was also found to be smaller in isolated hearts perfused at 38 $^{\circ}\text{C}$ (beating spontaneously) (0.142 ± 0.001 (n=3)) then determined in situ (0.22 ± 0.006 (n=4)). The in vitro sulfate space was, however, larger than the morphometric space of 0.077 ± 0.006 (n=3) and is thought to represent increased anion permeability of the ventricular cell membranes. Further, when the heart rate was increased to 180 bpm, the sulfate space was observed to increase to 0.164 ± 0.003 (n=3). These data also support the idea of an influence of heart rate on ECV. (Supported by an Indiana Heart Association Grant-in-Aid)

T-Pos301 I_{TT} AND AFTERCONTRACTIONS IN SINGLE CARDIAC MYOCYTES DURING CALCIUM OVERLOAD.

J.R. Berlin, M.B. Cannell and W.J. Lederer. Univ. Maryland Med. School, Baltimore, MD 21201

Enzymatically-dissociated rat ventricular myocytes were voltage-clamped using a single microelectrode technique. Calcium overload was produced by inhibiting the Na-pump with a low K^+ (0.4 mM) superfusing solution. Depolarizations of 100 msec from -40 mV to 0 mV were applied at 0.5 Hz (see figure). The depolarization produced a synchronous contraction of the cell. On repolarization, a transient inward current (I_{TT}) was observed as was an aftercontraction. The peak of I_{TT} is about 80 msec ahead of the aftercontraction, a finding similar to results reported for other cardiac tissues. Additional fluctuations of current and shortening were present and appear to be correlated. The exact timing and magnitude of I_{TT} and of the aftercontraction were variable from pulse to pulse and appear to depend in part on the degree of calcium overload. Results from other experiments using fura-2 to measure intracellular calcium suggested that a transient elevation of intracellular calcium following repolarization may be the cause of both I_{TT} and the aftercontraction in these cells.

**T-Pos302 INFLUENCE OF RYANODINE ON REST INTERVAL-INDUCED CHANGES IN ELECTRICAL AND CONTRACTILE PROPERTIES OF CAT VENTRICULAR MYOCYTES.** L.S. Miller and S.H. Houser, Department of Physiology, Temple University School of Medicine, Philadelphia, Pennsylvania 19140.

Sarcoplasmic reticular (SR) Ca^{2+} release and accumulation are believed to influence excitation-contraction coupling in cardiac muscle through modulation of the $[Ca^{2+}]_i$ transient. In this study we assessed the contribution of the SR to action potential (AP) and contractile recovery after variable rest intervals using ryanodine, a putative blocker of SR Ca^{2+} release. Adult cat ventricular cells were isolated via standard enzymatic digestion. Cells were perfused with Tyrode's solution (2 mM Ca^{2+} , 35°C) and stimulated to contract by brief depolarizing pulses (.5 msec @ 1 Hz). They were then subjected to rest periods ranging from 15 sec to 5 min. In normal Tyrode's solution, the first postrest action potential (AP1) was progressively increased with increasing rest interval (TABLE 1), with subsequent AP's declining to steady state (SS). Contraction magnitude (CM) was reduced in the first beat and increased with subsequent contractions to SS. Ryanodine (10^{-6} M) did not significantly affect AP duration in SS; after rest intervals, however, AP1 was considerably lengthened (TABLE 1) and CM was markedly diminished in comparison to control.

TABLE 1	RMP(mV)	APD ₅₀ (SS) (msec)	% INCREASE APD ₅₀ OF AP1 vs SS				
			15 sec	30 sec	1 min	2 min	5 min
Rest Interval:							
Tyrode's (n=14)	-85±3	234±23	5.7±3	9.1±5	17.2±9	16.3±8	28.5±15
T + R (n=10)	-87±4	230±31	9.2±5	20.6±9	27.8±17	55.7±26	78.4±33

The results indicate that SR Ca^{2+} release affects the AP waveform and the magnitude of mechanical changes following rest intervals in cat ventricular cells. (Supported by NIH grants: HL33921 and HL33648; AHA SE Pennsylvania Chapter Research Fellowship)

T-Pos303 QUINIDINE BLOCKS CARDIAC POTASSIUM CHANNELS IN A TIME- AND VOLTAGE-DEPENDENT FASHION DM Roden, PB Bennett and LM Hondeghem, Depts. of Medicine & Pharmacology, Vanderbilt University, Nashville, TN 37232

Quinidine blocks sodium channels in a use- and voltage-dependent fashion. It also prolongs the action potential, particularly at slow heart rates (Roden and Hoffman, Circ Res 56:857, 1985), suggesting that its interaction with cardiac potassium channels may also be use- and voltage-dependent. To test this hypothesis, guinea pig cardiocytes were prepared by collagenase separation and voltage clamped using the whole cell attached patch clamp technique at 35°C. Only cells that were rod-shaped in 2 mM external calcium and had a resting potential negative to -80 mV were used. From a holding potential of -100, -70 or -40 mV, a conditioning pulse of variable length (250-1250 msec) to +20 mV was applied, followed by a 1250 msec test pulse to -30 mV. The amplitude of the tail current (at -30 mV) was used as an indicator of the potassium channels that were conducting at +20 mV. Under control conditions, tail current amplitude was independent of holding potential. However, in the presence of quinidine (2 μM), tail current decreased as holding potential was made more negative. As the conditioning pulse was lengthened, this voltage-dependent reduction in tail current became less evident. These results indicate that quinidine blocks potassium channels preferentially at negative potentials and unblocks them at potentials in the plateau range, i.e., its action is modulated by membrane potential. We conclude that these voltage- and time-dependent actions of quinidine on this cardiac potassium channel contribute to the rate-dependent actions of quinidine on action potential duration.

T-Pos304 OUTWARD CURRENTS IN CANINE ATRIAL MYOCYTES. Bubien, James K. and W.T. Woods, Jr., Department of Physiology and Biophysics, University of Alabama at Birmingham, Alabama 35294.

Myocytes from 0.1% collagenase-treated canine right atria provided giga-ohm-sealed inside-out membrane patches for ion conductance studies. Current/voltage (I-V) plots, ion substitutions (gluconate for chloride), and responses to tetrathylammonium (1.0 mmole/l) were analyzed to elucidate outward currents. The first current was observed only at trans-patch command (t-p) potentials positive to -50 mV; its slope conductance was 10 ps. The I-V plot is similar to that of Kenyon and Gibbons, J. Gen. Physiol. 73:117-157, 1979). The probability of the channel being open was 10% at t-p potentials from -50 to 0 mV and it increased 50% at potentials positive to 0 mV. The second current was observed only at t-p potentials positive to 0 mV (increasingly outward at more positive potentials); its slope conductance was 105 ps. It exhibited bursting type transitions with gaps between bursts at 5×10^{-4} molar "intracellular" Ca^{++} . Kinetic analysis suggests that the gating frequency within bursts was not altered by voltage, but the burst length increased and the gaps between bursts decreased at more positive potentials. We conclude that we observed two different channels carrying outward current across the canine atrial cell membrane. The first peaked at +40 mV and the second was activated by "intracellular" Ca^{++} . Both have properties consistent with currents known to be carried by K^+ . [Sponsored by NIH (HL-30486) and USAMRDA (DAMD 17-84-R-0111)].

T-Pos305 DIFFERENCES BETWEEN ISOLATED SINUS NODE CELLS AND WORKING MYOCYTES IN THE CANINE RIGHT ATRIUM. Woods, W.T., Jr. and James K. Bubien, Department of Physiology and Biophysics, University of Alabama at Birmingham, Birmingham, Alabama 35294.

In histological sections and in isolated cell culture, there are marked structural differences (size, shape, cytoplasmic components, etc.) between sinus node pacemaker cells and atrial working muscle cells. To study the process of electrogenesis in these populations, structurally and electrophysiologically defined pacemaker cells were isolated from canine atria by 0.1% collagenase treatment and maintained in culture medium (Hamm's F12/DME). Ten canine sinus nodes (SN's) were mapped with microelectrodes, marked with thread, and perfused (SN artery) with canine physiological solution containing 3×10^{-5} M Ca^{++} and collagenase (150 U/ml) for 20 minutes. SN's were excised, minced, and shaken in the perfusing solution. Aliquots were collected at 15 minute intervals for 1 hour. The clear cytoplasm, single nucleus, and characteristic 8 ± 2 micron spherical shape characteristic of the nominal pacemaker cell was well preserved. These cells were electrically quiescent and had membrane potentials of -20 ± 5 mV. However, when they contacted dispersed quiescent atrial myocytes, spontaneous firing was observed in the myocytes. The current voltage curves (obtained from single channel patch clamp recordings) suggested that the membrane conductance characteristics of SN cells are different from those of atrial myocytes. Spontaneous firing of atrial myocytes may be induced by direct contact with SN cells rather than by an inherent property of automaticity in the SN cells. [Supported by NIH (HL-30486) and USAMRDA (DAMD 17-84-R-0111)].

T-Pos306 SAXITOXIN AND NITRENDIPINE BINDING BY SHEEP AND BEEF HEART PLASMALEMMA IS FOUND IN VESICLES OF BOTH SURFACE AND T-TUBULAR ORIGIN. D. D. Doyle, T. J. Kamp, H. C. Palfrey, R. J. Miller, and E. Page, University of Chicago, Chicago, Illinois 60637

Membranes from sheep and beef hearts were fractionated by centrifugation through a 10 - 40% sucrose density gradient into cell surface sarcolemma (CSS) and t-tubular (tt) vesicles. High affinity (HA) and low affinity (LA) ^3H -saxitoxin (STX) binding and HA ^3H -nitrendipine (NTD) binding were measured across the gradient. Distributions in the gradient of Na,K-ATPase activity, ^3H -QNB binding, ryanodine-sensitive Ca^{2+} -uptake (RSCaU), calsequestrin, and cAMP- and calmodulin-stimulated phosphorylation of two 250 - 300 kdalton "foot proteins" (FP) were used to further characterize the fractions. Three corresponding STX and NTD binding peaks centering around 19%, 27%, and 35% sucrose were identified and used to divide the gradient into three regions: I, II, and III. Na,K-ATPase and QNB were highest in I (presumed CSS). III (presumed tt vesicles complexed with junctional sarcoplasmic reticulum (SR)) had highest concentrations of RSCaU, calsequestrin, and FP. III also contained non-junctional SR sedimentable by Ca^{2+} oxalate-preloading, and mitochondrial NaN_3 -sensitive ATPase not precipitable with Ca^{2+} oxalate. II (presumed tt vesicles without junctional SR) had highest STX binding per mg protein and marked reduction in other markers concentrated in I and III. In contrast to skeletal muscle, the ratio (NTD binding sites in tt)/(NTD binding sites in CSS) was ≈ 1.0 . Significant amounts of both HA and LA STX as well as HA NTD binding sites were present throughout the gradient, indicating that Na and possibly Ca channels in heart are found in both surface and t-tubular sarcolemma. Supported by USPHS grant HL 20592, AHA grant 850-863, and NIH grants DA-02121 and MH-40165-01A1.

T-Pos307 EMERGENCE OF ELECTRICAL COUPLING BETWEEN HEART CELLS. H.J.Jongsma, M.B.Rook, A.C.G. van Ginneken. Dept. of Physiology. University of Amsterdam. 1105 AZ Amsterdam; the Netherlands

Membrane currents were measured in single isolated neonatal rat heart cells obtained by collagenase dissociation of whole hearts. Micro suction electrodes were applied to two cells and the I-V relation of each cell was measured. The total I-V relation has a flat region around the membrane resting potential presumably caused by an inward rectifying outward current; consequently the input resistance of the cells is quite high under resting conditions and not very voltage sensitive. Specific membrane resistance at the resting potential was calculated to be of the order of 10 KOhm-cm^2 .

Next, the cells were pushed together and membrane voltage of each of the cells was monitored continuously. After several minutes of contact, action potentials in one cell elicited subthreshold membrane potential displacements in the other one. At this moment transcellular conductance was calculated to be 100 pS which would amount to one junctional channel. Fully synchronized action potentials were recorded when transcellular resistance had decreased to 50 MOhm which amounts to 20 intercellular junctional channels. Transcellular current measurements indicate that the intercellular resistance is not voltage dependent.

T-Pos308 ACCESSIBILITY OF THE ACETYLCHOLINE RECEPTOR δ CHAIN C-TERMINUS TO HYDROPHILIC REAGENTS IN RECONSTITUTED VESICLES. Pierre McCrea, Jean-Luc Popot*, and Donald Engelman, Dept. of M.B.&B., Yale U., New Haven, Ct., and *Institut de Biologie Physico-Chimique, Paris, France

Each of the five Acetylcholine Receptor (AChR) subunits, $\alpha_2\beta\gamma\delta$, is believed to have the same number of transmembrane crossings. Attempts have been made to predict and determine the number. (J.-L. Popot, J.-P. Changeux, *Physiol.Rev.*, 1984). Since the N-terminus of each subunit is extracellular, the problem of distinguishing between an even and odd number of transmembrane passes may be solved by localizing the C-terminus. Recent antibody studies appear to support the cytoplasmic location of the C-termini. (E.F. Young et al., *PNAS*, 1985; M. Criado et al., *PNAS*, 1985).

Most of the AChR isolated from *Torpedo* sp. electric organ is present as a dimer, formed by a disulfide bridge joining two AChR via the penultimate C-terminal cysteine of the δ subunit. We have used this bridge as a marker of the C-terminus. Its accessibility to hydrophilic reducing reagents has been tested in reconstituted vesicles. The outward facing AChR may be labeled exclusively using ^{125}I -bungarotoxin. The ability of formally charged reductants such as glutathione to access the disulfide in intact and disrupted vesicles may then be compared using sucrose gradients or SDS-PAGE. No difference in reduction rates has been observed. The reduction into A and B fragments of tryptically cleaved diphtheria toxin trapped inside the same vesicles, on the other hand, was accelerated ~5 times by vesicle disruption. Although not a direct demonstration, the observed accessibility is consistent with that which one would expect of an extracellular disulfide. It is therefore most compatible with models that propose an even number of transmembrane crossings.

T-Pos309 STRUCTURAL ANALYSIS OF MEMBRANE-BOUND AND DETERGENT-SOLUBILIZED NICOTINIC ACETYLCHOLINE RECEPTOR. Michael P. McCarthy, Alok K. Mitra, and Robert M. Stroud. Dept. of Biochemistry and Biophysics, U. of California, San Francisco, CA 94122.

The nicotinic acetylcholine receptor (AChR) from *Torpedo californica* is a large, multi-subunit, transmembrane protein which acts as a chemical receptor and ion channel. We have investigated the relationship between the structure of the AChR and the mechanisms by which it performs its several functions by analyzing oriented arrays of both native membrane-bound and detergent-solubilized AChR in the electron microscope. Crude preparations of membrane-bound AChR reproducibly form ordered, two-dimensional crystalline tubes after incubation at 4°C for >4 weeks. These tubes are well ordered and diffract to 26 angstroms. Upon solubilization in β -octylglucoside, small three-dimensional crystals of the AChR grow by vapor diffusion against organic solvents at room temperature and low pH. Images of negatively-stained specimens prepared from fragmented or sectioned regions of these crystals show reflections out to a resolution of 30 angstroms in the optical diffractometer. Computer analysis allows us to map the projected structure of the AChR in these two states. The agreement between the structures observed for both membrane-bound and detergent-solubilized AChR is noteworthy, suggesting that either the packing forces involved in crystallization impose a single morphology upon the AChR, or more likely, that both detergent- and membrane-bound AChR are quite similar in structure, as suggested by a number of biochemical studies.

T-Pos310 SWINE TRACHEAL SMOOTH MUSCLE MUSCARINIC RECEPTOR AND ELECTROPHYSIOLOGICAL PROPERTIES.

Jerry M. Farley, C. M. Yang, H. M. Huang, P. Murali Mohan and Terry M. Dwyer. Depts. Pharmacol. & Toxicol. and Physiol. & Biophysics, Univ. MS Med. Ctr., Jackson, MS 39216-4505.

Activation of muscarinic receptors leads to contraction of tracheal smooth muscle. Swine tracheal muscle is no exception, contracting in response to the cholinergic agonists acetylcholine and bethanechol. [^3H] quinuclidinyl benzilate (QNB) binds with high affinity to tissue homogenates with a maximum receptor density of 1.8 pmoles/mg protein. The muscarinic receptors of swine tracheal cells are of the M_2 subtype as determined by inhibitor displacement of [^3H] QNB binding. The displacement of [^3H] QNB by cold pirenzepine, QNX, QNB, atropine and scopolamine is best described by competition for a homogenous population of binding sites with K_D 's of 256, 0.8, .02, 5.5, $7.2 \times 10^{-9}\text{M}$, respectively. Displacement of [^3H] QNB by the agonists carbachol and pilocarpine was best fit by a 2-site model, K_{D1} ; 49, 1.2 and K_{D2} ; 2.2, $5.4 \times 10^{-6}\text{M}$, respectively.

Muscarinic receptor activation is also known to alter membrane permeability to ions although the identities of the channels involved are not clear. In intact tissue the resting membrane potential of smooth muscle cells was 60 ± 5 mV. Spontaneous electrical activity was not generally observed except in a few cells where aborted action potentials were seen. Tetraethyl ammonium evoked spontaneous activity in the cells. For single channel recording, relaxed tracheal smooth muscle cells were isolated by enzymatic dispersion using 0.1% collagenase (type 1), 0.01% DNAase and 0.1% BSA in a standard Hepes buffered Ringer solution. Patch clamp studies on tracheal cells demonstrate the existence of Ca^{++} activated K channels which may be important in smooth muscle cell excitability. (Supported by Army contract #DAMD17-83-C-3248.)

T-Pos311 IS THE HYDROLYSIS OF PHOSPHATIDYLINOSITOL-4,5-BIPHOSPHATE (PIP_2) INTO INOSITOL-1,4,5-TRIPHOSPHATE (IP_3) THE PRIMARY STEP OF HORMONAL ACTIVATION OF INOSITOL LIPID METABOLISM? R. Rubio, P.T. Hawkins and R.H. Michell. Dept. of Physiology, University of Virginia, Charlottesville, Virginia 22908 and Dept. of Biochemistry, University of Birmingham, Birmingham, England.

Activation of PIP_2 specific phosphodiesterase may be the primary target of Ca^{++} mobilizing-hormones. This proposition is supported by the fact that in several cell systems, a time course of hormonal activation shows a rapid drop in the levels of PIP_2 paralleled by a rise in IP_3 . We have performed similar experiments in rat lipocytes stimulated either with oxytocin or vasopressin in the presence of 10 mM LiCl. We confirmed the findings reported in other cell systems, namely within 0-15 sec. after hormone addition, PIP_2 and phosphatidylinositol-4-phosphate (PIP) gradually decreased with a reciprocal rise in IP_3 and inositol-1,4-bisphosphate (IP_2). We reasoned that if the initial activation step is the PIP_2 hydrolysis to IP_3 one would expect within the first 15" incubation with a hormone: a reciprocal equal change in PIP_2 and IP_3 , the drop in PIP_2 precede and be greater than the drop in PIP , the rise in IP_3 precede and be greater than the rise in IP_2 . The results did not agree with these predictions: $-\Delta\text{PIP}_2$ was 8 times greater than $+\Delta\text{IP}_3$, PIP_2 and PIP drop simultaneously being $-\Delta\text{PIP}$ 4 times larger, finally IP_3 and IP_2 rise parallelly being $+\Delta\text{IP}_2$ 6 times greater. In addition, our recent chromatographic results show that the various inositol derivatives may be mixture of at least two isomeres. Although these results may not invalidate the proposal of primary activation of PIP_2 -phosphodiesterase. They indicate that more rapid, sensitive and discriminating kinetic techniques are required, to determine whether PIP_2 hydrolysis is the primary step of agonist action.

T-Pos312 PHARMACOKINETICS OF DRUG DELIVERY VIA VESICLES TARGETED TO THE HEPATIC ASIALOGLYCOPROTEIN RECEPTOR Paul R. Dragsten, Gail Sauer, David B. Mitchell, and Theresa Baker, The Procter and Gamble Company, Cincinnati, Ohio 45247

We have quantitatively assessed the utility of vesicles targeted to the hepatic asialoglycoprotein receptor as a drug delivery system for treatment of human liver diseases. Small, unilamellar vesicles (60-80nm diameter) containing in their membrane the molecule digalactosyl diglyceride are efficiently removed from circulation by the liver. Using an isolated, perfused rat liver system we show that this interaction is via the hepatic asialoglycoprotein receptor, and that the uptake process proceeds with minimal leakage of vesicle contents. At low lipid doses, the single pass extraction of vesicles by the liver is 50%, which means that this vesicle formulation operates at nearly optimal efficiency as a drug delivery system to the liver. Binding of vesicles to the liver was determined to saturate at 1.3 mg total lipid per rat liver, and the maximum steady state turnover rate of vesicles at 37°C was 22µg lipid/min. This implies that the recycling time for the vesicle receptors is around 60 min. The *in vivo* time course of vesicle distribution is quantitatively in accord with predictions from the perfused liver experiments. We have incorporated this data into a pharmacokinetic model for targeted vesicle delivery of drugs to the liver which takes into account saturation of vesicle uptake and serum-induced vesicle leakage.

T-Pos313 EFFECTS OF THE CALMODULIN INHIBITOR STELAZINE ON LDL RECEPTOR MOTION ON CELL SURFACES. Richik N. Ghosh, David Gross and Watt W. Webb, School of Applied and Engineering Physics, Clark Hall, Cornell University, Ithaca, NY 14853-2501.

Both clusters and single molecules of the LDL receptor can be localized on cell surfaces by using the intensely fluorescent ligand diI-LDL (Barak and Webb, J. Cell Biol. 90, 595-604, 1981). Using quantitative digital video fluorescence microscopy, we examined LDL receptor dynamics on human fibroblasts treated with the calmodulin inhibiting drug Stelazine (trifluoperazine dihydrochloride). Tracking the motions of discrete ligand-receptor clusters on J.D. (GM2408A) fibroblasts, we find mobilities an order of magnitude larger than previously measured on untreated J.D. cells (Gross and Webb, Biophys. J. 41, 215a, 1983). On normal fibroblasts (GM3348), internalization of the LDL receptors seems to be inhibited as suggested previously (Gross and Webb, 8th International Biophysics Congress, 1984). By integrating the intensities of the fluorescent diI-LDL spots, ligand-receptor cluster sizes were determined. Stelazine treatment reduced the cluster size distribution of normal cells from the usual range of >4 LDLs per cluster (Gross and Webb, Biophys. J., submitted) to a distribution of ≤4 LDLs for about 50% of the clusters. This small cluster size distribution was maintained over time (1 hour), and mimics the distribution on J.D. cells untreated with Stelazine (*ibid.*).

This work was supported by grants from the NSF (DMB 83-03404), ONR (N00014-84-K-0390), NIH (GM33028) and the Cornell Biotechnology Program.

T-Pos314 FLUORESCENT LABELING OF A COMMON CELL SURFACE PROTEIN WITH AN INTRINSIC PROBE: EXCHANGE OF FITC BETA-2-MICROGLOBULIN INTO CLASS I MHC ANTIGENS ON LIVING CELLS. J. Hochman, T. Wei, M. Weir, and M. Edidin, Department of Biology, Johns Hopkins University, Baltimore, MD 21218

Class I MHC antigens are a set of polymorphic glycoproteins important in cell mediated immune responses which are present on the surface of most mammalian cells. They consist of a transmembrane heavy chain noncovalently associated with beta-2-microglobulin (β_2M), a small water soluble subunit. We have intrinsically labeled MHC antigens on the surfaces of living cells by exchanging single labeled FITC derivatives of human β_2M with the native subunit. Chromatography of fluorescein β_2M on hydroxylapatite separated three peaks containing single labeled derivatives of β_2M . These derivatives labeled class I heavy chains on suspended and adherent cells from human, mouse, and dog, but did not label Daudi cells, which do not express the class I heavy chain. Mouse T lymphoma cells (RDM4 and EL4) labeled with β_2M from peaks B and C were recognized by monoclonal antibodies to class I MHC antigens suggesting that the exchange did not significantly alter the conformation of the antigens. The exchange of the human β_2M derivatives with the native protein bound to class I heavy chains on EL4 and RDM4 was measured using flow cytometry. Derivatives of β_2M in peaks B and C exhibited saturable high affinity binding while that in peak A showed diminished binding. The binding of all three derivatives was reversible and could be blocked with excess unlabeled β_2M . Applications of this intrinsic labeling technique to understanding the membrane properties and immunological function of the MHC antigens will be discussed.

T-Pos315 BIOLOGIC AND PHYSICAL CHARACTERIZATION OF IMMUNOGLOBULINS FLUORESCENTLY LABELED ACROSS DISULFIDE BONDS. Beverly Packard, Akira Komoriya, and Michael Edidin. Biology Department, The Johns Hopkins University, Baltimore, MD. 21218 and Revlon Biotechnology Research Center, Rockville, MD. 20850

As previously reported (Biophys. J. 47:591a (1985)), we have designed and synthesized crabscein, a fluorescent label that is directed at disulfide bonds of proteins. By virtue of its insertion across a disulfide bond in an IgG, it is rigidly attached to the macromolecule and has a rotational correlation time of the segment of protein to which it is covalently bound. Exhaustive trypsinization of the crabscein-labeled IgG yielded a single fluorescent fragment; the amino acid sequence of this fragment indicated that the label had incorporated across the disulfide bond in the F_c domain most distal to the F_{ab} arms.

IgEs represent a class of immunoglobulins which binds to mast cells via their F_c domains; therefore, we chose to label an IgE with crabscein to examine the dynamics of the interaction between a physiologic ligand and its cellular receptor. We have a biologically active IgE that contains ca. one crabscein per IgE and are pursuing dynamic measurements of this interaction.

T-Pos316 LATERAL DIFFUSION OF CLASS I MHC ANTIGENS INTRINSICALLY LABELED WITH FLUORESCENT BETA-2-MICROGLOBIN. Marjorie L. Wier, Jerome Hochman, and Michael Edidin. Department of Biology, The Johns Hopkins University, Baltimore, MD 21218.

Class I major histocompatibility antigens consist of a transmembrane heavy chain which is noncovalently associated with a water soluble light chain, beta-2-microglobulin (β_2M). The MHC antigens can be intrinsically labeled by exchanging FITC conjugated β_2M for cell surface β_2M and this property has been used to label the MHC antigens on human, mouse, and dog cells. Using the fluorescence recovery after photobleaching technique (FRAP), we compared the lateral diffusion of MHC molecules on cells labeled with FITC β_2M with that on cells labeled with FITC conjugated Fab fragments of monoclonal antibodies directed against Class I antigens. Lateral diffusion of MHC molecules was examined on mouse and human lymphocytes and on normal and transformed human fibroblasts. In all cases, the average lateral diffusion coefficient and percent recovery were equivalent for both labels. The measured lateral diffusion coefficients ($1-5 \times 10^{-10}$ cm²/sec) and mobile fractions (40-60%) for β_2M or antibody were similar to those observed for other membrane proteins. When fibroblasts were plated on extracellular matrix materials, the average mobile fraction of the intrinsically labeled MHC antigens was decreased (from 58% to 32%) and the percent of cells showing no measurable recovery increased from 0-27%. These measurements were consistent with previously reported results on cells labeled with antibody (Biophysics J. 47:203a). The results provide further evidence that the antibody label does not significantly alter the lateral diffusion of the MHC molecule and suggest that β_2M can be useful as a membrane label for many types of cells.

T-Pos317 MOLECULAR PARAMETERS INFLUENCING RECEPTOR CROSSLINKING AND HISTAMINE RELEASE IN HUMAN BASOPHILS. Donald MacGlashan, Jr., Renee Z. Dintzis and Howard M. Dintzis, Dept. of Medicine, Dept. of Biophysics and Dept. of Cell Biology and Anatomy, Johns Hopkins Medical School, Baltimore Md. 21205.

It has long been known that multivalent antigens interacting with IgE antibody molecules bound to IgE receptors on the surface of basophils and mast cells are responsible for triggering such cells to release histamine and other mediators of the allergic response. As part of a study of the molecular properties of antigenic molecules necessary for triggering cell receptor mediated function in various cells of the immune system, we have studied the response of human basophils to polyacrylamide molecules multivalently coupled to DNP (dinitrophenyl) groups. In order to initiate histamine release with antigens, basophils were passively sensitized with a monoclonal IgE with specificity for DNP ($K_a = 7 \times 10^{-7}/M$). The surface IgE density was systemically varied, as was the polymer size, epitope valence and spacing. Varying surface IgE density 10 fold had no measurable effect on the concentration of antigen for optimal histamine release as predicted by some models of basophil histamine release, although cell sensitivity to antigenic challenge increased 100 fold (for equal histamine release). Varying epitope density 100 fold ($DNP_1 \rightarrow DNP_{100}$) altered both the apparent optimal concentration for release (a 100 fold shift to lower concentrations) and dramatically increased the cell sensitivity (10^6 fold shift, 50% maximal response at $\approx 10^{-4}$ $\mu g/ml$). Significantly, basophils were able to respond to linear polyacrylamide antigens substituted with only 2 or 3 DNP groups. Interestingly, maintaining a constant epitope density but varying molecular size (valence increase of 11 to 53) had little effect on the shape of the dose response curve. Based on these experiments and the fact that some predictions on the behavior of basophils towards these antigens have not been experimentally verified, we believe that this system represents a useful experimental model of antigen induced crosslinking reactions capable of guiding theoretical models.

T-Pos318 CELLULAR UPTAKE AND INTRACELLULAR LOCALIZATION OF A FLUORESCENT CHOLESTEROL ESTER ANALOG BY DIGITAL IMAGING FLUORESCENT MICROSCOPY. M. Picardo, R. Homan, L. C. Smith, and H. J. Pownall, Baylor College of Medicine, Houston, Texas 77030

A fluorescent cholesterol ester analog (DPH-Chol) containing 3-(p-(6-phenyl)-1,3,5-hexatrienyl)phenylpropionic acid as the acyl chain was used to monitor the location and rate of uptake of low density lipoprotein (LDL) cholesterol ester by living cultured human fibroblasts. DPH-Chol was incorporated into LDL by exchange with reassembled high density lipoprotein donors and partially purified cholesteryl ester transfer protein. By digital imaging fluorescence microscopy (DIFM), we observed the time-dependent uptake of DPH-Chol into the perinuclear region of cells. Following uptake, fluorescence was also present in other less well-defined regions of the cell. Cellular internalization of LDL labeled with both DPH-Chol and a lysosome specific carbocyanine dye (DiI(18)) resulted in colocalization of fluorescence suggesting that DPH-Chol was taken into the lysosomes with LDL. TLC of lipid extracts from fibroblasts incubated for 24 hours with the labeled LDL showed that DPH-Chol was metabolized within the cells and was an acyl chain donor for glyceride synthesis. The cytoplasmic hydrolysis of the fluorescent cholesteryl ester was inhibited by including chloroquine in the incubation medium. Competition studies with radiolabeled (^{125}I) LDL indicated that uptake of the DPH-Chol labeled LDL was receptor-mediated and saturable after 6 hours incubation. A comparable rate of uptake was observed for live cells with DIFM. In conclusion, the DPH fluorophore is an effective fluorescent marker for visualizing the transport of lipids into cells via LDL. The use of DPH lipid analogs in conjunction with DIFM yields both spatial and temporal information for the cellular uptake and metabolism of lipids.

T-Pos319 ENZYMATIC PROBE OF INTERACTIONS BETWEEN GANGLIOSIDE Gd_{1a} AND ENKEPHALINS. M. Myers and E. Freire, Department of Biochemistry, University of Tennessee, Knoxville, TN 37996.

Previously we have shown by high sensitivity differential scanning calorimetry (DSC) that the enkephalin analogue (D-ala²) methionine enkephalinamide has a profound effect on the thermotropic behavior of dipalmitoylphosphatidylcholine (DPPC) bilayers containing ganglioside Gd_{1a} . In this report, we present further evidence of ganglioside Gd_{1a} -enkephalin interaction using (D-ala²) methionine enkephalinamide and methionine enkephalin (tyr-gly-gly-phe-met). Both these peptides may serve as substrates for the enzyme tyrosinase which *in vivo* catalyzes the hydroxylation of tyrosine to dopa and dopa to dopaquinone. The K_m for the reaction using methionine enkephalin is $1.5 \times 10^{-4}M$ while that of the (D-ala²) methionine enkephalinamide reaction is $3.0 \times 10^{-4}M$. The interaction of Gd_{1a} with the enkephalin molecule causes a decrease in the initial velocity of the enzymatic reaction. In the case of (D-ala²) methionine enkephalinamide, micellar ganglioside is more effective in inhibiting the reaction than vesicle-bound ganglioside. With methionine enkephalin, however, the converse is true. Analysis of the inhibition kinetics yields an association constant of $0.8 \times 10^5 M^{-1}$ for methionine enkephalin to membrane-bound ganglioside Gd_{1a} . The physical state of the membrane (i.e., gel or liquid crystalline) seems to have little or no effect on the extent of the decrease in initial velocity as evidence by experiments utilizing Gd_{1a} incorporated into both DPPC and DMPC suv's. The specific interactions observed thus far suggest that gangliosides may have an *in vivo* role in opiate receptor functioning. (Supported by NIH grant NS-20636.)

T-Pos320 PHORBOL ESTER INDUCED ALTERATIONS IN CELL SURFACE ORGANIZATION OBSERVED BY PHOTOELECTRON MICROSCOPY. D.L. Hablston, G.B. Birrell, K.K. Hedberg, and O.H. Griffith, University of Oregon, Eugene, Oregon, 97403.

Photoelectron microscopy (PEM), the electron optics analog of fluorescence microscopy, has been shown to be a useful technique for the examination of uncoated biological surfaces (Birrell et al., PNAS 82, (1985) 109; Mrsny and Griffith, J. Reprod. Fert. 74, (1985) 127). For example, surface details of cultured cells, red cell ghosts, and sperm can be observed. Photoelectron labels have also been developed (Griffith and Birrell, TIBS, 10 (1985), 336). In the present study, PEM was used to document the release of fibronectin from fibroblast cell surfaces resulting from exposure to the potent tumor promotor, TPA. Normal human foreskin fibroblasts were exposed to TPA at 100 ng/ml for various periods of time, fixed, and labeled for both immunofluorescence and immunophotoelectron visualization of cell surface fibronectin. In photoelectron micrographs of labeled cells, a decrease in the amount of cell surface fibronectin was evident 30 min after the addition of TPA to the culture medium. It is difficult to see this early effect by immunofluorescence because the presence of substantial amounts of fibronectin remaining beneath the cell culture obscures the initial changes taking place on the upper cell surface. The unique surface sensitivity of PEM makes it useful for the detection of early phorbol ester induced alterations in cell surface organization (supported by NIH grant CA 11695).

T-Pos321 DISTRIBUTION OF GLUCOSE TRANSPORTERS AND INSULIN RECEPTORS ON PLASMA MEMBRANES AND TRANSVERSE TUBULES OF SKELETAL MUSCLE. Elena Burdett[§], Troy Beeler[†], and Amira Klip[§], [§]The Hospital for Sick Children, Toronto, Ont. M5G 1X8, Canada, and [†]USUHS, Bethesda, Maryland.

Skeletal muscle is the primary target of insulin, and a major function of the hormone in this tissue is stimulation of glucose uptake. Glucose is taken up by muscle cells through a system of facilitated diffusion, constituted by a polypeptide of Mr ~40,000 (Klip et al., Arch. Biochem. Biophys., 226, 198, 1983). In muscle, the plasma membrane is physically continuous with the invaginated transverse tubules which transmit the electrical signal for excitation-contraction coupling. Studies with dissected muscles indicate that there may be specific functions segregated in each plasma membrane and transverse tubules. This study was performed to analyze the distribution of glucose transporters and insulin receptors in isolated surface membranes from rabbit skeletal muscle.

Plasma membranes were prepared according to Seiler and Fleischer (J. Biol. Chem. 257, 13862, 1982), and transverse tubules according to Roseblatt et al. (J. Biol. Chem. 256, 8140, 1981). The origin of the isolated membranes was confirmed by the presence of nitrendipine binding sites in transverse tubules but not in plasma membranes.

Insulin receptors, detected by saturable binding of ¹²⁵I-insulin, were present in the same proportion in plasma membranes and transverse tubules, and showed similar dissociation constants. Glucose transporters, detected by D-glucose-sensitive binding of [³H]-cytochalasin B, were enriched in the transverse tubules relative to the plasma membranes. The dissociation constant was the same in both membrane fractions. The differential distribution of glucose transporters may be of physiological consequence in the action of the hormone.

Supported by the Medical Research Council of Canada.

T-Pos322 FACTORS INVOLVED IN POTASSIUM-INDUCED REVERSE-TRANSFORMATION OF CELLS INFECTED WITH A TEMPERATURE-SENSITIVE TRANSFORMATION MUTANT VIRUS. C.-N. Lai, G.E. Gallick, S.A. Maxwell, B.R. Brinkley* and F.F. Becker. Departments of Pathology and Tumor Biology, University of Texas System Cancer Center, Houston, TX, and Department of Cell Biology, University of Alabama, Birmingham, AL.

It was previously found that K⁺ at high concentrations (52-72 mM hypertonic KCl) induced reverse-transformation in 6m2 cells, a clone of rat kidney cells (NRK) infected with a temperature-sensitive transformation virus. The K⁺ treated cells grown at permissive temperature (33°C) exhibit flat morphology and reduced soft-agar growth, characteristics of cells grown at 39°C, a temperature not permissive for transformation. In the current study, the flattening of cells at 33°C induced by K⁺ was observed by electron microscopy to occur within 6 h of exposure, and was similar to that produced by temperature shift to 39°C. A potassium effect on P-85^{gag-mos} was observed within 1 h and its activity was approximately 50% of control at 2 h. After 3 days at 72 mM KCl (hypertonic), P-85^{gag-mos} content and synthesis were reduced by 75% compared to untreated cells at 33°C. The CMTC and F-actin cables were affected more slowly by potassium. Only after 3 days was the CMTC of K⁺ treated cells a fine reticulum network similar to NRK cells, and the F-actin cables, similar to, but not as well defined as NRK. The cables were particularly well developed near the membrane with frequent cross-patching, although less extensive than in NRK cells. As with temperature shift, the effect of potassium on 6m2 cells occurred first at the level of P-85^{gag-mos} activity while changes in CMTC and F-actin cables occurred later. The results of this study indicate that the decline of P-85^{gag-mos} and/or the effect on the cytoskeletal system were not sufficient to account for the degree of reverse-transformation induced by K⁺.

T-Pos323 INTER-RECEPTOR SPACING IN IgE RECEPTOR AGGREGATES ON THE SURFACE OF RBL CELLS. T. A. Ryan, A. K. Menon, D. Holowka, B. Baird and W. W. Webb, Depts. of Physics (T.A.R.), Applied Physics (W.W.W.) and Chemistry (A.K.M, D.H., B.B.), Cornell University, Ithaca, NY 14853.

A measure of the average inter-receptor spacing in large patches of crosslinked IgE receptors on the surface of rat basophilic leukemia (RBL) cells has been provided by digital fluorescence microscopy measurements. By comparing the fluorescence intensity of diffusely distributed ^{125}I -FITC-IgE-receptor complexes with that inside a patched area one may obtain an estimate of the magnitude of the decrease in receptor spacing after aggregation. A measurement of the specific activity of the ^{125}I -FITC-IgE, the ^{125}I counts per cell and the average cell geometry allows one to calculate average inter-receptor distances for both the diffuse and patched receptors. Assuming a smooth cell surface, we find that the inter-receptor distance for the diffuse IgE-receptor complex is $\sim 420\text{\AA}$. By comparing the fluorescence intensity of the diffuse receptors to that of the patches induced by crosslinking with a rabbit polyclonal anti-IgE antibody we find that the inter-receptor spacing of the crosslinked receptor complexes is $\sim 185\text{\AA}$. Furthermore by measuring samples with varying initial labeled receptor densities we have found that the final inter-receptor distance in the crosslinking induced aggregate is strongly dependent on the original diffuse density. Concurrently a lower bound of $\sim 100\text{\AA}$ was obtained with fluorescence energy transfer measurements for the average inter-receptor distance between pairs of IgE-receptor complexes crosslinked by antibodies. These results suggest that the dimensions of the IgE-receptor complex or the crosslinker do not completely determine the inter-receptor spacing or the organization of the receptors in large aggregates. Supported by grants from NIH (GM33028), NSF (DMB 83-03434), ONR (N00014-84-K-0390) and NIH (AI18306).

T-Pos324 PROTEOLYTIC MAPPING OF THE AGONIST AND ALLOSTERIC ANTAGONIST BINDING SITES ON THE NICOTINIC ACETYLCHOLINE RECEPTOR (AChR) α -SUBUNIT. Steen E. Pedersen, Evan B. Dreyer and Jonathan B. Cohen, Washington University School of Medicine, St. Louis, MO 63110.

Proteolytic cleavage by *S. Aureus* V8 protease of the α -subunit of the AChR from *Torpedo californica* yields two major bands, when analyzed by SDS-PAGE, of 20 and 18 kDa. The smaller, 18 kDa, band was found to contain carbohydrate by direct binding of fluorescein isothiocyanate-labelled concanavalin A. Treatment with endoglycosidase H resulted in altered migration of the 18 kDa band, also indicating the presence of carbohydrate on this fragment. If the α -subunit was affinity labelled with [3 H]maleimidobenzyl trimethyl ammonium iodide ([3 H]MBTA) or photoaffinity-labelled with [3 H]d-tubocurarine prior to cleavage with V8 protease, only the 20 kDa fragment contained the reactive sites. The upper, 20 kDa, band also specifically bound [125 I] α -bungarotoxin after electrophoretic transfer onto Zetabind paper. When the α -subunit was radiolabelled with [3 H]-meproadifen mustard, an affinity label for the allosteric antagonist binding site, the V8 protease cleavage pattern revealed an additional minor band at 21 kDa that contained the radiolabel. This band was apparently related to the 20 kDa band as it also contained the [3 H]MBTA-reactive site. N-terminal amino acid sequence analysis revealed that the 20 kDa fragment begins at Ser 173 and that the 18 kDa fragment begins at Val 46. The cleavage pattern generated by V8 protease was unaffected by the absence or presence of disulfide reducing agents, indicating the lack of disulfide linkages between the two predominant bands. These data suggest that only sequence beyond Ser 173 contributes to the agonist and allosteric binding sites, and suggests that Cys 128 or Cys 142 do not contribute to the labile disulfide bond near the agonist binding site.

T-Pos325 SINGLE CHANNEL STUDIES REVEAL THREE CLASSES OF ACETYLCHOLINE-ACTIVATED CHANNELS IN MOUSE SKELETAL MUSCLE. J.A. Steele and J.H. Steinbach, Depts. of Anesthesiology and Anatomy/Neurobiology, Washington Univ. School of Medicine, St. Louis, MO 63110.

Noise analysis of ACh-activated channels at the endplates of rat muscle have shown that there is a 3-fold decrease in mean channel open time during development (Fischbach & Schuetze, J. Physiol. 303:125, 1980). However, the properties of AChR channels which are present extrajunctionally at early stages of development have not been studied. We utilized single channel recording techniques to examine these AChRs. Recordings were made at low ACh concentrations (100 nM) from cell-attached patches on isolated fibers obtained by enzymatic treatment of flexor digitorum brevis muscles of newborn C3H mice. We compared these results to data obtained from extrajunctional receptors on denervated (1 wk) adult fibers. For the adult denervated muscle, two classes of AChR currents were apparent. One had a single channel conductance of 45 pS and a mean burst duration (minimum closed time 2 ms) of 2.2 ms at -25 mV to V_m (21°C). The other had a conductance of 33 pS and a mean burst duration of 6.7 ms. For the neonatal muscle, there was a single class of AChR channels with a conductance of 35 pS and a mean burst duration that was 2-3 times longer than that of the small conductance channel on the denervated fibers. The basis for the differences is unknown but our results suggest that 3 classes of AChRs appear during development.

(Supported by NIH NS 22356; JAS supported by AHFMR postdoctoral fellowship.)

T-Pos326 A DRUG WHICH ALTERS PROTEIN GLYCOSYLATION AFFECTS ACh RECEPTOR SINGLE CHANNEL CURRENTS IN BC3H-1 CELLS. M. Covarrubias*, J.H. Steinbach*, M.M. Smith# and J.P. Merlie#. *Depts. of Anesthesiology and Anatomy/Neurobiology, and #Dept. of Pharmacology, Washington University School of Medicine, St. Louis, MO 63110.

We have used single channel records to study the effect of deoxynojirimycin on acetylcholine receptor function. This drug inhibits cellular processing of sugar moieties on proteins, and changes the electrophoretic mobility of at least the alpha subunit of the ACh receptor synthesized by BC3H-1 cells. We studied the function of modified ACh receptors by blocking existing receptors with α -bungarotoxin, then treating the cells with deoxynojirimycin (1 mM) for 48 hours. Currents were elicited with a low concentration of ACh (100 nM) at room temperature, either cell-attached or with inside-out patches. The single channel conductance does not change in treated cells, compared to normal controls from the same set of cultures. However, our observations show a marked increase in the proportion of channel openings which are isolated, brief duration events (mean open time 0.2 to 0.5 msec). The proportion of brief openings depends on membrane potential, but increases from 10%-20% (control) to 40%-60% (treated). These observations suggest that the carbohydrate moiety may influence the function of the ACh receptor. We are investigating the basis for this effect.

(Supported by NIH grants to JHS and JPM. MMS supported by NIH training grant T32 NS07057.)

T-Pos327 RECONSTITUTION OF ACETYLCHOLINE RECEPTOR FROM *TORPEDO CALIFORNICA* IN POLYMERIZABLE LIPIDS. *Dalziel, A.W., **Price, R., **Singh, A., ***Yager, P. *Georgetown University, Washington DC, **Geo-Centers, Newton Falls, MA, ***Naval Research Laboratory, Code 6190, Bio/Molecular Engineering Branch, Washington, DC 20375-5000

As a first step in developing biologically based sensors we have incorporated acetylcholine receptor into polymerized vesicles. The receptor was purified from electroplax tissue of *Torpedo californica* by affinity chromatography. While solubilised receptor was bound to the affinity column exogenously-added cholate-solubilised 1,2 dioleoyl-*sn*-glycero-3-phosphocholine was exchanged for endogenous lipids. Reconstituted vesicles formed from purified receptor and several lipids including a polymerizable phospholipid, bis (1,2(hencosa 10,12 diynoyl))-*sn*-glycero-3-phosphocholine were examined by electron microscopy. Freeze fractured samples demonstrated that vesicles ranging from 60nm to 1800nm were formed depending on the lipid added prior to reconstitution. When vesicles containing polymerizable lipid were frozen to -70°C and irradiated with ultraviolet light (254nm) a red polymeric phospholipid formed.

Modifications to previously developed spectrophotometric methods of measuring ion flux resulted in a convenient assay for acetylcholine receptor based on the fluorescence quenching of an entrapped fluorophore by Cs⁺ ions. The fluorophore 1,3,6,8 pyrenetetrakisulfonic acid was substituted for compounds used in previous assays because it is commercially available, it has a high molar extinction coefficient, and it is extremely polar. Internal volume of the vesicles was determined after lysis with octylglucopyranoside provided the concentration of fluorophore was low enough to prevent self quenching.

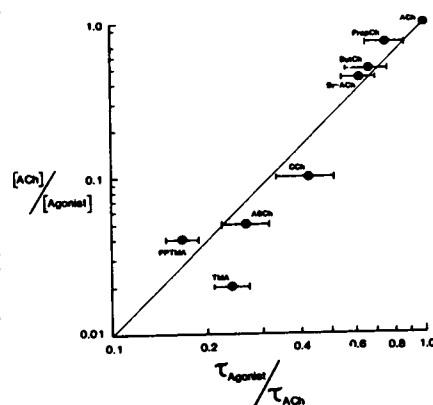
T-Pos328 ALTERATIONS IN THE RATE OF RECEPTOR DEGRADATION DURING DEVELOPMENT OF *XENOPUS* MYOTOMAL MUSCLE. P. Brehm, Dept. of Physiology, Tufts Medical School, Boston, MA. 02111.

The turnover rate of acetylcholine (ACh) receptors was studied on developing myotomal muscle from *Xenopus laevis*. Tail musculature was dissected from tadpoles (stages 33 to 49) and maintained in organ culture. Prior to organ culture each tail was treated with 40 nM ¹²⁵I alpha-bungarotoxin for 60 min and washed extensively. ACh receptor degradation was assessed by the time-dependent release of radioactivity from each tail. The relationship between released counts (% total) and time in organ culture was fit to a single exponential to estimate the rate constant of receptor degradation. At stage 34 of embryonic development the rate constant was 72 hr⁻¹ (half-life=50 hrs). Beginning at stage 41, the rate constant progressively decreased until stage 47, after which no further decrease beyond 306 hr⁻¹ (half-life=213 hours) was observed. Surprisingly, no significant component corresponding to the embryonic rate constant of 72 hr⁻¹ was present in the degradation curves from any tails beyond stage 35 even though extrajunctional receptor density remains high at these stages. This finding is consistent with a developmental decrease in the degradation rate for extrajunctional receptors. It could be argued that tails which showed slow degradation had fewer extrajunctional receptors. To the contrary, however, tails with slower degradation rates invariably exhibited the highest binding. A consistent inverse correlation was found to exist between receptor number and the degradation rate for all stages beyond 35. These data suggest that the maintenance of high extrajunctional receptor density throughout the life of the muscle, as measured electrophysiologically, is a consequence of slow receptor degradation over the entire muscle surface. NIH Grant NS18205

T-Pos329 AGONIST EFFICACY AT THE MOTOR ENDPLATE: IS AGONIST POTENCY RELATED TO CHANNEL OPEN TIME? D.J. Adams, Dept. of Pharmacology, Univ. of Miami Sch. Med., Miami, FL 33101

The dose-response and single channel characteristics of the nicotinic receptor to different cholinomimetic agonists were investigated in frog and rat skeletal muscle. The endplate region of single frog muscle fibers was voltage clamped using the vaseline-gap method. Agonists were bath applied at equipotent concentrations producing -20 to -30nA currents at -70mV. Power density spectra of current fluctuations produced by each different agonist were fitted by a single Lorentzian curve to determine the single channel conductance and apparent channel open time (burst duration). The single channel conductance for the eight agonists tested were similar (20-27pS; cf. Gardner et al. (1984) Nature 309, 160). Dependence of single channel open time on concentration of carbachol (CCh), acetylthiocholine (ASCh) and tetramethylammonium (TMA) was studied with the patch-clamp method in rat cultured myotubes. The open time distributions indicate that the brief open times obtained for the low agonist concentrations studied is not a consequence of rapid ion channel block by the agonist (Sine & Steinbach (1984) Biophys. J. 46, 277). The relation described by Figure 1 suggests that the efficacy of these agonists are only partly determined by burst duration.

Figure 1: Relation between apparent open times and the potencies of various agonists. The ratio $\tau_{\text{agonist}}/\tau_{\text{ACh}}$ is plotted as a function of $[\text{ACh}]/[\text{agonist}]$ on logarithmic co-ordinates. $[\text{ACh}] = 1 \mu\text{M}$ and $[\text{agonist}]$ is the concentration of the agonist that is equipotent with 1 μM ACh.



T-Pos330 THE INTERACTION OF LOCAL ANESTHETICS WITH THE NICOTINIC ACETYLCHOLINE RECEPTOR: AN ELECTRON SPIN RESONANCE STUDY. Michael P. Blanton, Elizabeth McCardy, Tim Gallaher, Howard H. Wang, Department of Biology, University of California, Santa Cruz, CA 95064.

Using electron spin resonance spectroscopy (ESR) the interaction of the spin-labeled tertiary and quaternary amine local anesthetic (abbreviated as C6SL and C6SLMEI respectively) with the nicotinic acetylcholine receptor (AChR) were examined. When native membrane preparations (*Torpedo californica*) were equilibrated with the agonist, acetylcholine prior to the addition of C6SL, the spin-labeled probe interacted with the receptor in a similar manner as when agonist and anesthetic were added simultaneously. In contrast, preincubation for more than five minutes with agonist, decreased the interaction of the quaternary amine analog (C6MEI) with the AChR. The data is interpreted in terms of a four state model of the allosteric transition of the AChR molecule; where A is the active, conducting state of the receptor, D is the desensitized, high-affinity (non-conducting) state of the receptor, and R is the resting state. The results suggest that the permanently charged quaternary amine analog is restricted in its ability to interact with the receptor in the desensitized state (D) (preincubation with agonist 10^{-4} M converts +99% of the AChR molecules into the D state), while the tertiary amine analog (pK 7.2-7.4) is able to freely interact with the desensitized receptor. We propose that the uncharged form of the anesthetic is able to diffuse into the lipid bilayer and gain access to the ion channel via a hydrophobic pathway. The anesthetic then binds to its receptor site in the charged state and is pharmacologically active.

T-Pos331 ANION-SELECTIVE CHOLINERGIC RECEPTORS IN DISSOCIATED GIANT FIBER LOBE (GFL) NEURONS OF SQUID. R.H. Chow (Intr. by Ana Lia Obaid), Department of Physiology, University of Pennsylvania, Philadelphia, PA 19104.

In the squid stellate ganglion, GFL neurons give rise to hundreds of individual axons which fuse to form the third order giant axon. Postsynaptic potentials from GFL neurons have been described (Miledi 1967, J. Physiol. 192:379-406), but the associated transmitter is unknown. Transmitter-activated receptors in these neurons are readily studied in isolated cells which are dissociated, maintained in culture, and voltage-clamped according to procedures previously described (Bookman et. al. 1985, Biophys. J. 47:222a). Cells were prepared one to five days before experiments. To optimize recording conditions, only cells without axonal stumps and with diameters < 40 μ m were selected. The membrane potential was clamped using the whole-cell patch clamp technique. Currents were recorded at 25 C in response to agonists applied with a pressure microinjection system. Cells were bathed in ASW, and the patch pipettes contained (mM) 125 KCl, 50 KF, 100 KGlutamate, 10 HEPES, and 10 EGTA. Application of 5 mM carbachol in ASW evoked inward currents with maximum amplitudes of 2-5 nA at a holding potential of -80 mV. These currents peaked within 350 ms and relaxed to baseline over several seconds. Similar responses were not obtained when ASW was applied. The responses showed desensitization, and varying the ratio of internal to external Cl concentrations resulted in shifts of the reversal potential close to that predicted by the Nernst equation for Cl. Replacement of internal K by N-methyl-D-glucamine and tetraethylammonium did not affect the reversal potential. Bath application of d-tubocurarine reversibly blocked the carbachol response. These preliminary results demonstrate the presence of anion-selective cholinergic receptors in GFL neurons.

T-Pos332 CHANNEL OPENING KINETICS OF THE ACETYLCHOLINE RECEPTOR: CHEMICAL KINETICS AND SINGLE-CHANNEL CURRENT MEASUREMENTS.

Jayant B. Udgaonkar and George P. Hess, Section of Biochemistry, Molecular and Cell Biology, 270 Clark Hall, Cornell University, Ithaca, New York 14853 USA.

Chemical kinetic measurements on *E. electricus* electroplex vesicles, using carbamoylcholine (Carb) (50 μ M to 20 mM) at 12°C, yielded values for K_1 (dissociation constant for receptor activation), ϕ (channel-closing equilibrium constant), α (inactivation rate coefficient) and \bar{J} (ion flux specific reaction rate) of 1 mM, 3.6, 10 s⁻¹ and 4×10^{-4} M⁻¹ s⁻¹ respectively. The single-channel measurements were done on the same electroplex using Carb (50 μ M to 2 mM) at 12°C. The single-channel conductance is ~ 50 pS. Channel open times fit a single exponential distribution: a unique open-channel state concurs with the minimum model proposed on the basis of the chemical kinetic measurements. The channel-closing rate constant (k_o) shows a voltage dependence of 60 mV/e-fold change and has a value of 1100 s⁻¹ at 0 mV. At high concentrations of Carb, the apparent lifetime of the open-channel form is decreased by the inhibition caused by binding of Carb to a regulatory site. Closed times within a burst fit a double exponential distribution: a concentration-independent time constant interpreted to be the rate constant for the dissociation of Carb from the regulatory site, and a concentration-dependent but voltage-independent time constant interpreted to be the rate constant for channel opening (k_o). Analysis of the mean closed times on the basis of the minimum model gives values for K_1 and k_o of 0.6 mM and 440 s⁻¹ respectively. The values for K_1 and ϕ ($= k_o/k_o^o$) at 0 mV, and the values for α and \bar{J} calculated from the single-channel current measurements, compare well to the values obtained from the chemical kinetic measurements.

T-Pos333 BIOSYNTHESIS OF THE TORPEDO CALIFORNICA ACETYLCHOLINE RECEPTOR α -SUBUNIT¹ IN YEAST.

Norihisa Fujita¹, Nathan Nelson², Thomas D. Fox², Toni Claudio³, and George P. Hess¹
¹Cornell University, Ithaca, NY 14853; ²Roche Institute, Nutley, NJ 07110; ³Yale University, New Haven, CT 06510. Intr. by G.W. Feigensohn.

Yeast cells transformed with a plasmid containing cDNA for the α -subunit of the Torpedo californica acetylcholine receptor synthesize a protein that has the expected molecular weight, antigenic specificity, protease digestion, and ligand-binding properties. The subunit is inserted into the yeast plasma membrane, the first demonstration that yeast has the apparatus to make such an insertion with a foreign protein. The α -subunit constitutes approximately 1% of the yeast membrane proteins, and its density in the plasma membrane of yeast and of the receptor-rich electroplax of Electrophorus electricus are about the same. In view of the widely available technology for obtaining large quantities of yeast proteins, yeast may prove to be an ideal way for amplifying the amounts of interesting membrane-bound proteins available so that physical and biochemical studies can be made easily.

(Supported by a grant from the Cornell Biotechnology Program, which is supported by the N.Y.S. Science and Technology Foundation and a consortium of industries.)

T-Pos334 SELECTIVE BINDING OF POTENTIOMETRIC PROBES ALLOWS OPTICAL RECORDING OF ELECTRICAL ACTIVITY FROM DIFFERENT CELL TYPES IN ELASMOBRANCH CEREBELLAR SLICES IN VITRO. B.M. Salzberg, A.L. Obaid and A. Konnerth, University of Pennsylvania, Philadelphia, PA 19104 and the Marine Biological Laboratory, Woods Hole, MA 02543.

We have used potentiometric probes and optical recording techniques to monitor electrical activity from 124 loci simultaneously in a slice preparation from the skate (Raja erinacea) cerebellum. This new preparation is a robust and highly organized structure, with many advantages for neurophysiological studies. Handcut coronal slices (~700 μm thick) were mounted in a recording chamber containing oxygenated elasmobranch Ringer's solution and stained for 60 minutes in 0.2 mg/ml of the pyrazo-oxonol dye RH 482. A brief stimulus (< 50 μs), applied to the molecular layer by means of a teflon-coated platinum bipolar electrode, evoked large changes in extrinsic absorption that spread rapidly from the site of stimulation, but were confined to the molecular layer. These signals represent the action potential in a beam of parallel fibers. This action potential has a width of 3-5 msec (22°-24°C), is eliminated by TTX and prolonged by TEA, and exhibits a prominent after-hyperpolarization that is blocked by 50-100 μM Cd⁺⁺, suggesting the presence of a gK(Ca).

When the slice was stained with RH 155, a close analogue of RH 482, the parallel fiber optical spike was followed by a large, slow second component that reached a maximum in 80 msec and lasted for more than 500 msec. The kinetics of this component, the sensitivity of its amplitude to the volume of the extracellular space, and the delayed recovery introduced by ouabain (1 μM), all suggest that this signal reflects transient changes in [K⁺]_o and is probably of glial origin. Supported by NIH grants NS 16824 and NS 12253 and a fellowship from the Alexander-von-Humboldt Foundation to AK.

T-Pos335 OPTICAL MEASUREMENTS OF CALCIUM TRANSIENTS TRIGGERED BY EXCITATORY AMINO ACIDS IN SPINAL CORD NEURONS UNDER VOLTAGE CLAMP. A.B. MacDermott*, M.L. Mayer†, G.L. Westbrook†, S.J. Smith§ & J.L. Barker*. (Intr. by C.A. Colton). *Lab. Neurophysiol., NINCDS, †Lab. Dev. Neurobiol., NICHD, NIH, Bethesda, & §Section on Molecular Neurobiol., Yale Univ. Sch. Med., New Haven.

Mammalian spinal neurons have three receptor types for excitatory amino acids characterized by the use of selective agonists and antagonists. One of these receptors is activated by N-methyl-D-aspartic acid (NMDA) and antagonized by 2-amino-5-phosphonovaleric acid (2-APV); the ion channel linked to this receptor is cation selective and shows a voltage-dependent block by physiological concentrations of Mg²⁺. The reversal potential of the response to NMDA varies with the extracellular Ca²⁺ concentration (Mayer and Westbrook, in prep.) suggesting that Ca²⁺ as well as monovalent cations are permeant.

We have used the whole-cell patch recording technique to load cultured spinal cord neurons with the calcium indicator dye arsenazo III (ArIII) using a polychromator to measure ArIII absorbance changes while monitoring inward currents evoked by excitatory amino acids under voltage clamp. Optical signals were monitored at 570, 610, 660 and 700 nm; [Ca²⁺]_i transients were recorded as differential signals either 660-570 nm or 660-700 nm. Experiments were performed at 25°C in HEPES-buffered saline containing 2.5 mM Ca²⁺, 0 mM Mg²⁺ and 1 μM TTX. Our results provide direct evidence for an NMDA-triggered increase in intracellular Ca²⁺, which begins during the NMDA-evoked conductance change, varies with the driving force for inward current and is blocked by Mg²⁺. L-glutamate, a mixed agonist acting at both NMDA and non-NMDA receptors also triggered [Ca²⁺]_i transients, however kainic acid was much less effective in producing an ArIII signal.

T-Pos336 SINGLE CHANNEL RECORDINGS FROM RABBIT CORNEAL ENDOTHELIUM IN VITRO
J.P. Koniarek, G. Markowitz, L.S. Liebovitch, and J. Fischbarg. Depts. of Physiology and Ophthalmology, Columbia Univ., N.Y., N.Y. 10032.

Cell-attached and inside-out patches were obtained from the apical membrane of corneal endothelial cells using Boralex glass micropipettes. Seals were readily obtained at pH 8.1. Several different types of voltage dependent channels were observed. The most frequently occurring channel (seen in some 40% of the patches) had a conductance of about 70 pS. For a cell attached patch, current flowed from the pipette into the cell when no voltage was applied to the pipette and reversed at -50 mV (pipette minus bath), which approximately coincides with the intracellular potential. The ratio of open to closed times was between 1:10 and 1:20 at the normal cell resting potential. Ion substitution experiments suggest that this channel is not very ion selective. Another channel, observed less frequently (in about 20% of the patches) had a conductance of 180 pS. In this case, the current reversed at 0 mV, which points to a K channel. The ratio of open to closed times for this channel was about 1:1. Lowering the [NaCl] inside the patch pipette revealed yet another channel with a conductance of about 66 pS. In this case, the current reversed when about -25 mV was applied to the patch pipette. This channel exhibited flickering behavior consistent with the presence of one open and two closed states. Supported by USPHS EY 01080 and EY 04624.

T-Pos337 MECHANISM OF MALAT TRANSPORT IN ISOLATED BARLEY VACUOLES

R. Hedrich, U.I. Flügge* and J.M. Fernandez

Max-Planck-Institut für biophysikalische Chemie, D-3400 Göttingen, W.-Germany

*Institut für Biochemie der Pflanze, Universität Göttingen, D-3400 Göttingen, W.-Germany

These are the first patch clamp studies on isolated vacuoles. The vacuole is an intracellular organelle which covers up to 90% of the plant cell volume and functions as a storage for sugars and ions.

Using whole-vacuole recordings we measured a large inward current upon application of external ATP. This current was observed in symetric solutions and at a holding-potential of 0 mV. The current amplitude follows michaelis menten kinetics for ATP, $K_m = 1$ mM and $I_{max} = 85$ pA. This current is due to an H^+ -ATPase as it is blocked by TBT ($1 \mu M$), known to inhibit other H^+ -ATPases. In voltage clamp, the current voltage, relationship revealed an inward rectifier as the only ionic conductance. This ionic current is mediated by ionic channels with a single-channel conductance of 24 pS in symetric 50 KCl. The inward rectifier appears to discriminate poorly between anions and cations and allows large organic anions, such as malate, to cross the vacuolar membrane.

We propose that the H^+ -ATPase described above provides the driving force for the uptake of malate into the vacuolar space, during photosynthesis. Whereas at night malate can be rapidly released into the cytoplasm through the inward rectifier observed in the vacuolar membrane. Malate is then metabolised in the mitochondria to keep the energie status of the cell.

T-Pos338 SINGLE CHANNEL RECORDINGS IN SEA URCHIN SPERM. A. Guerrero, J.A. Sanchez and A. Darszon.

Depts. of Biochem. and Pharmacol. CINVESTAV-IPN, Mexico City.

Ionic fluxes through the plasma membrane play a fundamental role in the physiology of sperm (activation and acrosome reaction). Recently, we have shown that several types of K^+ channels are present in bilayers derived from sea urchin sperm plasma membranes formed at the tip of patch pipettes (Lievano et. al. Dev. Biol. in press). We have now initiated the characterization of the ionic channels in situ by patch clamping sperm from *Strongylocentrotus purpuratus* and *Lytechinus pictus* sea urchin. To facilitate gigaseal formation heads were detached from their flagella and suspended in ASW. The isolated heads retained their capacity to undergo the jelly and high pH induced-acrosome reaction. Gigaseals could be formed by applying negative pressure through the pipette, thus bringing the sperm head in contact with the microelectrode tip. Pipettes contained ASW. Membrane currents were filtered at 1 kHz and stored on tape. Gigaseals could be formed in 6% of the attempts (1145), and about half showed single channel activity. In some cases the "on cell" configuration was indicated by the presence of unitary activity at 0 mV and by relaxations of membrane currents with time constants of 20-70 msec., indicating a membrane conductance $< 2-7$ pS ($C_m = 1 \mu F/cm^2$) in accordance with the value of 6 pS estimated for the sperm head (assuming $C_m = 3 \times 10^{-5}$ S/cm²). In other experiments only one membrane was evident. I-V curves, created using single channel events, showed conductances of ca. 40, 70 and 180 pS which suggests the presence of three different types of channels. These conductance values agree with those recorded from K^+ channels in bilayer experiments.

ASW = artificial sea water.

The support of CONACyT is acknowledged (grants PCCBBEU-020405 and ICCBXNA-021503).

T-Pos339 CHOLINERGIC CONTROL OF A CHLORIDE CONDUCTANCE MAY REGULATE GLIAL CELL MEMBRANE POTENTIAL IN CRAYFISH. Donald G. Brunder and Edward M. Lieberman, Dept. of Physiology, East Carolina Univ. School of Medicine, Greenville, NC 27834.

The resting membrane potentials of the glial cells of the giant axons of the squid and crayfish are low (-40 to -45 mV) compared to values reported for other glial cells. Previous work has indicated that this low potential is not entirely due to K^+ alone, i.e. the glial cell is not a potassium electrode. In addition crayfish and squid glial cells hyperpolarize in response to cholinergic agonists. Chloride removal (isethionate substitution) hyperpolarizes the crayfish glial cell to the same level as carbachol (-55 to -60 mV). This hyperpolarization is not blocked by SITS but is partially blocked by furosemide. The membrane potential response to altered $[K^+]_o$ is also more Nernstian in chloride-free solutions. Reducing Na^+ to 5 mM (from 160 mM) has little effect on the glial cell membrane potential but it does decrease the carbachol-induced hyperpolarization. Effects of furosemide and low Na suggest a Na/K/Cl co-transport process may be involved in the maintenance of the Cl^- gradient. Analysis of data obtained by combinations of carbachol, ouabain, and different $[K^+]_o$ suggests that $[K^+]_i$ increases in the presence of carbachol; this increase is blocked by 2 mM ouabain.

The data are consistent with a glial cell membrane potential that is due to a hyperpolarizing K^+ influence together with a depolarizing influence of Cl^- . Carbachol acts by blocking the Cl^- conductance. The result is a K^+ uptake which can be blocked by ouabain. If Na/K transport occurs at the pre-carbachol rate the K^+ in the perineural space could be reduced at a rate of 125 mM/sec. This would have great importance in perineural ion homeostasis especially to regulate K^+ in the adaxonal space during stimulation. Supported by ARO DAAG29-82-K-0182 and NSF INT 8117183.

T-Pos340 GLUTAMATE RESPONSE OF ISOLATED ADULT AND NEONATE MEDULLARY NEURONS. J.A. Drewe and D.L. Kunze, Department of Physiology and Biophysics, University of Texas Medical Branch, Galveston, Texas 77550.

Glutamate is the proposed excitatory neurotransmitter for the primary synapse of the baroreceptor afferents in the medial and dorsomedial nucleus tractus solitarius (M-NTS). Medullary neurons, 10-15 μ M, acutely enzymatically dissociated from the guinea pig M-NTS were studied under voltage clamp conditions at 20°C. Whole cell patch clamp recording with 2-5 M Ω electrodes filled with either 130 mM KCl or CsCl, 5 mM NaCl was used to investigate the current response to pressure application of 0.1 mM L-glutamate. I-V curves of the glutamate-induced current (n=14) revealed 1) an inward current at negative potentials with an apparent increase in conductance 2) a current reversal at 1.8 mV and 3) no apparent voltage dependence. Morphologically similar neurons dissociated by filtration from the 1-3 day old rat 4th ventricle obex region of the medulla, grown in serum tissue culture for 1-6 days were studied under identical voltage clamp conditions with 130 mM KCl as the pipette solution. I-V curves of the glutamate response (n=8) revealed 1) an outward current at potentials hyperpolarized to reversal potential with an apparent decrease in conductance 2) a current reversal near the estimated K⁺ reversal potential and 3) a marked voltage dependence such that no glutamate-induced current change was observed at voltage more positive than -40 mV. The voltage dependent conductance and glutamate response were simultaneously blocked by 1 mM Ba⁺⁺. We conclude that glutamate, in the adult neurons, modulates a voltage independent ligand coupled conductance. In contrast, in the neonate neurons glutamate is proposed to modulate a voltage dependent K⁺-conductance. Supported by DHHS HL27116.

T-Pos341 EFFECTS OF SOMATOSTATIN-14 AND -28 UPON THE LIGHT RESPONSES OF RETINAL GANGLION CELLS AND HORIZONTAL CELLS IN THE ISOLATED RETINAS OF WILD-TYPE (C57BL/6J) PEARL MUTANT, AND PEARL REVERTANT MICE. Hitoshi Suzuki and Lawrence H. Pinto, Department of Biological Sciences, Purdue University, West Lafayette, IN 47907.

We recorded action potentials from on-center retinal ganglion cells and membrane potentials from axon bearing horizontal cells in isolated (retinal pigment epithelium removed), superfused retinas of wild-type (C57BL/6J +/+), pearl mutant (pe/pe) and pearl revertant (pe^{+2P}/pe^{+2P}) mice. When wild-type or revertant retinas were bathed in solutions with low (< 1 nM) concentration of somatostatin-28 (SS-28), but not SS-14, "excitatory" effects (increase of maintained discharge rate and enhancement of the response to a small centered stimulus) were observed upon 35 of 37 retinal ganglion cells studied. When wild-type, revertant or mutant retinas were bathed in solutions having a high (> 1 nM) concentration of either peptide "inhibitory" effects (decrease of maintained discharge rate and diminution of the response to a small, centered stimulus) were observed. The "excitatory" effects were reversible, but the "inhibitory" effects were sometimes irreversible. The "excitatory" effects of SS-28 were lessened in wild-type and revertant animals by simultaneous application of SS-14. In pearl mutants, "excitatory" effects upon retinal ganglion cells (33 of 34 studied) were observed when the retina was bathed in solutions having a low (< 1 nM) concentration of either SS-14 or SS-28. Bathing the retina in solutions having a high (5-10 nM) concentration of SS-14 made the dark, resting membrane voltage of the horizontal cell of pearl mutants, but not of wild-type mice, more negative. These results show that SS-28 is probably the active form in wild-type retinas and suggests that either (1) somatostatin receptor molecules, (2) post-receptor processing or (3) endopeptidase enzymes may be altered in pearl mutants.

T-Pos342 FLUORESCENT DYE MEASUREMENTS OF A LIGHT-INDUCED PROTON PERMEABILITY IN VERTEBRATE ROD PHOTORECEPTOR DISK MEMBRANES. H. Gilbert Smith, Phoebe Rice, and Roger S. Fager, GTE Laboratories, Inc., Waltham, MA 02254 and Dept. of Physiology, University of Virginia, Charlottesville, VA 22908.

We have used the membrane-permeant, charged fluorescent dye, 3,3'-dipropylthiadicarbocyanine iodide (diS-C3(5)), to monitor electrical potentials across the membranes of isolated bovine disks. Calibration curves obtained from experiments where a potential was created across the disk membrane by a potassium concentration gradient and valinomycin show an approximately linear relation between dye fluorescence and calculated membrane potential from 0 mV to -130 mV. Light exposure in the presence of a permeant buffer like imidazole causes a rapid decay of the membrane potential to a new stable level. Addition of CCCP, a proton ionophore, in the dark produces the same effect as illumination. If the permeant buffer, imidazole, is replaced by the impermeant buffer, HEPES, neither light nor CCCP can discharge the gradient. Permeant bases other than imidazole such as ammonia can also support the light-induced discharge of the potential. We interpret the changes in membrane potential measured upon illumination to be the result of a light-induced increase in the permeability of the disk membrane to protons. A permeant buffer is required to prevent the build-up of a pH gradient which would inhibit the sustained proton flux needed for an observable change in membrane potential. (RSF was supported by NIH grant EY0-1505.)

T-Pos343 TWO NOVEL CATION CHANNELS IN NERVE TERMINALS. *J.R. Lemos* and E.L. Stuenkel. Békésy Lab of Neurobiology, Honolulu, Hawaii 96822 and Worcester Foundation for Experimental Biology, Shrewsbury, MA 01545

Single channel currents were recorded from nerve terminals isolated from the sinus gland of *Cardisoma carnifex*. Two novel channel types have been observed in inside-out excised patches: 1) The first, or "f", channel shows brief (0.1-2 msec) transitions to the open state occurring in bursts with intervals of 0.1-2 sec. This channel, in symmetrical K^+ , has a mean slope conductance of 69 ± 3.6 pS. The single channel I-V curve is not changed by substitution of K_2SO_4 or Na_2SO_4 for KCl, but does show rectification when CsCl is substituted. Na^+ goes through the channel just as easily as K^+ since the reversal potential, with equal concentrations of KCl outside and NaCl inside, remains 0 mV. Furthermore, this concentration of Na^+ on the inside of the patch causes this type of channel to remain open for longer periods upon depolarization. 2) The second, or "s", channel exhibits much longer (secs) openings with rapid flickering back to the closed state. This channel has a mean conductance of 213 ± 6.1 pS in symmetrical K^+ . It is rarely observed in solutions having low $[Ca^{++}]$, and is activated by increasing $[Ca^{++}]$ above 10^{-6} M. Ion substitution experiments indicate that this channel also has nearly equal permeabilities for Na^+ and K^+ , but, unlike the "f" channel, allows Cs^+ to pass through. The "s" channel has the characteristics of a Ca-activated cation channel, but exhibits a much larger slope conductance than has been observed in other cells. These two previously undescribed channel types may be unique to nerve terminal membranes.

T-Pos344 CALCIUM-ACTIVATED SLOW INWARD CURRENT IN NEUROSECRETORY CELL BODIES. R. Valdiosera*, C. Onetti* and U. García* (Intr. by R. Valle), CINVESTAV IPN, México D.F. and Centro de Investigaciones Biomédicas, Universidad de Colima, México.

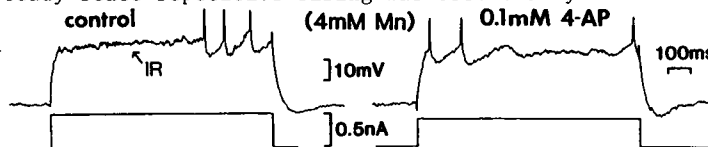
Recently we reported the properties of calcium currents in neuron somata of the crayfish X-organ (García et al., Soc. Neurosci. Abstr., Vol.11, Part 1, p.520, 1985). The decay time course of these currents show two time constants, suggesting the existence of two inward currents. Here we report experiments designed to test this possibility. Whole cell clamp recordings (Hamil et al., Pflug. Arch. 391:85, 1981) were performed in axotomized neurons of the crayfish (*Procambarus clarkii*) X-organ at room temperature (22°C). Cells dissection and experimental procedures were as previously reported. The composition of the pipette solution was (in mM): Cs-aspartate 220, Ca-EGTA buffer 5 ($[Ca^{2+}] = 10^{-9}$ to 10^{-8} M) and MOPS 10 (pH= 7.3); and the bathing solution: TRIS- CH_3SO_3 205 and $Ca(CH_3SO_3)_2$ 20 (pH= 7.3). Depolarizing voltage pulses (400 msec long) from a holding potential of -50 mV, preceded by a 200 msec conditioning pulse to inactivate the fast inward current, elicit slow inward currents starting at -40 mV reaching a maximum peak value of -50 $\mu A/cm^2$ at 20 mV in 200-300 msec, with an apparent reversal potential near the Ca^{2+} equilibrium potential. The magnitude of these currents incremented 50% when Na^+ substituted TRIS $^+$ and were blocked by the addition of Cd^{2+} (2 mM) to the bath. However, when intracellular $[Ca^{2+}]$ was increased up to 0.1-1 mM, the slow inward currents remain even in the presence of Cd^{2+} (2-5 mM) in the external solution. In this condition, the current magnitude was independent of the holding potential. Our results suggest that these slow inward currents are due to the Ca-dependent activation of a voltage independent non-specific cationic conductance. This conductance could be important in the pacemaker activity.

T-Pos345 ELECTROPHYSIOLOGICAL PROPERTIES OF MOUSE CHROMAFFIN CELLS *IN SITU*. V. Nassar, E. Rojas & H.B. Pollard. LCBG, NIADDK, National Institutes of Health, Bethesda, MD. 20205.

Chromaffin cells secrete catecholamines and other factors in response to complex stimuli acting on receptors and related channels on the plasma membrane. Until now, isolated cells have been primarily studied by electrophysiological techniques, but we have now devised methods of studying these cells *in situ*. The adrenal gland was microdissected, cut into halves, mounted in a 300 μ l chamber, and perfused with Krebs bicarbonate buffer at 37 °C. For intracellular recording and current injection, single microelectrodes were filled with 1.5M KCl - 0.5M K citrate (200 - 300 M Ω). Average resting potential was -54.3 ± 8.8 mV (n=21). A sudden elevation of K^+ from 5 to 12.5 mM depolarized the cells and elicited action potentials. Intracellular current injection showed a normal delayed outward rectification, and the input resistance, estimated from the slope of the linear portion of the current-voltage relationship, was 102.8 ± 15 M Ω (n=12). Application of depolarizing current pulses (0.1 - 0.2 nA) invariably induced action potentials, and electrical activity was often elicited at the end of an hyperpolarizing current (0.1 - 0.2 nA). Exposure to acetylcholine caused a depolarization from -54 to -34 mV which was followed by a marked increase in spike frequency of cells. Since the input resistance measured in these cells *in situ* is much lower than that for cultured cells (500 M Ω to 5 G Ω), the unavoidable conclusion is that the cells are electrically coupled in the gland. These data indicate that the *in situ* approach may yield information more indicative of the state of chromaffin cells in nature, and more illustrative of regulatory mechanism inherent in the system.

T-Pos346 A-CURRENT AND Ca-DEPENDENT TRANSIENT OUTWARD CURRENT CONTROL THE INITIAL REPETITIVE FIRING IN HIPPOCAMPAL NEURONS. Johan Storm, Department of Neurobiology and Behavior, SUNY at Stony Brook, NY 11794.

The transient K current I_A is known to control slow repetitive firing in molluscan neurons. Hippocampal cells also have an I_A -like current, and are able to fire at low frequencies. The role of I_A in CA1 pyramidal cells was studied in rat hippocampal slices, using current clamp and single electrode voltage clamp techniques. Holding at -60 to -90mV, 10-35mV depolarizing voltage clamp commands elicited a fast-activating transient outward current, which seemed to contain 3 components: a fast one (inactivation time constant $\tau_1 \sim 0.2$ s) which was abolished by Ca-free medium with 3mM Co; an intermediate one ($\tau_2 \sim 3$ s) which was blocked by 0.1mM 4-aminopyridine (4-AP), but not by 0 Ca/3 Co (as typical of I_A); and a slow component ($\tau_3 \sim 10$ s) which was resistant to 4-AP and 0 Ca/3 Co. In current clamp, depolarizing current steps elicited an initial ramp (IR), which delayed and slowed the initial discharge for 0.3-1.5s. The IR was ascribed to the transient currents, because the time course, voltage dependence and sensitivity to 4-AP and Ca were the same. Thus, conditioning depolarization abolished the IR; Co, Cd, Mn or 0 Ca reduced the initial 1-3s of the IR; and 4-AP blocked part of the remaining IR. In contrast, the steady state repetitive firing was essentially unaffected by 4-AP (in the presence of 4mM Mn). Thus, I_A in CA1 cells seems to control the initial rather than the steady state discharge, unlike its role in molluscs. (Supported by a Fulbright fellowship to J.S., and NIH grant NS 18579 to Dr. P. R. Adams.)



T-Pos347 INITIATION OF B-CELL PROLIFERATION IS INDEPENDENT OF EARLY CHANGES IN THE CYTOSOLIC FREE Ca^{2+} CONCENTRATION. Erik Wiener*, Deborah Leberman*, John Cebra*, and Antonio Scarpa*, U. of Penna., Depts. of Biochemistry/Biophysics*, and Biology*, Philadelphia, PA 19104.

The effects of lipopolysaccharides (LPS), 12-O-tetradecanoyl phorbol-13-acetate (TPA), rabbit IgG antimouse Fab (RAMIgGαFab) and its F(ab')₂ fragment on the cytosolic free $[Ca^{2+}]_f$ ($[Ca^{2+}]_f$), 3H -thymidine, and 3H -uridine uptake were measured in murine B-lymphocytes. LPS (0.4 μg/ml to 50 μg/ml) induced a 20-120 X increase in the 3H -thymidine uptake, a 3-7 X increase in 3H -uridine uptake, and had no effect on the $[Ca^{2+}]_f$. TPA marginally increased 3H -thymidine and 3H -uridine uptake, but had no effect on the $[Ca^{2+}]_f$. TPA suppressed the changes in the $[Ca^{2+}]_f$ induced by RAMIgGαFab and the F(ab')₂ fragment, but stimulated their proliferative response. RAMIgGαFab induced a change in $[Ca^{2+}]_f$ which saturated at 10 μg/ml, but concentrations as high as 50 μg/ml had no significant effect on the 3H -thymidine or 3H -uridine uptake. In contrast, pretreating the cells with 16 nM TPA for 3 min. virtually abolished the increase in the $[Ca^{2+}]_f$ induced by 2 μg/ml of RAMIgGαFab, but stimulated a RAMIgGαFab induced increase in 3H -thymidine uptake 85 X relative to controls. In the presence of TPA, RAMIgGαFab (0.4 μg/ml-10 μg/ml) induced a 2-30 X increase in 3H -uridine. High doses of the F(ab')₂ fragment (10 μg/ml and 50 μg/ml) increased 3H -thymidine (3 and 15 X) uptake, 3H -uridine uptake (1.3 and 3.5 X), and the $[Ca^{2+}]_f$. Lower doses only increased the $[Ca^{2+}]_f$. 16 nM TPA virtually abolished the $[Ca^{2+}]_f$ increase induced by 2 μg/ml F(ab')₂, yet it stimulated the F(ab')₂-induced uptake of 3H -thymidine and 3H -uridine by 120 X and 10 X, respectively. Since these experiments dissociate the increase in $[Ca^{2+}]_f$ from proliferation, we conclude that initiation of B-cell proliferation is independent of changes in $[Ca^{2+}]_f$.

T-Pos348 PHORBOL ESTERS ATTENUATE THE GLUCAGON INDUCED INCREASE IN CYTOPLASMIC FREE Ca^{2+} CONCENTRATION IN RAT HEPATOCYTES. James M. Staddon and Richard G. Hansford (Intro. by Prof. P. L. Pedersen). NIH, Gerontology Research Center, 4940 Eastern Ave., Baltimore, MD 21224.

Hepatocytes were isolated from rats and then loaded with the fluorescent Ca^{2+} -indicator quin2. Glucagon (10nM) caused a sustained (5min) increase in the fluorescence of the quin2 loaded cells; this was interpreted as an increase in cytoplasmic free Ca^{2+} concentration ($[Ca^{2+}]_c$). If 100nM-PMA (phorbol myristate acetate, a putative activator of protein kinase C) was added prior to glucagon then the increase in $[Ca^{2+}]_c$ was greatly reduced. If PMA was added after glucagon then the increased $[Ca^{2+}]_c$ was partially reversed. The effects of PMA on the glucagon induced increase in $[Ca^{2+}]_c$ were not mimicked if $[Ca^{2+}]_c$ was increased by ionomycin. Thus an event between occupancy of the glucagon receptor and the mechanism by which $[Ca^{2+}]_c$ was increased appears to be a prerequisite for the action of PMA. Similar results to those with glucagon were obtained if forskolin (to activate adenylate cyclase) or dibutyryl-cAMP (to circumvent the mechanisms involved in cAMP generation) were used instead of glucagon. The observations with dibutyryl-cAMP indicate that, although other sites of action cannot be excluded, PMA acted distally to cAMP generation. Glucagon appears to increase $[Ca^{2+}]_c$ by releasing intracellular sources of Ca^{2+} and increasing net influx of Ca^{2+} across the plasma membrane; this is indicated by the observation that in the absence of extracellular Ca^{2+} glucagon caused only a transient increase in $[Ca^{2+}]_c$. Thus PMA could attenuate the action of glucagon on $[Ca^{2+}]_c$ by interfering either with the increased net influx of Ca^{2+} across the plasma-membrane or the release of intracellular stores of Ca^{2+} .

T-Pos349 TRANSIENT AND SUSTAINED INCREASES IN THE CONCENTRATION OF INTRACELLULAR FREE CALCIUM IN PARATHYROID CELLS: DIFFERENTIAL INHIBITION BY CALCIUM ANTAGONISTS. E.F. Nemeth and Antonio Scarpa, Intr. by A.V. Somlyo, Dept. Biochem/Biophysics, Univ. of Penna., Philadelphia, PA 19104

The concentration of intracellular free calcium ($[Ca^{2+}]_i$) in dissociated parathyroid cells (PTCs) has been measured with the fluorescent indicator fura 2. In PTCs loaded with fura 2, step-wise increases in the extracellular calcium concentration ($[Ca]_o$) of 0.5 mM between 1.0 and 3.0 mM evoked rapid and transient increases followed by smaller but sustained increases in $[Ca^{2+}]_i$. Pre-treatment of PTCs with La^{3+} (20 μ M) or the organic Ca channel blockers D600 and verapamil (50 μ M each), depressed the sustained increases in $[Ca^{2+}]_i$ without affecting the transient phases. When sustained, steady-state increases in $[Ca^{2+}]_i$ were obtained by exposure to high $[Ca]_o$ (2 mM), the subsequent addition of La^{3+} produced a rapid fall in $[Ca^{2+}]_i$ to levels approaching those obtained in low $[Ca]_o$ (0.5 mM). Qualitatively similar results were obtained with D600 or verapamil. Transient increases in $[Ca^{2+}]_i$ also occurred in the absence of any change in $[Ca]_o$ by doubling $[Mg]_o$. These Mg-induced intracellular Ca^{2+} transients were not followed by large and sustained increases in $[Ca^{2+}]_i$ and were not inhibited by pretreatment with La^{3+} or D600. The ability of extracellular Mg to elicit a transient increase in $[Ca^{2+}]_i$ unaccompanied by a sustained increase indicates that the transient and sustained phases can be readily separated. This finding, together with the ability of Ca antagonists to preferentially inhibit the sustained, steady-state increase in $[Ca^{2+}]_i$, suggests that the two phases of increased $[Ca^{2+}]_i$ evoked by extracellular Ca are mediated by two distinct mechanisms and that extracellular Ca contributes to the maintenance of the steady-state level of $[Ca^{2+}]_i$ in PTCs. Supported by NIH grant AM-33928.

T-Pos350 DOES HEAT SHOCK PROTEIN HAVE A PROTECTIVE ROLE IN THE PLASMA MEMBRANE OF THE *XENOPUS LAEVIS* OOCYTE ? R.T. Kado, E. Brault and H. Duclozier. Lab. de Neurobiologie Cellulaire et Moléculaire, C.N.R.S. Gif Sur Yvette, 91190 FRANCE.

Cells heated to temperatures 2 to 10 °C above normal respond by producing specific Heat Shock Proteins (hsp). In spite of their occurrence in all organisms studied, little is known about the functional role of the hsp (Heat Shock, Schlesinger, Ashburner and Tissières Eds., Cold Spring Harbor Lab. 1982). We report on voltage clamp and fluorescence experiments examining a possible membrane function for the hsp in oocytes of *Xenopus laevis*. This oocyte is known to translate a 70 KD hsp from its maternal messenger stores when exposed to temperatures above 30°C which is blocked by cycloheximide or emetine. The membrane electrical properties were unchanged after a 30 minute exposure to 33°C and returned to the normal temperature of 16°C. If, on the otherhand, the oocyte had been treated with either blocker, we observed signs of damage beginning at the electrode penetration sites. The treated oocytes also had low potentials and resistance on return to normal temperature. Because of this apparent membrane effect with HS after suppression of protein synthesis, we examined the effects of HS on the membrane fluidity using the pyrene dimer fluorescence technique. In these experiments, 30 min. temperature pulses from 5°C to various temperatures up to about 29°C gave a linear increase in fluidity response with temperature. At temperatures above 30°C however, a membrane rigidification was found. This decrease in fluidity began within about 1 min. of attaining 33°C and exponentially reached a plateau with a time constant of about -4 min. This rigidification was reversed if the oocyte had been treated with either of the synthesis inhibitors used. These results are very preliminary but may indicate a direct or indirect role for hsp in decreasing membrane fragility during exposure to elevated temperatures.

T-Pos351 AMILORIDE, AN INHIBITOR OF Na^+/H^+ EXCHANGE, INHIBITS ALSO ACETYLCHOLINESTERASE ACTIVITY. David Dannenbaum and Kurt Rosenheck, Dept. of Membrane Research, The Weizmann Institute of Science, Rehovot, Israel.

In the course of work on Na^+ transport in plasma membrane vesicles, derived from adrenal medullary chromaffin cells, we have made the chance observation that the plasma membrane acetylcholine esterase (EC 3.1.1.7) (AChE) is inhibited by amiloride. We have investigated this inhibitory activity in more detail, using the colorimetric method of Ellman et.al. for AChE assay. Lineweaver-Burk plots at varying concentrations of amiloride indicated that inhibition is non-competitive. K_i , calculated from either the ordinate intercepts of these plots or by Dixon analysis, was $\sim 20 \mu$ M. Similar results were obtained for amiloride inhibition of AChE from electric eel (Sigma) and that of red blood cell ghosts (freshly drawn blood). The K_i 's for these systems were $\sim 60 \mu$ M and $\sim 40 \mu$ M, respectively. For comparison, the K_i 's of eserine (Sigma) were determined for the electric eel and the chromaffin cell plasma membrane vesicles AChE's. These experiments showed that the inhibitory activity of amiloride is about two orders of magnitude lower than that of the standard blocker. This seems to be the first instance recorded of a guanidinium derivative acting as a reversible blocker of AChE. It may be assumed that the guanidinium group can substitute reasonably well for the quaternary ammonium group of the substrate at the active site of the enzyme.

D. Dannenbaum was the recipient of a summer studentship conferred by the Weizmann Institute of Science.

T-Pos352 THE NMDA RECEPTOR ANTAGONIST APV BLOCKS EPILEPTOGENESIS BUT NOT EPILEPTIFORM ACTIVITY IN AN IN VITRO MODEL OF SEIZURES. William W. Anderson, H. Scott Swartzwelder and Wilkie A. Wilson, Epilepsy Ctr, VA Med Ctr, and Dept Pharmacol, Duke Univ, Durham, NC (Intr. by C.L. Lingle).

The ability the NMDA receptor antagonist DL-2-amino-5-phosphonovalerate (APV) to block epileptiform burst induction by NMDA and stimulus train induced bursting (STIB) (Stasheff et al, Brain Res 344:296, 1985) was studied in the CA3 pyramidal cell layer of the rat hippocampus.

Bath application of 10 uM NMDA induced strong spontaneous and triggered bursting (18 and 17 spikes/burst, S/B) in 70% of the slices while in NMDA. After NMDA washout, spontaneous and triggered bursting (11 and 8 S/B) continued in >63% of the slices that were bursting in NMDA.

100 uM APV blocked all effects of 10 uM NMDA when applied prior to NMDA. When 100-200 uM APV was added to 10 uM NMDA during NMDA activation, triggered bursting was reduced but not blocked (S/B decreased by 60%). When 100 uM APV was applied following NMDA washout, triggered bursting was reduced but not blocked (S/B decreased by 40%), and spontaneous bursting was not blocked.

In ACSF, electrical stimulation of s. radiatum (2s, 60/s trains; 10 trains once every 5 min) induced spontaneous and triggered bursting in 67% of the slices. However, when 100-500 uM APV was applied before the stimulus trains, spontaneous bursting was induced in 0 of 12 slices, and triggered bursts (of max. 3 S/B) were induced in 2 of 12 slices. When 100-500 uM APV was applied after bursting was induced by electrical stimulation, triggered bursting was reduced but not blocked (S/B decreased by 42%), and spontaneous bursting was blocked in half the slices.

These data are consistent with NMDA receptor activation being necessary for the induction of epileptiform burst activity by electrical stimulation, but only contributing to and not necessary for the generation of individual, previously induced bursts. Supported by Veterans Administration.

T-Pos353 NOISE-INDUCED NEURAL IMPULSES Klaus Schulten and Herbert Treutlein, Dept. of Physics, Technical University of Munich, 8046 Garching, Fed. Rep. Germany

The firing pattern of neurons shows a stochastic scatter in the lag time between pulses and a large variation in the average pulse frequency. This behaviour cannot be accounted for by deterministic non-linear dynamic processes like the Hodgkin-Huxley model. We demonstrate that a noise term added to deterministic models can explain the observed firing patterns of neurons very well. For this purpose we consider the Bonhoeffer-van der Pol model which describes neuronal activity in terms of two variables (V =potential and x). Previous investigations involved only models which lack the ability to recover the resting state and therefore, cannot describe trains of neural pulses. By means of a Monte Carlo solution of the Fokker-Planck equation corresponding to the stochastic Bonhoeffer-van der Pol model we show that the stationary probability distribution $p(V,x)$ for noisy neurons is bimodal, jumps between the two regions of maximum probability representing noise-induced limit cycles, i.e. the pulse trains of nerve cells. The dependence of the pulse frequency on the system parameters and on the noise amplitude is investigated.

T-Pos354 NEURAL CODING ANALYSIS, Judith E. Dayhoff, Stanford University, and Judith Dayhoff Assoc. (Address: Box 4029, Mountain View, CA 94040)

Neural coding refers to the mechanisms by which sensory and motor information is represented when transmitted along nerve fibers. Neural coding also includes any underlying encoding schemes used in the integrative processing of the central nervous system. Numerous candidate codes have been proposed and studied experimentally. One candidate code suggests that different neural firing rates represent different sensory stimuli or different neuromuscular signals. In another candidate code, the firing of different cells has different biological meaning. Alternatively, nerve firing patterns could represent specific sensory or neuromuscular information. Another coding scheme emphasizes the potential significance of groups of neurons firing in near synchrony. Independent of research on neural coding, a wide variety of coding schemes have arisen in other fields such as computer science, communications, genetics, and cryptography. The special characteristics of these codes are used here to compare and analyze the candidate neural codes. Concepts such as error-detection, error-correction, dynamic information compaction, reading frames, comma-free characteristics, and decryptability are used to address the neural coding schemes. Some of the proposed neural schemes show structure that allows error-detection, error-correction, and other powerful signaling characteristics.

T-Pos355 COMPUTER SIMULATION OF ACTION POTENTIAL CONDUCTION IN PRESYNAPTIC AXONS. R.M. Siegel and E.Y. Isacoff. The Salk Institute, La Jolla, CA and McGill University, Montreal, QUE.

Conduction properties of presynaptic axons were modeled after terminal preganglionic axons of cat superior cervical ganglion as 0.2 μ m diameter fiber with a 100% tapered widening (axonal bifurcation) or a 3 μ m long, 1.4 μ m diameter dilation (synaptic bouton). Active membrane currents were given by the Hodgkin-Huxley (HH) equations with an added electrogenic sodium pump and potassium conductance with the properties of the calcium-activated conductance (CagK). To simplify the computations, the pump current and the CagK were modeled as linearly summing, exponential decaying processes activated with fixed amplitude and delay following an AP. The partial differential equations for the cable properties of the nerve were solved using the implicit integration method of Moore. When only the HH equations were used, the presence of either a bouton or bifurcation produced a localized reduction in AP conduction velocity just proximal to the inhomogeneity. Addition of the CagK altered APs late in a 40Hz burst by slowing conduction velocity in the uniform part of the axon and producing conduction block near the site of the diameter change. For a given value of the CagK, fewer APs in a burst were blocked at lower firing rates. Pump activity produced little conduction slowing and no conduction failure. It is suggested that activation of conductances following an AP can produce a potent reduction in the safety factor for conduction of subsequent APs through both boutons en passage and bifurcations. The likelihood of inducing conduction block in this way depends on conductance summation, i.e. upon conductance time constant and interstimulus interval.

T-Pos356 NERVE IMPULSES COULD BE ELICITED IN AN AXON BY LASER BEAMS. Chyuan-Yih Lee,
325 Spedding Hall, Iowa State University, Ames, IA 50011.

Under normal physiological conditions, the nerve impulses will be elicited whenever the Na permeability is sufficiently raised. According to a two-state electron transfer (ET) model,¹ the Na permeability is proportional to N_2 , the density of ET complexes at the higher energy state. In physiological systems or conventional experiments, the Na permeability (and thus N_2) is usually raised by depolarizing a membrane. In principle, the ET complexes could also be excited to the higher energy state by laser beams with wavelengths in the charge transfer band.² The energy gap between the two electronic states was estimated¹ to be about 0.1 eV in the resting axon. Because of the Franck-Condon principle, the energy of the charge transfer band is likely to be somewhat higher.

1. C. Y. Lee, Bull. Math. Biology, 45(1983), 759-780.
2. D. DeVault, Q. Rev. Biophysics, 13(1980), 387-564.

T-Pos357 MECHANOTRANSDUCING ION CHANNELS: IONIC SELECTIVITY AND COUPLING TO VISCOELASTIC COMPONENTS OF THE CYTOSKELETON. Z.C. Yang, F. Guharay and F. Sachs. Dept. Biophysics, SUNY, Buffalo, NY 14214.

Ion channels sensitive to membrane tension are present in the membrane of chick skeletal muscle (Guharay and Sachs, 1984,5).^{*} We have recently observed the channels also in dorsal root ganglion cells of the rat. Earlier kinetic analysis revealed a four-state system (3 closed and 1 open state) where only one rate constant depends on tension (exponentially on the square of membrane tension). Even the smallest eigenvalues of this system predict macroscopic relaxations in the ms range. To test this prediction, steps of pressure were applied and the average current was measured. The observed current had no inactivation but the onset followed a sigmoidal time course with a delay of 2-3 s, orders of magnitude longer than predicted. This delay is reduced by pretreatment with cytochalasins. The simplest interpretation seems to be that force is initially held by a viscoelastic actin network which relaxes and transfers tension to the channels.

New information of ionic selectivity shows that the I/V curve is super linear in the hyperpolarizing quadrant. At room temperature:

$$K(73pS) \sim NH_3(70pS) > Cs(62pS) > Na(52pS) > Li(30pS)$$

at a potential of -100mV. The superlinearity increases with conductance of the species. For K, the slope conductance increases from 50pS at -70 mV to 103pS at -120mV.

^{*}J. Physiol. 363:119; 352:685.

Supported by NINCDS-13194 and US Army DAAG2985K0135

T-Pos358 WATER AND PROTON INVOLVEMENT IN EXCITABILITY

V. Vasilescu, Eva Katona and Mioara Tripşa

Department of Biophysics, Medical Faculty, Bucharest, Romania

Comparative studies on nerve, isolated nerve fibre, retina and muscle cells allow us to demonstrate the role of water and protons in neuroexcitability. The present work is a survey of experimental data obtained using various nondestructive techniques in the investigation of the excitation process in different biosystems, in normal and deuterated media, at different pH and pD values. Effects of water-heavy-water and proton-deuteron exchange, of pH variation and of temperature on the early stages of the excitation process as well as on the energetics of various excitable systems were followed up. Quantum mechanical studies of the structure of different anesthetics and of their interaction with various macromolecular structures were also undertaken. Physico-chemical mechanisms underpinning anesthetic action, essential role of water-stabilized macromolecular conformations and of active groups involved in neuroexcitability or its reversible abolishment in various conditions as well as dependence of excitation-energy coupling on the presence of intracellular protons - more evident in systems in high activity - are disclosed by data analysis. As a conclusion strong involvement of water and protons in the normal evolution of excitation process is pointed out.

T-Pos359 HALOTHANE RAISES THRESHOLD, SLOWS IMPULSE CONDUCTION AND DISRUPTS RECOVERY MECHANISM

IN SINGLE AXONS OF FROG SCIATIC NERVE. Raymond SA, Butterworth JF, Roscoe RF. Brigham and Women's Hospital, Boston, MA 02115 and Bowman Gray School of Medicine, Winston-Salem, NC 27103

We measured firing threshold of myelinated axons to investigate effects of halothane concentrations which produce general anesthesia in humans and animals. We report a previously unknown action of halothane on recovery of excitability following impulse activity and an hypothesis regarding the mechanism of anesthesia. Axons teased from excised nerves were recorded with suction electrodes. Nerve trunks were stimulated with Ag/AgCl electrodes. Resting threshold and conduction latency were measured using current pulses of fixed amplitude whose duration was automatically adjusted to hold the probability of firing at 50%. Anesthetic concentrations of halothane caused dose-dependent increases in resting threshold and slowed conduction. Step increases in halothane were followed by transient decreases in threshold (the dip) and step decreases in halothane were followed by transient increases in threshold (the bump). The dip transient may be related to the agitation and excitement seen in patients as they lose consciousness when anesthesia is induced. Halothane-induced increases in resting threshold were not sufficient to block conduction. However, activity-dependent processes were greatly altered. Halothane diminished both superexcitability and depression (Raymond, J Physiol 290:273, 1979). This suggests a novel mechanism for general anesthesia: disruption of the normal dependence of excitability on impulse firing patterns. We predict that drugs which reduce activity-dependent threshold changes will cause unconsciousness even if they do not raise resting threshold. (Supported by BRSR S07RR05489-22 and a grant from Ohmeda, Inc.)

T-Pos360 DERIVATION OF SEVERAL VOLTAGE AND CURRENT CLAMP CIRCUITS FROM A FUNDAMENTAL CLAMP CIRCUIT.

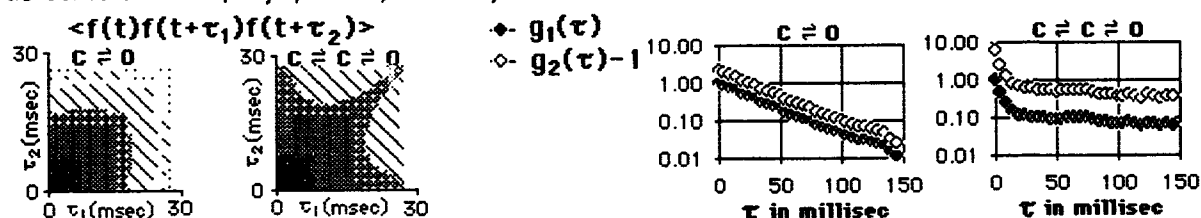
Gunter N. Franz and Ronald Millecchia. Department of Physiology, West Virginia University Medical Center, Morgantown, WV 26506.

F.J. Sigworth (J. Physiol. 307: 97-129, 1980) has published the block diagram for a "general" voltage clamp circuit. The equation associated with this circuit (equ. A5, p. 125) has been accepted by others (J.W. Moore et al., Biophysical J. 46: 507-514, 1984) as representing "the general case of a voltage clamp with R_s compensation" (ibid. p. 509). In this paper we demonstrate that the "general" scheme of Sigworth represents a rather special case: (1) it implies that the clamp amplifier is a voltage-controlled current source with infinite output impedance rather than the usual (nearly ideal) voltage-controlled voltage source; (2) it fails to describe several topologically differing clamp and compensation schemes. Here we show how three basic clamp schemes can be derived from one fundamental circuit. The Sigworth block diagram represents a subset of the general set. We present the basic set of circuit and block diagrams and tabulations of transfer functions, two-port parameters, and open-loop gains for all basic clamp schemes. The two-port parameters characterize clamp fidelity in terms of the voltage amplification factor (ideally 1) and the output impedance (ideally ∞) of the clamp circuit.

T-Pos361 USE OF CORRELATION FUNCTIONS TO STUDY PATCH CLAMP DATA

L. Liebovitch, J. Fischbarg, and J. Koniarek, Dept. Ophthalmology, Columbia U., NY 10032

Channel kinetics are usually obtained from patch clamp data by analyzing the open and closed time histograms. However, correlation functions can also be used for the same purpose. Since the correlation methods analyze the whole data record at once, they can be faster and simpler than using open/closed time histograms. We extended our earlier techniques (B.B.A., 1985 813:132, *Math. Biosci.*, in press) by using the functions $g_n(\tau) = \langle f(t+\tau)f(t) \rangle / \langle f(t) \rangle^2$ and 3-point correlation functions $\langle f(t)f(t+\tau_1)f(t+\tau_2) \rangle$, also known as cumulants or polyspectra, to study multistate channels.



T-Pos362 STOCHASTIC THEORY OF MEMBRANE SENSITIVITY: AN ANIMATED COMPUTER GRAPHICS TUTORIAL.
Franklin F. Offner, Department of Biomedical Engineering, Northwestern University, Evanston, IL 60201

The high sensitivity of the conductance of membranes to their environment, which has been difficult to understand by classical treatments, may be explained by the interaction of channel gates which open and close stochastically, with the time-varying field within the channels (Offner, 1984, *Biophysical J.* 46:447-461). In order to facilitate the understanding of the theory, an animated graphics tutorial program has been developed, which shows physically how the cycling of the gates will affect the electric field, and how this interaction may result in a very large increase in sensitivity. It also demonstrates how Ca^{++} may interact with conformational gates, to increase their sensitivity. The use of the program will be demonstrated, and the program disk will be made available to those who may wish a copy.

T-Pos363 ESTIMATION OF OPEN PROBABILITIES OF CHANNELS FOR MEMBRANE PATCHES CONTAINING MORE THAN ONE CHANNEL K. H. Iwasa and S. S. Yeandle, Laboratory of Biophysics, NINCDS, NIH Bldg. 36, Room 2A-29 Bethesda, Maryland 20892

Among the properties of channels most readily available from single channel recording is the fractions of time the channels are open. We intend to provide statistical criteria in estimating open probability of channels in two- or many-channel patches. For simplicity we only consider two-channel patches; an extension to patches with more channels is straightforward. We do not consider effect of noise or of filtering [Colquhoun and Sigworth, 1983], but we start from level (or amplitude) histograms, in which the component of each current level is well defined. The estimation of the open probabilities of channels from steady state current records is a statistically non-trivial question, because the sampled points are not independent of each other. We have generated simulated current records of two identical, independent channels under voltage clamp, and sampled at certain intervals to obtain the level histograms. We found that an extension of the chi-square minimization is useful in fitting the level probabilities to the binomial distribution to obtain the open probability. The conventional method of obtaining open probability by using all available data points is justified, provided that the record is long enough compared with the relaxation time of the channels involved, in order to find the best fit to the model considered. The statistical significance of the fit, however, requires caution. If the kinetic properties of the channels (i.e. the transition scheme and the range of the transition rates) are known, it is possible to generate the cumulative distribution function, and to determine the statistical significance of the fit.

T-Pos364 MOLECULAR-BASED CALCULATIONS OF ION FLUX IN GRAMICIDIN CHANNELS -- PETER GATES AND ERIC JAKOBSSON, DEPARTMENT OF PHYSIOLOGY AND BIOPHYSICS, PROGRAM IN BIOENGINEERING, UNIVERSITY OF ILLINOIS, URBANA, ILLINOIS 61801

It is shown that a "mean free energy" (defined by $A_m = kT \ln \int e^{-A/kT} d(\frac{x}{\delta})$, where δ =length of channel) can be calculated for an ion in a gramicidin channel from the experimental saturation properties of the small signal conductance. This calculation is based on the fact that the small signal conductance is measured in a near-equilibrium situation. The mean free energy calculation provides a constraint on the validity of energy profiles proposed for ion permeation.

In this paper we use this constraint to evaluate potential profiles suggested by the results of various published molecular dynamics and Monte Carlo calculations.¹ We further use the method of Brownian dynamics² to calculate full current-voltage curves for energetically possible potential profiles.

We thank Professor Peter Jordan for providing dipole and image forces used in our calculations.³ Support was received from the Bioengineering Program and the Research Board of the University of Illinois, and from the National Institutes of Health.

1) Fischer and Brickmann (1983) *Biophys. Chem.* 18: 323; Lee and Jordan (1984) *Biophys. J.* 46: 805; Kim, Vercauteron, Welte, Chim, and Clementi (1985) *Biophys. J.* 47: 327; Kim, Nguyen, Swaminathan, and Clementi (1985) *J. Phys. Chem.* 89: 2870; Etchebest and Pullman (1985) *J. Biomol. Structure & Dynamics* 2: 859. 2) Cooper, Jakobsson, and Wolynes (1985) *Prog. Biophys. & Mol. Biol.* 46: 51; Gates & Jakobsson (1985) *Biophys. J.* 47: 432a. 3) Jordan (1984) *J. Membr. Biol.* 78: 91.

T-Pos365 INTERDEPENDENCE OF BURST LENGTH AND NUMBER OF OPENINGS PER BURST IN STOCHASTIC MODELS OF SINGLE ION CHANNELS. R.K. Milne, R.O. Edeson, and B.W. Madsen. Dept. of Mathematics, University of Western Australia, Dept. of Anaesthesia and Intensive Care, Sir Charles Gairdner Hospital, and Dept. of Pharmacology, University of Western Australia, Nedlands, Western Australia, 6009. (Intro. C. Lewis)

The joint distribution, conditional distributions, and conditional means for burst length (T) and number (N) of openings per burst have been derived for three-state Markov models of agonist-only and channel blocking mechanisms of bursting. For both models the mean burst length ($E\{T|N = r\}$) increases linearly as a function of the number of openings per burst, but the conditional mean number of openings per burst ($E\{N|T = x\}$) is a non-linear strictly increasing function of burst length (x), which is asymptotically linear for large x . In both models, the asymptotic intercept of the latter conditional mean is less than, equal to, or greater than unity according as mean channel closed-time is less than, equal to, or greater than mean channel open-time. For parameter values typical of the nicotinic receptor, there is a clear distinction between the models: the asymptotic intercept is less than unity for the agonist-only model and greater than unity for the blocking model. A practical consequence of the interdependence of T and N is that truncation of burst length measurements can bias the interpretation of data. (Supported by SCGH Res. Foundation, Faculty of Anaesthetists RACS, and CTEC.)

T-Pos366 ON THE ORIGIN OF VALENCE SELECTIVITY IN A GRAMICIDIN LIKE CHANNEL. A MOLECULAR DYNAMICS STUDY. Shen-Shu Sung and Peter C. Jordan, Dept. of Chemistry, Brandeis University, Waltham, MA 02254

In previous work (1) we have studied the potential energy profile of cations with several water molecules in a simplified model of the gramicidin channel. We now extend this approach to consider anion occupancy with the aim of establishing whether the valence selectivity of gramicidin is a thermodynamic or a kinetic phenomenon. There are significant qualitative differences between the potential energy profiles for anion and cations, even for ions of the same size. Cationic potential profiles reflect the periodicity of the gramicidin helix, exhibiting series of 15 local minima. Anionic profiles show far less structure; there is a minimum near the channel center and, depending upon the number of water molecules included in the simulation, minima near the channel entrances. We will contrast some properties of hydrated Cl^- and Cs^+ ions in the model channel. These will include: the static energy barrier to ion entry into the channel; the binding energy; the solvation structure at binding sites; the solvation structure at saddle points. The significance of aqueous hydrogen bonding to the polar moieties of gramicidin and to the Cl^- will also be considered.

1) Lee, W.K. and P.C. Jordan, 1984. *Biophys J.*, 46: 805-819.

T-Pos367 CONTRIBUTION OF BULK SOLUTION ACCESS RESISTANCE TO THE CONDUCTANCE OF H^+ , K^+ and Li^+ IN THE GRAMICIDIN CHANNEL. E. Radford Decker and David G. Levitt, Dept. of Physiology, Univ. of Minnesota, Minneapolis, MN 55455

The relative importance of the access resistance at the channel mouth in determining cation conductance in gramicidin was evaluated in two series of experiments. In the first series, the H^+ conductance at pH 3.75 was measured in the absence and presence of 1M formate. At this pH (= pK formate), formate should act as a source/sink for H^+ , reducing the access resistance. The presence of formate increased the H^+ conductance by more than seven-fold at 200 mV. This suggests that the access resistance contributes at least 85% of the total resistance to H^+ at 200 mV. Lactate and oxalate were less effective in increasing conductance. In the second series of experiments, measurements were made of the H^+ , K^+ and Li^+ conductance in the presence and absence of high concentrations (1M) of non-conducting cations. If access resistance is limiting, the high non-conducting cation concentration should reduce the voltage drop at the channel mouth, decreasing the conductance. In the presence of 1M Tris, conductance at 200 mV decreased by 51% for H^+ (pH 3.75), 27% for 10 mM K^+ , and 11% for 20 mM Li^+ . The 50% reduction in conductance and the shape of the current-voltage relationships seen with H^+ agree with the theory (Lauger, *BBA* 455(1976):493-509) for the case where access resistance is the only rate limiting step in channel conductance. No decrease in conductance was seen with 1M choline. This may reflect the ability of Tris, with its unsubstituted amine group, to move closer to the channel mouth than choline. The results suggest that the access resistance is the major rate limiting step for H^+ conductance and significantly limits K^+ conductance.

T-Pos368 MODIFICATION OF SQUID AXON SODIUM CHANNELS BY DELTAMETHRIN. Leslee D. Brown and Toshio Narahashi, Dept. of Pharmacol. Northwestern Univ. Med. Sch., Chicago, IL 60611

Modification of sodium channels by deltamethrin, a potent synthetic pyrethroid, has been studied with squid axons using voltage clamp techniques. Pyrethroids have been shown previously to prolong sodium current. After internal treatment with deltamethrin (10 μ M), a depolarizing step to -20 mV from a holding potential of -80 mV elicited the normally activating and inactivating transient sodium current. However, when a long (500 ms) depolarizing step was given activation of modified sodium channels was observed late in the pulse. Deltamethrin appears to modify a fraction of sodium channels in such a way as to slow activation dramatically. This would also explain the slight decrease in peak sodium current seen after deltamethrin. Upon repolarization from a depolarizing pulse a large sodium tail current appeared. This tail current had a dual exponential decay with a fast time constant of 50 ms and a slow time constant of 1000 ms at -80 mV. At -100 mV the fast time constant was decreased to 30 ms and the slow time constant to 700 ms. In addition to slowing activation deltamethrin also appears to slow channel closing. Increasing the depolarizing pulse duration beyond 50 ms allowed more modified channels to open thereby increasing the amplitude of both the fast and slow phases of the tail current. However, the time constants of decay were independent of pulse duration. The process of modified channel closing is not dependent on the number of modified channels open. In all experiments currents were blocked by 1 μ M TTX. Supported by NIH grant NS 14143.

T-Pos369 BLOCK OF SODIUM CHANNELS AND REMOVAL OF SODIUM INACTIVATION BY CHLORAMINE-T IN CRAYFISH GIANT AXON. James M. C. Huang and Jay Z. Yeh. Dept. of Pharmacol. Northwestern University, Chicago, Ill. 60611. (Intr. by C. H. Wu)

Modification of sodium channels by chloramine-T (Ch-T) was examined in crayfish giant axons using the double sucrose gap voltage clamp technique. Internally or externally applied Ch-T (1-5 mM) was equally effective in removing fast inactivation from sodium channels. This action of Ch-T did not seem to be voltage-dependent, since prolonged depolarization could not prevent the sodium channel from being modified by Ch-T. This contrasts with our earlier findings of voltage dependent removal of Na channel inactivation with pronase or N-bromoacetamide (NBA) (Salgado et al., Biophys. J. 47: 567-571, 1985). The slow inactivation mechanism was still present in the modified channels. Similar to findings with pronase or NBA, the voltage dependence of activation and reversal potential of the modified current were not affected. However, unlike pronase or NBA, during treatment with Ch-T, a distinct blocking phase (up to 80% blockade) occurred, which recovered upon washing out Ch-T. Thus, Ch-T exerted two actions on the sodium channels: one was to remove inactivation irreversibly and the second was to block the channels reversibly. Supported by NIH grant GM-24866.

T-Pos370 BURST ACTIVITY OF NA CHANNELS REVEALS SLOW INACTIVATION KINETICS. Fred Quandt, Dept. of Physiology, University of Calgary, Faculty of Medicine, Calgary, AB., Canada T2N 4N1.

The gating of single Na channels by the process of slow inactivation has been studied using patches of membrane from N1E-115 neuroblastoma cells. In order to directly study slow inactivation, the process of fast inactivation was eliminated by applying an enzyme to the internal surface of excised patches (see Soc. for Neuroscience abstracts 9:674, 1983). The studies reported here utilized papain for this purpose. Currents due to the opening of Na channels can be observed in steady state measurements between -50 and -20mV, in the absence of fast inactivation. Opening of Na channels can occur in bursts under these conditions. For one typical experiment at -40mV, the mean interburst interval was found to be 9.6 sec, the burst length was 450 msec, the mean open time was 5 msec, and the closed time within a burst was about 1 msec (22°C). The interburst interval increased for more depolarized potentials. Since the mean burst length is similar to the time constant for slow inactivation, it likely represents the mean time to arrive at the slow inactivation state of the channel from either closed or open states. The interburst interval would then represent the time in which the channel occupies the slow-inactivated state, and therefore the inverse of the sum of the rates of reaction from slow-inactivated to closed, and slow-inactivated to open states of the Na channel. The reduced probability of opening of the Na channel from the slow-inactivated state compared to that from the closed states, and the slow recovery from slow-inactivated to closed states, may explain the ability of Na channels to hibernate. Supported by the Medical Research Council of Canada and The Alberta Heritage Foundation for Medical Research.

T-Pos371 THE FATTY ACID COMPOSITION OF THE SODIUM CHANNEL POLYPEPTIDE FROM EEL ELECTRIC ORGAN. S.R. Levinson, A.W. Pike[#], & P.V. Fennessey[#], Dept. Physiology and [#]Mass Spectrometry Research Resource, U. Colorado Medical School, Denver CO 80262. As we have reported, the sodium channel polypeptide of the electric eel is unusually hydrophobic; this can be seen in its ability to bind up to 6 times its weight of the detergent SDS. It appears likely that this hydrophobicity is due to a post-translational modification of the channel protein, since the newly-synthesized, unprocessed polypeptide core appears to bind normal amounts of detergent. A possible cause of such hydrophobic behavior could be fatty acylation of the protein; such modifications have now been described for a number of proteins, both cytosolic and membrane-associated. To determine the fatty acid content of the eel channel, the polypeptide was purified on a reducing SDS column, extensively dialyzed, and extracted in chloroform/methanol to remove detergent and loosely-associated lipids. Tightly-bound fatty acids were then methyl-esterified and analyzed and identified by combined gas chromatography/mass spectrometry. Significant amounts of fatty acyl moieties are found by these methods, representing up to 10% of the weight of the polypeptide. Most of the fatty acid is palmitate, while lesser amounts of stearate and traces of myristate were also found. At present, it is uncertain what fraction of this lipid is covalently bound to the protein (e.g. by ester or amide linkages). In any case, despite fairly rigorous removal procedures, unprecipitated amounts of fatty acids appear to be associated with the eel sodium channel protein. Since the sodium channel both structurally and functionally interacts with a hydrophobic phase in the membrane, these findings could be relevant to the understanding of channel conformation and mechanism. Supported by NIH NS-15879 and RR-01152, and the Muscular Dystrophy Association.

T-Pos372 SODIUM CHANNELS AND ACETYLCHOLINE RECEPTORS: A COMPARISON OF THEIR DISTRIBUTION NEAR THE ENDPLATE AND THE TENDON OF SKELETAL MUSCLE. J.H. Caldwell and R.L. Milton, Dept. of Molecular and Cellular Biology, National Jewish Center for Immunology and Respiratory Medicine and Dept. of Physiology, Univ. of Colorado Medical School, Denver, CO 80206.

Sodium current density, measured with a loose patch voltage clamp, is much greater near the endplate than in extrajunctional regions far from the endplate. We have made longitudinal and circumferential maps of sodium current in the immediate vicinity of endplates. Sodium current in snake muscle decreased circumferentially about fourfold from the endplate (20 mA/cm²) to the antipode 60 μ m away (4.6 mA/cm²). The rate of decrease longitudinally was about the same as that in the circumferential direction, which is also true for acetylcholine receptor (AChR) maps in perijunctional regions of rat muscle (Bekoff and Betz, 1977) and raises the possibility that these channels are regulated together.

Although coordinate regulation of Na channels and AChRs may exist at the neuromuscular junction, this cannot be true for the entire muscle fiber since AChR and Na channel densities are dissimilar near the tendon. AChR density increases at the tendon of soleus muscle (Miledi and Zelena, 1966). We have measured sodium current density at the tendon in intact rat soleus muscle and find that it falls about threefold, e.g., from 7 mA/cm² (500 μ m from the end) to 2 mA/cm² (25 μ m from the end). This implies that separate mechanisms exist for controlling AChR and Na channel distributions in muscle. (Supported by grants from the NSF [BNS-8418742] and the MDA.) Bekoff and Betz, *J. Physiol.* **271**, 25-40 (1977). Miledi and Zelena, *Nature* **210**, 855-856 (1966).

T-Pos373 BIOCHEMICAL CHARACTERIZATION OF THE RAT AND THE RABBIT SKELETAL MUSCLE SODIUM CHANNEL SUBUNITS. R.H. Roberts, R.D. Gordon, J.M. Casadei and R.L. Barchi. University of Pennsylvania, Philadelphia, PA, 19104.

The voltage sensitive sodium channels from rat and rabbit skeletal muscle have been shown to contain a large (260kDa) and one or two smaller (37-40 kDa) subunits. The subunits of the rabbit channel have been separated by Sepharose 6B chromatography under reducing and denaturing conditions and their amino acid compositions determined (z values 0.40 and 0.36 for large and small subunits respectively). Carbohydrate analysis of the purified subunits indicated that the large subunit and the small subunit were 26% and 32% carbohydrate by weight, with N-acetyl hexosamine and sialic acid as the predominant monosaccharides. Enzymatic deglycosylation of the 38 kDa subunit with endo F resulted in a stepwise reduction in molecular weight to a sharp single band of 26.3 kDa. Using known amounts of large and small subunits calibrated by absolute amino acid analysis, the densitometric intensity of SDS-PAGE autoradiographs of each subunit was correlated with the amount of protein applied to each gel. Based on the deglycosylated molecular weights for the two subunits and densitometric scans of purified rabbit and immunopurified rat muscle sodium channel, we have calculated a subunit stoichiometry of one 260 kDa subunit to one small subunit of 37-40 kDa in these mammalian systems.

T-Pos374 Fast sodium current inactivation: whole cell and single channel studies.

Morier, N. and Payet, M.D., Dept. Biophysics, Fac. Medicine, Univ. Sherbrooke, Quebec, Canada J1H 514

The fast sodium current was studied on isolated myocytes from newborn rats. Patch clamp technique is used in whole cell and patch on-cell configurations. At negative voltages, the inactivation phase could be described by one exponential. At potentials more positive than -30 mV, two exponentials are required. The time constant of the fast component ranges between 8 ms and 1.5 ms reaching a plateau for voltages more positive than -20 mV. Time constant-voltage relationship of the slower component is U-shaped and the minimum value is found at -20 mV.

Single channel conductance was found to be 10 pS. At negative voltages, two types of events with different amplitude were observed. At positive voltages, late events with long opening time were occurred. Average currents with and without these late events clearly demonstrated that the second slower component of the inactivation is produced by late openings. Two populations of Na channels with different kinetics are postulated.

Supported by MRCC and FGMC. Morier, N. is FCAR fellow and Payet, M.D., FCMC scholar.

T-Pos375 MODIFICATIONS OF THE NA CHANNEL INACTIVATION PROCESS DO NOT AFFECT THE BLOCK OF NA CURRENT BY TTX AND STX IN FROG NERVE AND MUSCLE FIBERS. P.A. Pappone, Dept. of Animal Physiology, Univ. of Calif., Davis, CA 95616. It has been suggested that external amino group with a high pK forms part of the STX binding site (Strichartz, JGP 84:281, 1984). Modification of external amino groups by trinitrobenzenesulfonic acid (TNBS) indicate that such groups affect Na channel inactivation gating. I tested whether the same surface amino groups are involved in inactivation gating and toxin binding by assessing the effects of TNBS modification on the block of Na current by tetrodotoxin (TTX) and saxitoxin (STX). Nerve or muscle fibers were voltage clamped using the vaseline gap method. Treatment of the fibers with TNBS (10 mM, 2-8 min, pH 9.5) resulted in a shift in the voltage dependence of steady-state Na current inactivation of -14.3 mV (muscle) or -8 mV (nerve). The block of Na current by TTX or STX measured before and after TNBS treatment was identical. These results indicate that the TNBS-modifiable groups involved in inactivation gating are not involved in toxin binding. In contrast to the results in biological systems, the block of batrachotoxin (BTX)-activated Na channels reconstituted into artificial lipid bilayers by STX and STX analogs is highly voltage dependent, although independent of the charge of the blocking molecule. These results raise the possibility that the toxins bind to a membrane group involved in Na channel gating whose behavior is altered by BTX. Since one of the most prominent effects of BTX is the removal of Na current inactivation, I tested the effects of removing inactivation in muscle fibers with low internal pH on Na current block by STX. Preliminary results indicate that block of Na channels by STX is not affected by destruction of the inactivation process. These results suggest that the binding of TTX and STX to Na channels is independent of inactivation gating.

T-Pos376 KINETIC ANALYSIS OF RECENT STRUCTURAL MODELS OF THE SODIUM-CHANNEL PROTEIN Gilbert Baumann and George S. Easton, Dept Physiol, Duke Univ Med Ctr, Durham, NC 27710, and Grad Sch Bus, Univ Chicago, Chicago, IL 60637.

Working from the primary structure of the sodium-channel protein (Noda et al., Nature 312:121, 1984), several researchers (Noda et al., loc cit.; Kosower, FEBS LETTERS 182:234, 1985; Guy and Seetharamulu, PNAS (in press); Greenblatt et al. (pers. comm.)), including ourselves (J. Gen. Physiol. 86:11a, 1985), have proposed models of its tertiary structure. All these models (except one) are based on the presence in the protein of four homologous domains, each containing several segments with high structure-forming potential. These segments are capable of spanning the membrane and providing regions of contact with its hydrophobic core, sensing the transmembrane voltage, or lining the channel itself. If a simple molecular mechanism is assumed based on the concept of reversible interaction among the domains, then these four-domain models can account for many kinetic features of sodium gating. The fit between model and data follows naturally from the basic concept rather than from adjusting parameters in an ad hoc scheme. Based on the mechanism, experiments can readily be designed that test its applicability in some of these models. Also, from such a mechanism, experimentally testable molecular explanations can be offered for data not accounted for by the Hodgkin-Huxley formalism. (Research supported by NSF grant BNS 84-00101 and grant Z-3397 from the North Carolina Board of Science and Technology.)

T-Pos377 TETRODOTOXIN-INSENSITIVE Na-CHANNELS FROM DENERVATED RAT MUSCLE IN PLANAR LIPID BILAYERS. X. Guo, S.H. Bryant and E.G. Moczydlowski, Dept. of Pharmacology & Cell Biophysics and Dept. of Physiology & Biophysics, Univ. of Cincinnati Coll. of Medicine, Cincinnati, OH 45267

Previous work has shown that a fraction of the Na-channel current of rat skeletal muscle becomes insensitive to tetrodotoxin (TTX) within several days after denervation. To study the properties of single Na-channels present in denervated muscle, a plasma membrane fraction was isolated from 30 g of right lower hind limb muscles from 11 rats on the 7th day after surgical removal of a 1 cm piece of right sciatic nerve. Incorporation Na-channels into planar lipid bilayers (7PE:3PC) cast from decane was observed in the presence of batrachotoxin to remove inactivation. Single Na-channels were characterized with respect to toxin sensitivity by addition of $1 \mu\text{M}$ TTX to the chamber (0.2 M NaCl, pH 7.4, 22°C). Two distinct types of Na-channels were identified. One type with a conductance of 21 pS was blocked 92% of the time at +50 mV by $1 \mu\text{M}$ TTX, while a second type with a conductance of 24 pS was blocked only 36% of the time under the same conditions. In experiments from 12 bilayers, 9 TTX-insensitive channels and 24 TTX-sensitive channels were observed with both types of channels often incorporating together in the same bilayer. Preliminary analysis of the single channel blocking kinetics revealed that the TTX-sensitive channels are identical to those observed in preparations from normal muscle with a K_D of about 30 nM TTX at 0 mV. Compared to such normal channels, TTX-insensitive channels have a 4-fold faster off-rate and a 10-fold slower on-rate for TTX with a K_D of 1000 nM TTX at 0 mV. Both types of channels exhibit a similar voltage dependence of TTX binding rate constants. The blocking kinetics of the TTX-insensitive channels are similar to that of Na-channels from dog heart in planar bilayers (Uehara and Moczydlowski, in preparation). These results indicate that macroscopic Na-currents in denervated muscle can be explained by two subtype populations of Na-channels with different toxin receptor sites. (Supported by AHA, MDA, NIH AM35128, NS03178 and Searle Scholars Program/The Chicago Community Trust.)

T-Pos378 CHARACTERIZATION OF MAMMALIAN VOLTAGE-ACTIVATED SODIUM CHANNEL GENES. G. MANDEL, S. COOPERMAN, M. MONTMINY, R. BARCHI, P. BREHM, AND R. GOODMAN. (Intr. by F. Moody-Corbett), Dept. of Medicine, Tufts-New England Med. Ctr., Boston, MA., 02111.

Complementary DNA's (cDNA) encoding rat muscle and neuronal sodium channel proteins have been isolated and characterized by sequence analysis. The mammalian cDNA's were identified by hybridization to a cDNA encoding the large subunit of *Electrophorus electricus* sodium channel. An oligonucleotide, homologous to 18 base pairs in the 3' end of the eel cDNA, was synthesized and used to screen a cDNA library prepared from electroplax mRNA's. One clone was sequenced and found to be identical to 2300 nucleotides in the 3' end of the published eel sodium channel gene sequence. This cDNA was then used to screen bacteriophage lambda gt11 rat muscle and brain libraries. Several muscle and brain clones were isolated using hybridization conditions of moderate stringency. The cDNA's that have been sequenced contain regions of greater than 80% amino acid homology with the eel electroplax sodium channel protein. These regions correspond to hydrophobic domains within the large subunit sodium channel. The cDNA's are being used as probes to measure sodium channel gene activity in developing neuronal and muscle cells. Supported by NIH Grant NS 22518.

T-Pos379 BTX-MODIFIED SODIUM CHANNELS FROM EEL ELECTROPLAX IN PLANAR BILAYERS. E. Recio-Pinto, D.S. Duch⁺, S.R. Levinson⁺ & B.W. Urban, Depts. Anesthes. & Physiol., Cornell U. Med. Coll., New York, NY 10021 and ⁺Dept. Physiology, U. of Colorado Med. School, Denver, CO 80262.

The highly purified, large molecular weight TTX-binding polypeptide (2000-2900 pmol TTX bound/mg protein) from eel electroplax was reconstituted into liposomes as previously described (Duch and Levinson, *Biophys. J.* 47:192a, 1985). From measurements of sodium fluxes in the presence of veratridine it was estimated that 85% to 100% of the TTX-binding polypeptides conducted sodium ions. Other polypeptides present constituted less than 10% of the total purified protein (SDS-PAGE).

In the presence of BTX, vesicles containing the purified TTX-binding polypeptide were fused with planar bilayers made from neutral phospholipid solutions containing PE/PC (4:1) in decane, following procedures used for dog brain synaptosomes (Green et al., *Ann. NY Acad. Sci.* 435:548, 1984). Channel activity similar to that of brain sodium channels was detected. At +60 mV the channels had a fractional open time of 0.98. The I/V curve was linear between -110 mV and +80 mV with a single channel conductance of 24 pS (symmetrical 0.5 M NaCl, 10 mM hepes, pH 7.4); submaximal TTX levels did not alter the single channel conductance. Some channels functioned for more than five hours without any detectable change in the I/V curve. TTX block was voltage dependent with K_D 's of about 5, 20 and 90 nM at -60, 0 and +60 mV, respectively. Steady-state channel activation had an average mid-point potential of -80 mV. These values are very similar to the ones reported for sodium channels from dog brain synaptosomes (Green et al., 1984), except for the observed larger spread of the midpoint potentials from the voltage-dependent gating. The latter has also been reported for reconstituted purified rat brain sodium channels (Hartshorne et al., *PNAS* 82:240, 1985).

T-Pos380 Local anesthetics block Na currents in chloramine-T treated squid axons. G.K. Wang, M.S. Brodwick, D.C. Eaton, and G.R. Strichartz, Anesthesia Research Labs, Harvard Medical School, Boston, MA, and Department of Physiology and Biophysics, University of Texas Medical Branch, Galveston, TX.

We have studied the effects of QX-314 and etidocaine on Na currents in the control, pronase, and chloramine-T (CT) pretreated squid axons under voltage clamp conditions. Chloramine-T, a non-cleaving, oxidizing reagent, was applied to remove the Na channel inactivation in a manner similar to pronase. We found that both local anesthetics, when applied internally at 1 mM, elicit a tonic block of Na currents, a time-dependent block during single depolarizations, and a use-dependent block after repetitive depolarizations in the control and CT treated axons. Little time-dependent or use-dependent block occurs in pronase-treated axons. A profound time-dependent block appears at large depolarizations ($E_m > +60$ mV) in the CT treated axons, suggesting that the binding interaction remains even in the absence of functional Na inactivation. The voltage dependence of the use-dependent block in the CT treated axons differs slightly from that in the control; an 8% reduction of the maximal use-dependent block and a shift of the voltage-dependence in the hyperpolarizing direction were found in the CT treated axons. Nevertheless, the recovery from this use-dependent block is comparable between the control and CT modified axons, suggesting that the unbinding kinetics of the bound drug from the Na channel is little changed. These results together demonstrate that QX-314 and etidocaine are able to interact with the activated open channels in a voltage- and time-dependent manner. Also evident is that inactivation *per se* does not appear to be a prerequisite for the local anesthetic action. A generalized modulated receptor scheme is suggested for the interactions between the local anesthetic and the Na channel. Supported by NIGMS-GM 35401, GM 35647, and NS 11963.

T-Pos381 SLOW INACTIVATION IN MAMMALIAN MUSCLE.

W. Stühmer and L. Simoncini,
Dept. of Membrane Biophysics, MPI für Biophysikalische Chemie, 34 Göttingen, F.R.G.

We have used the loose-patch voltage clamp method (Stühmer, Roberts and Almers in *Single Channel Recording*, eds. Sakmann and Neher, Plenum, 1983) to investigate the slow inactivation process in intact rat extensor digitorum longus muscle fibres.

The slow inactivation was elicited by application of a steady hyper- or depolarising potential to the inside of the patch pipette and the corresponding changes in peak sodium currents measured as a function of time. These peak currents could be well fitted by a single exponential (with exclusion of the first 10 seconds during which the normal and intermediate inactivation take place) with time constants in the range of one to four minutes.

The steady state values of peak currents as a function of effective membrane potential as measured by the position of the fast inactivation curve could be well fitted by a function identical to the one used to describe the fast inactivation process. This gave a potential of -101 mV at which half of the sodium channels are slow inactivated. In fact, more than 50% of the sodium currents could be recovered by hyperpolarizing fibres, even if they had resting potentials more negative than -90 mV.

These results indicate that the slow inactivation process is important in regulating the availability of sodium channels with a slow time constant as a function of membrane potential.

T-Pos382 A CALCIUM-ACTIVATED SODIUM CONDUCTANCE CONTRIBUTES TO THE FERTILIZATION POTENTIAL IN THE EGG OF THE NEMERTEAN WORM, *CEREBRATULUS LACTEUS*. Douglas Kline^{1,2}, Laurinda A. Jaffe^{1,2}, and Raymond T. Kado^{1,3}. ¹Marine Biological Laboratory, Woods Hole, MA. 02543 U.S.A., ²Dept. of Physiology, Univ. of Connecticut Health Center, Farmington, CT. 06032 U.S.A., and ³Laboratoire de Neurobiologie Cellulaire, Centre National de Recherche Scientifique, Gif-sur-Yvette 91190 FRANCE.

The egg of the nemertean worm *Cerebratulus lacteus* produced a fertilization potential lasting 80 min; starting from about -65 mV, the potential shifted to a Ca^{2+} -dependent peak at about +44 mV and a Na^+ -dependent plateau at about +24 mV. To establish the background for studying the fertilization potential, we first analysed the conductance properties of the unfertilized egg. Current-voltage relations of the unfertilized egg showed a fast inward Ca^{2+} current and a slow inward Ca^{2+} -dependent Na^+ current. The Na^+ conductance showed selectivity for Na^+ over K^+ and was blocked by microinjection of EGTA. EGTA and BAPTA injections also indicated that the Ca^{2+} -activated Na^+ conductance contributed to the fertilization potential. Pressure injection of 5 to 9 mM BAPTA:CaBAPTA in a 10:1 ratio (about 10^{-7} M Ca^{2+}) reduced the amplitude of the fertilization potential. Injection of 5 to 9 mM BAPTA:CaBAPTA in a 1:1 ratio (about 10^{-6} M Ca^{2+}) shifted the egg's potential to the level of the fertilization potential plateau. Intracellular Ca^{2+} stores were probably important in generating the fertilization potential, since perfusion with zero Ca^{2+} sea water had only a small effect on the fertilization potential plateau, and the fertilization potential in sea water containing 10 mM Cd^{2+} had a normal plateau potential. Supported by NIH grant HD14939 to L.A.J., and NIH Training Grant HD07098 to the Embryology Course at the Marine Biological Laboratory, Woods Hole, MA.